FLUIDIC ARMAMENT TURRET SYSTEM M-28 TURRET 2-AXIS DAMPER

Richard Evans, et al

Honeywell, Incorporated

Prepared for:

Rock Island Arsenal

August 1974

Security Classification

DOCUMENT CONTROL DATA · R & D AD/A-000917

Security classification of title, body of abstract and indexing annotation must be entered when the overall report is classified

1 ORIGINATING ACTIVITY (Corporate author)
Honeywell Inc.
Government and Aeronautical Products Division
1625 Zarthan Ave.,
Minneapolis, Minnesota 55416

2a. REPORT SECURITY CLASSIFICATION
Unclassified

2b. GROUP

3 REPORT TITLE

Fluidic Armament Turret System

4 DESCRIPTIVE NOTES (Type of report and inclusive dates)
Final Report 16 June 1972 to 31 March 1974

5 AUTHOR(S) (First name, middle initial, last name)

Richard Evans
J. Robert Sjolund

6 REPORT DATE	7a. TOTAL NO. OF PAGES	7b. NO. OF REFS
August	99	

8a. CONTRACT OR GRANT NO.	9a. ORIGINATOR'S REPORT NUMBER(S)
DAAF03-72-C-0164	
b. PROJECT NO Task W0522	2760-45682
c.	9b. OTHER REPORT NO(S) (Any other numbers that may be assigned this report)
d.	

10 DISTRIBUTION STATEMENT

11 SUPPLEMENTARY NOTES	12. SPONSORING MILITARY ACTIVITY
	Rock Island Arsenal Rock Island, Illinois

13 ABSTRACT

The results of a program to build and test a Fluidic Armament Turret System (FATS) are reported The FATS is a two-axis hydrofluidic-electronic hybrid inertial damping system for the XM28 turret. The program includes analysis, hardware design, fabrication, and testing. Turret performance is finally compared with and without the turret damper during firing tests from an AH-1G Helicopter, at the Honeywell Proving Grounds.

DD FORM 1 NOV 1473 REPLACES DD FORM 1473, 1 JAN 64, WHICH IS OBSOLETE FOR ARMY USE.

Security Classification

FOREWORD

This study was conducted under ARMY Contract DAAF03-72-C-0164, "Fluidic Armament Turret System (FATS) XM28 Turret 2-Axis Damper". The work was administered under the direction of Rock Island Arsenal. Mr. P. Townsend was the project monitor. The work was conducted during the period of 16 June 1972 through 31 March 1974.

This report was prepared by the AFS Fluidic Systems Group of the Government and Aeronautical Products Division, Honeywell Inc., 1625 Zarthan Ave., Minneapolis, Minnesota 55416.

The number assigned to this report by Honeywell Inc. is W0522.

TABLE OF CONTENTS

TABLE OF CONTENTS (Concluded)

LIST OF ILLUSTRATIONS

LIST OF ILLUSTRATIONS (Continued)

LIST OF ILLUSTRATIONS (Continued)

LIST OF ILLUSTRATIONS (Concluded)

SECTION I

INTRODUCTION

A hybrid two-axis turret damper system that would inertially stabilize an M-28 helicopter turret having the standard electro-hydraulic position loop control was developed. The system concept was conceived earlier, on Contract DAAF03-72-0021, and then revised within this program to the final version.

The final version of this system includes:

- The basic M-28 electro-hydraulic position control.
- A two-axis hydrofluidic vortex rate sensor and amplifier package for sensing azimuth and elevation axes rates of the turret guns.
- Two fluidic-to-electrical transducers.
- An electronic signal amplification and conditioning circuit.
- Electrical switching for activating or deactivating the system.

The overall objective of the program was to develop a flightworthy fluidic turret damper system, optimized to provide maximum damping of aircraft disturbances in the turret's azimuth and elevation axes. To achieve this overall objective, the following basic objectives were initially set up:

1. Provide inertial damping of 1) turret motions resulting from aircraft motions, and 2) structural flexure resulting from gun firing.
2. Provide this damping without seriously degrading the accuracy and response of the turret to gunner commands.
3. Provide simple interface capability with existing electrical turret controls, to facilitate the addition and evaluation of the fluidic system.
4. Provide above functions for a relatively low cost, with high reliability in the weapon shock environment.
5. Conduct a turret structural investigation to locate the source of resonance encoutered in the M-28 turret during the earlier feasibility programs, and formulate methods of eliminating the problem.

Early in the program it was realized that items 1 and 2 above could not be completely satisfied with the initial mechanization, and a change in the program was recommended. The structural flexure problem was recognized as being caused by one of two factors: a relatively low frequency distortion resulting from average firing torques, and high frequency distortions occurring at firing frequencies and helicopter structural frequencies. Because of system bandwidth limitations, correction of only the first factor could be expected. Upon the acceptance of this recommendation a new mechanization was developed, fabricated, and tested both in the laboratory and in a helicopter during gun firing tests.

The complete program was a twenty-one and one-half month development effort to design, build, and evaluate a system to satisfy the above objectives.

The following conclusions can be derived from the results of the program:

- The low frequency turret resonance (17 Hz) is caused by hydraulic fluid compressibility in the elevation axis actuator and by gear train flexability in the azimuth axis.
- The general concept of hydrofluidic turret stabilization for future turrets was verified.
- No feedback control effects were detected due to turret inertia causing helicopter structural deformation.
- Fluidic system performance was unaffected by gun fire shocks.
- A high response hydrofluidic rate sensor (25 to 50 Hz) is practical for future high response systems.
- An optimized system that includes gunsight reticle compensation (for stabilization system inputs) would effectively reduce round dispersion.

The following recommendations are made:

- A cost effectiveness study involving the value of improvement in dispersion considering mission and target mix factors, turbulence environment, gunner human factors, and related developments in alternate sight/control means should be conducted.
- A development program to add gunsight reticle compensation to the FATS system should be considered.
- Consider use of non-highpassed FATS (Fluidic Armament Turret System) for stabilization of guns fired by the pilot from the stowed position.
- Consider use of hydrofluidic systems for other applications requiring environmental ruggedness.

SECTION II

SYSTEM ANALYSIS

INITIAL SYSTEM ANALYSIS

The first portion of the system analysis was conducted on a system concept that originated in a previous contract, DAAF03-71-C-0336.[1] This system was mechanized through use of simulation techniques on both an analog and a digital computer. This system is shown in Figure 1.

This mechanization was found to have serious shortcomings resulting from a compromise between damping effectiveness and degradation of the turret-performance-to-gunner inputs. The trade off at best ended up with insufficient damping and degraded gunner input performance.

A second factor preventing use of this concept was the 17 Hz resonance in the basic turret, since the resonance was further aggravated by this concept. Rate sensor delay time was also a significant limitation to attainable system bandwidth, approaching that contributed by the turret resonances.

To establish the validity of the computer analysis results; a test setup was devised using the actual turret with the existing electronic position control, a vortex rate sensor, a hydrofluidic amplifier, a pressure transducer, and an analog computer. With the analog computer, system gains and compensations could be varied readily and simulated inputs could be applied.

The results of this series of tests again showed the system to be undesirable due to stability problems at high frequency (structural resonance) and gunner input performance degradation. Some improvements were made in this system with the use of a notch filter. The block diagram of the "best" system is shown in Figure 2. Performance of this system is plotted on the graphs of Figures 3 and 4.

It was recommended that an effort be initiated to define a new mechanization that would accomplish the same goals while inherently avoiding some of the above indicated problems.

FINAL SYSTEM ANALYSIS

The M-28 turret position control system, with added fluidic rate stabilization, was analyzed to determine system configuration and potential performance. The objective of the design is to provide short-term inertial stabilization of gun angle with minimum degradation of response to gunner commands. The latter is facilitated by adding inputs consisting of only those angular gun rates produced by helicopter body motions. These can

---

(1) Hedeen, J. O., Final Report, Contract DAAF03-71-C-0336, (Security Class).

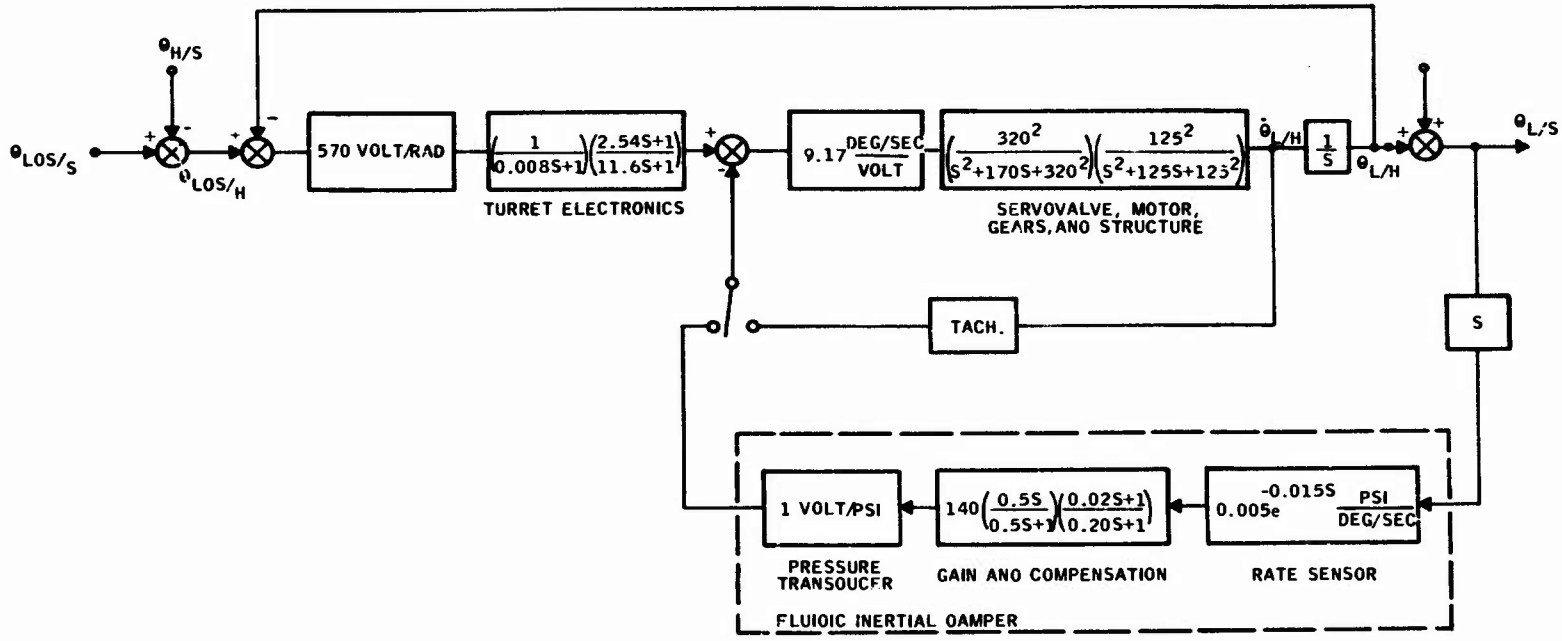

Figure 1. Block Diagram of Basic Traverse Axis

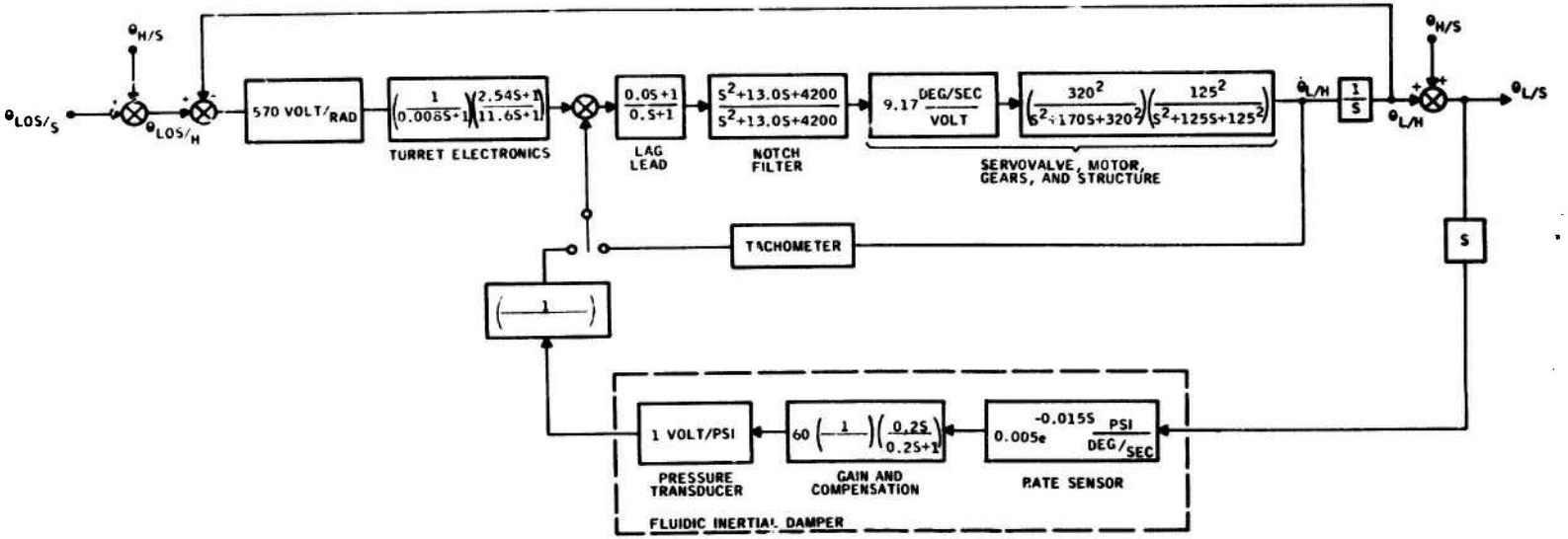

Figure 2. Block Diagram of Improved Traverse Axis

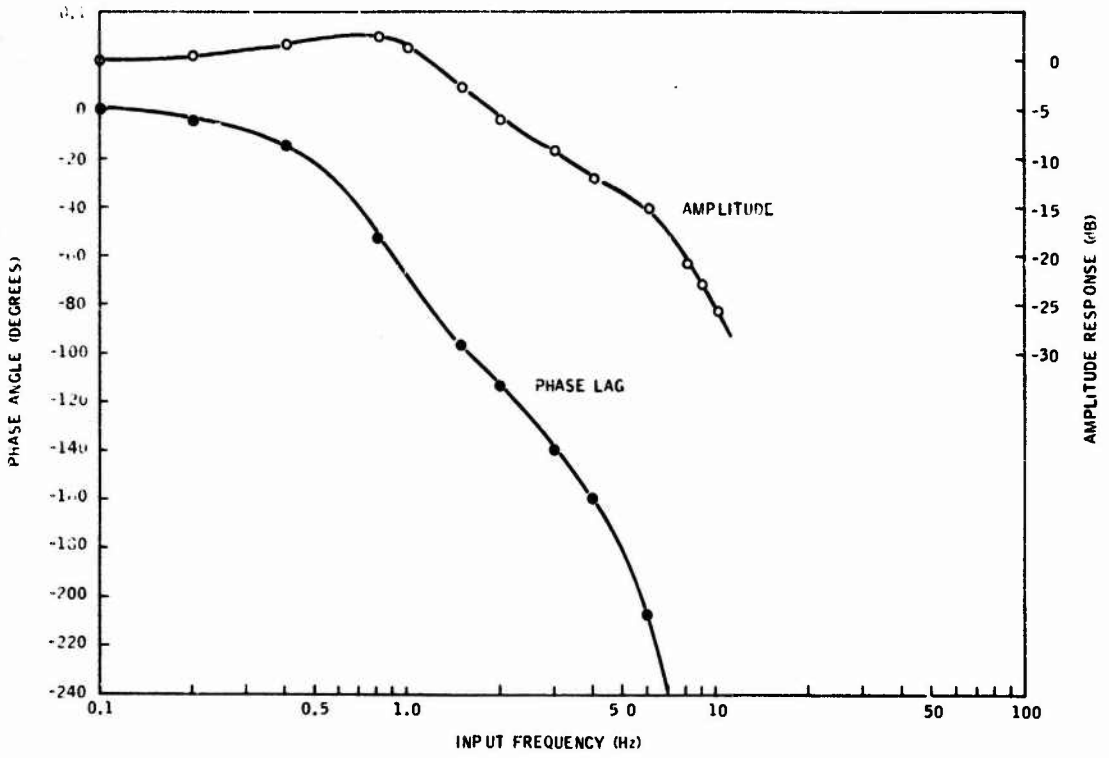

Figure 3. System Response to Disturbance Inputs

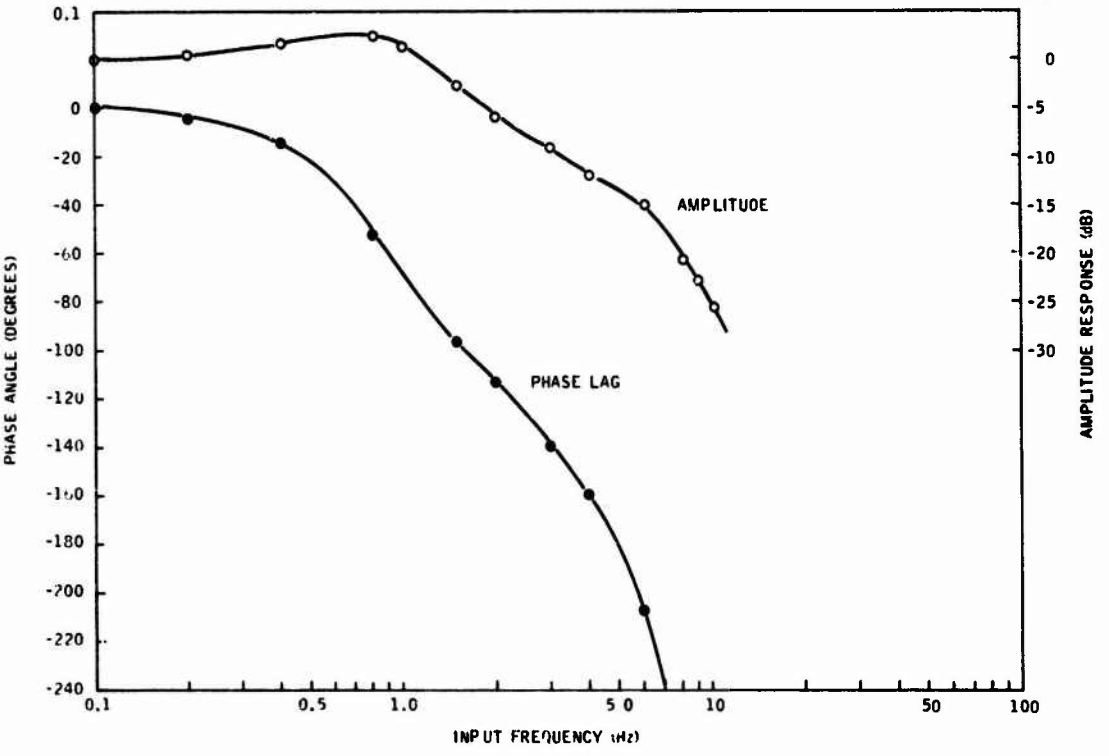

Figure 4. System Response to Gunner Inputs

be derived in alternate ways by using appropriate combinations of inertial rate and sensed turret angular rates relative to the helicopter. The short-term stabilization is effective for disturbances within the system response capabilities. This would include airframe oscillations resulting from rigid body and aerodynamic dynamic effects, as well as structural deformations due to lower frequency loads (e.g. "average" firing torques). This would exclude structural deformations at frequencies of the firing itself and natural frequencies of the helicopter structure.

Basic System Structure

Basic turret geometry is illustrated in Figure 5. For the indicated variables,

$$r_G = r_H \cos E_G + (p_H \cos A_G + q_H \sin A_G) \sin E_G + A_G \cos E_G \quad (1)$$

$$q_G = q_H \cos A_G - r_H \sin A_G + E_G \quad (2)$$

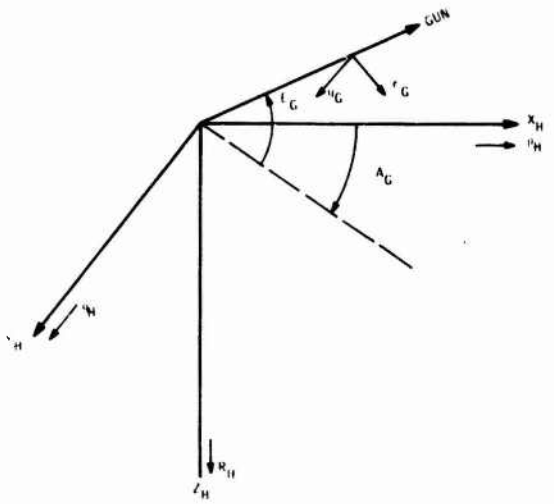

Figure 5. Basic Turret Geometry

Equations (1) and (2) relate boresight angular rates to helicopter body rates and turret angular rates. To keep the gun stabilized under helicopter motions, $q_G = r_G = 0$, thereby dictating required azimuth and elevation rates according to equations (1) and (2). If only two rate sensors are to be used, those must be oriented such that q_G and r_G are measured without effect from a p_G component (gun boresight roll rate). Otherwise, the roll rate component must also be measured in some other manner. The orientation with least complication in terms of required hardware is to place the azimuth sensor on the gun, thereby measuring gun azimuth rate directly. Hence, R_{RS} (azimuth rate sensor input) equals r_G. This signal is combined with the tachometer-generated A_G to derive the equivalent helicopter rate component parallel to r_G, namely $R_{RS} - A_G \cos E$. From this quantity a transient azimuth command can be generated to apply to the existing azimuth control loop:

$$A_{cmd} = \frac{-R_{RS}}{\cos E_G} + A_G \quad (3)$$

To produce only transient stabilization, the integration of A_{cmd} is replaced by $\frac{S}{(S+1)^2}$, hence

$$A_{cmd} = \frac{S}{(S+1)^2} \frac{-R_{RS}}{\cos E_G} + A_G \qquad (4)$$

note also that since the turret is being commanded as a function of derived helicopter rate, the input of equation (4) will have little effect on gunner input to gun position.

In the case of the elevation axis, an identical approach is used. Here an elevation command is generated as a function of helicopter rate parallel to the elevation axis to maintain zero gun rate according to equation (2):

$$E_{cmd} = -(q_H \cos A_G - p_H \sin A_G) = E_G - q_G \qquad (5)$$

Note here, however, the option exists of placing the rate sensor on the gun and combining with E_G, or placing the rate sensor on the turret platform aligned with the elevation axis. The choice is largely dependent on implementation convenience, although minor differences in performance will occur due to differing rate sensor and tachometer characteristics. Rate sensor placement on the turret platform eliminates a requirement for an elevation tachometer and would, therefor, appear preferable. Assuming this option is used, and again limiting the stabilization to only higher frequencies:

$$E_{cmd} = \frac{S}{(S+1)^2} -Q_{RS} \qquad (6)$$

Where Q_{RS} = elevation rate sensor signal.

The resulting overall system is shown in Figure 6.

It should be noted at this point that the added stabilization of the gun in conjunction with the standard fixed-reticle sight is a potential source of tracking error under helicopter angular rates in that the gunner has incomplete knowledge of the transient gun position. The shaping selected for the stabilization signal $\frac{S}{(S+1)^2}$ is designed to minimize this error source by blocking "steady state" rate signals. A more comprehensive solution would be provided by perturbing the sight reticle in proportion to gun position error relative to the gunner input, as indicated on Figure 6. This would also provide the added benefit of short-term reticle inertial stabilization.

Performance Analysis

The system analytical model used for the performance analyses reported in this section is illustrated in Figure 7. This model is improved in dynamic accuracy over previous models in that a 0.002-second valve log is included. The model relates gun angular position to both gunner (sight) inputs and to helicopter angular position. The dynamics and gain of the nominal loop electronics are illustrated, along with the dynamics of the turret structure and actuation. The indicated transfer functions for the latter are strictly applicable only to the azimuth axis, although the elevation

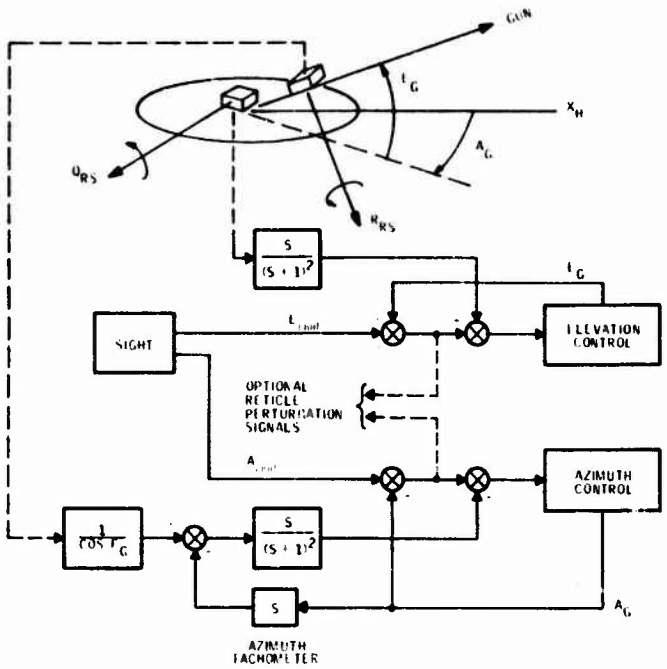

Figure 6. Turret Stabilization System

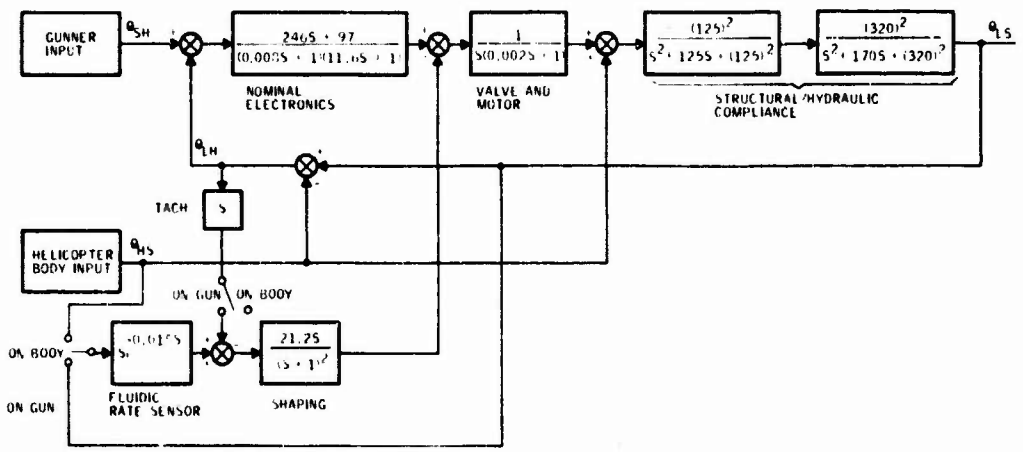

Figure 7. System Analytical Modeling (No Helicopter Structural Coupling)

dynamics appear comparable or somewhat less restrictive, based on prior analyses and frequency response measurements. The added rate stabilization is illustrated for both gun and body-mounted rate sensors, although the latter option only applies to the elevation axis.

The model of Figure 7 omits any coupling through the helicopter structure, as may be produced by turret inertial forces causing the helicopter angular rates which are sensed by the fluidic sensor. The "rigid body" rates associated with this effect are expected to be negligible because of low turret-to-vehicle inertia ratios. Helicopter flexibility may be significant, however, requiring added filtering to preclude undesirable coupling.

Also not analyzed are weapon-firing reaction forces as applied to both the helicopter structure and to the turret. It is expected that helicopter structural dynamics may also significantly influence these effects. Their overall contribution to fire control error is generally unknown.

The current feedback control system provides a relatively high bandwidth control of turret position relative to the helicopter, as demonstrated by the frequency responses of Figure 8. In the performance of this function, little if any benefit is realizable from added tachometer or rate sensor feedback with existing structural and hydraulic stiffness. No significant degradation in gunner tracking ability is anticipated due to turret response characteristics. Figure 8 shows responses for the rate sensor positions on the body and on the gun. The delay time of the fluidic rate sensor affects the latter, creating a minor resonance of approximately 6.4 Hz.

Turret motions due to air turbulence or firing bursts are in frequency range which is subject to only partial correction by the gunner. Effective gun stabilization by inertial sensing of helicopter rates appears feasible, however, with little effect on response to gunner commands. Figure 9 illustrates turret response to helicopter body angles with and without rate stabilization. The latter is shown for both rate sensor positions. A slight difference is evident due to fluidic delay time.

In event of unacceptable coupling through the helicopter structure, added filtering of the rate signal may be necessary which will degrade the inertial stabilization somewhat. Figure 9 also illustrates the response of turret position to helicopter motion with a 0.1 second first-order lag added to the nominal rate shaping; i.e.,

$$\frac{S}{(S+1)^2} \qquad \frac{S}{(S+1)^2\,(.1S+1)}$$

The case shown has the rate sensor on the gun, although the difference between mounting options becomes negligible with the added filter.

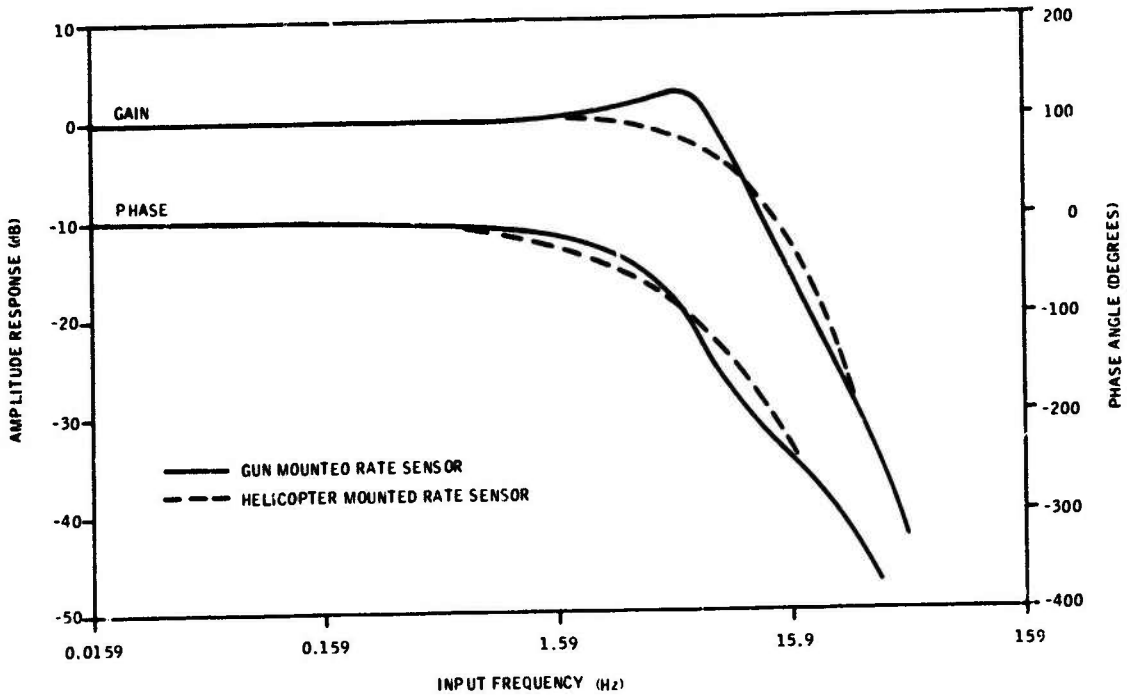

Figure 8. Frequency Response, Turret Position From Gunner

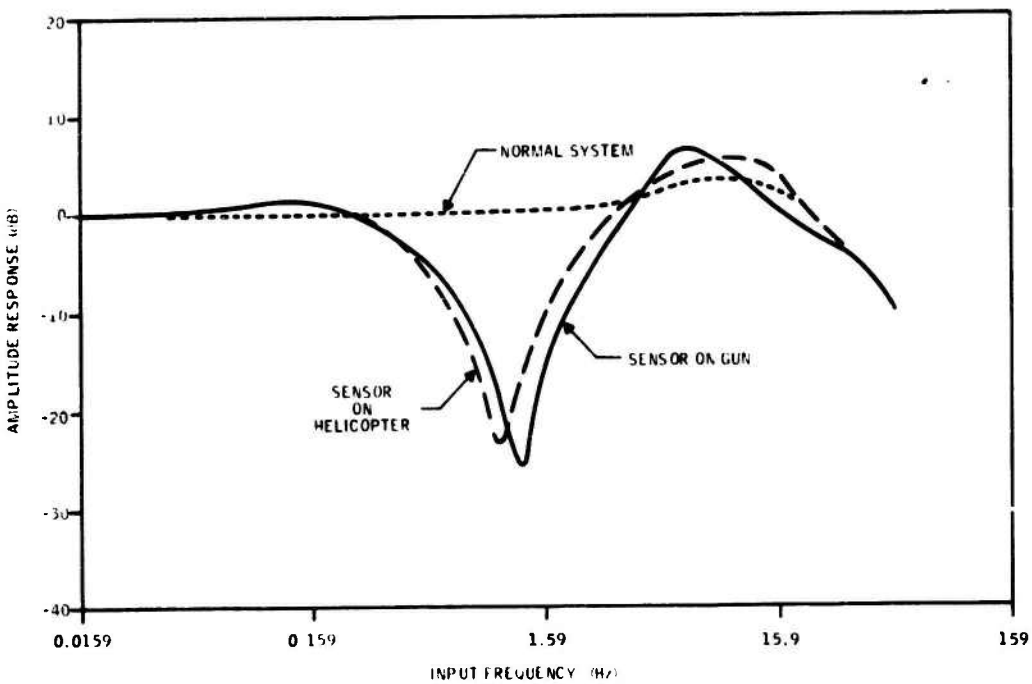

Figure 9. Amplitude Response, Absolute Turret Position from Helicopter Angle

SECTION III

STRUCTURAL ANALYSIS

In the final reports for contracts DAAF03-70-C-0076 and DAAF03-71-C-0336, a structural resonance problem was identified which was significantly limiting the design of an inertial damper for the turret. This problem consisted of a 10 Hz resonance in the elevation axis and a 13 Hz resonance in the azimuth axis as determined by laboratory testing of the turret while mounted on the functional test stand. A recommendation was made to the Army to investigate the source of these resonances.

The analysis effort was planned to pinpoint the source of the resonances and recommend a solution for their removal. This was to be accomplished by completing any one or all of the following steps:

1. Develop a structural math model of the functional test stand, considering the turret assembly to be infinitely rigid.

2. Develop a structural math model of the turret assembly, considering the test stand or helicopter mounting interface to be infinitely rigid.

3. Integrate the turret assembly math model with the functional test stand math model and then determine response of the entire system.

The order of the above steps was arrived at essentially due to the analyst's opinion that the functional test stand was not intended to model dynamically the turret/helicopter mounting interface. As a result, the low frequency resonances were thought to be a trait of the test stand and would not be present in an actual turret on the helicopter.

FUNCTIONAL TEST STAND

A structural finite element math model (Figure 10) of the functional test stand (Figure 11) was developed which consisted of 196 nodes, 27 elastic bar members, 39 rigid bar members, 135 triangular plates and 73 quadrilateral plates. The box section frame assembly was considered as steel, while the mount assembly was considered to be aluminum, with a total weight of 467 pounds. Mass was lumped at a total of 37 nodes, giving a total of 114 dynamic degrees of freedom. The turret rotary inertias were included based on WECOM information. The resulting math model consisted of a linear set of 918 algebraic equations with 918 unknowns.

Results indicate a structural resonance of the test stand in the elevation axis at 9.95 Hz (See Figure 12), a resonance in the azimuth axis as 16.2 Hz (See Figure 13), and another elevation axis resonance at 20.1 Hz. This corresponds fairly well with previous test data as illustrated in Table 1.

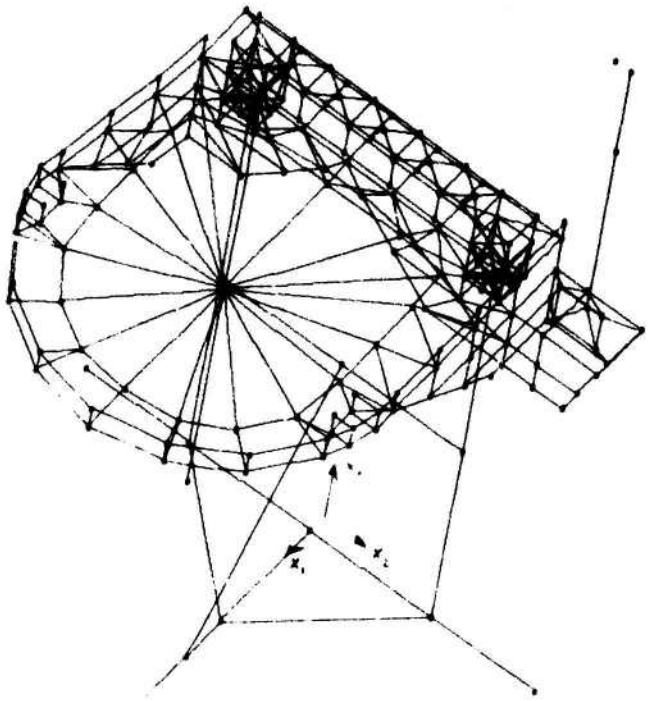

Figure 10. Math Model

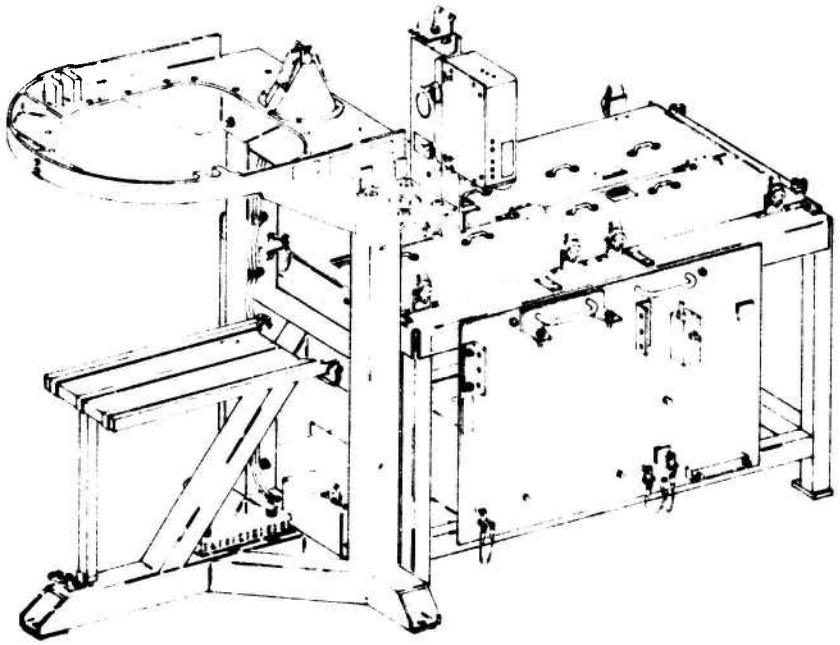

Figure 11.M-28 Functional Test Stand

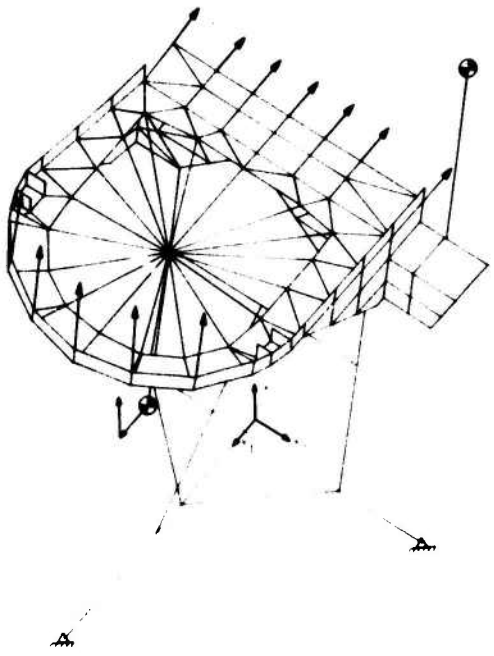

Figure 12. Functional Test Stand, Mode Shape, f_n = 9.95 Hz

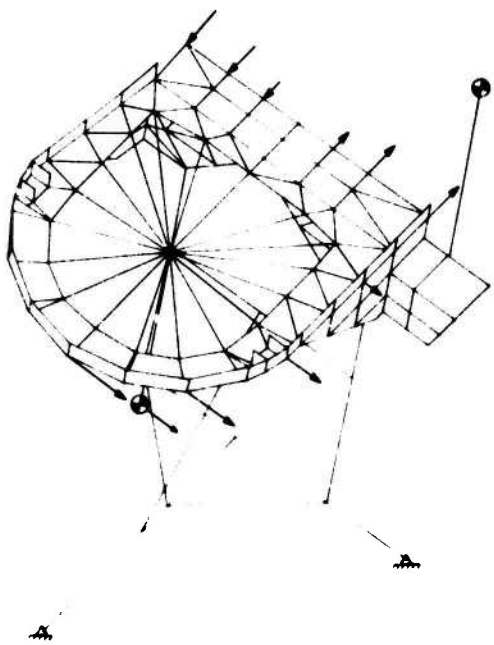

Figure 13. Functional Test Stand, Mode Shape, f_n = 16.2 Hz

TABLE 1. TURRET/TEST STAND RESONANCE FREQUENCIES

AXIS OF	LOWEST FREQUENCY (Hertz)	
PRIMARY RESONANCE	TEST*	ANALYSIS
ELEVATION	10	9.95
AZIMUTH	13	16.2
ELEVATION & AZIMUTH	20	20.1

* Test data taken from data sheets 1 and 7, Reference 2.

At this point, the solution to the resonance problem seemed to indicate stiffening of the test stand. Thus, a steel plate structure was attached from a structural column of the building to the test stand mount assembly (See Figure 14). The math model of the test stand was then modified to include the stiffening assembly. Analytical results indicated that a rather large rise in resonances should be expected, with the minimum occurring in the elevation axis at 33.7 Hz. Test data obtained with the stiffened test stand, however, did not verify so large a frequency shift. The rise in resonances in the elevation axis was from 10 Hz to 15 Hz, and in the azimuth axis from 13 Hz to 15 Hz. This indicates a resonance within the turret in each axis is approximately 15 Hz. Although the resonances at 15 Hz are not apparently in the test stand, it is important to note that by stiffening the test stand the resonances did increase, indicating that the test stand is not a very desirable dynamic test fixture.

TURRET ASSEMBLY

A structural finite element math model of the M-28 gun turret assembly (Figure 15) was developed to investigate the dynamic characteristics of the turret assembly irrespective of the mounting interface (See Figures 16, 17 and 18). This math model consisted of 190 nodes, 133 elastic beam elements, 23 triangular sandwich type plate elements, and 108 quadrilateral plate elements. The entire assembly was considered to be made of steel with a total weight of 266.5 pounds. Mass was distributed throughout the structure and lumped at 30 nodes, giving a total of 93 dynamic degrees of freedom. The rotary inertias and weight of the gun and saddle assemblies were based on WECOM data for an M-129 grenade launcher and an M-134 gun. The resulting math model contained 1013 static degrees of freedom and 93 dynamic degrees of freedom, requiring the solution for 927 linear simultaneous algebraic equations and 93 eigen values.

Results indicate there are five major structural resonances below 500 Hz:

RESONANT FREQUENCY (Hertz)	DESCRIPTION OF RESPONSE
38.9	Rocking motion of turret gun support structure in X_2 axis coupling with rotational motion of turret about X_3 axis (azimuth).

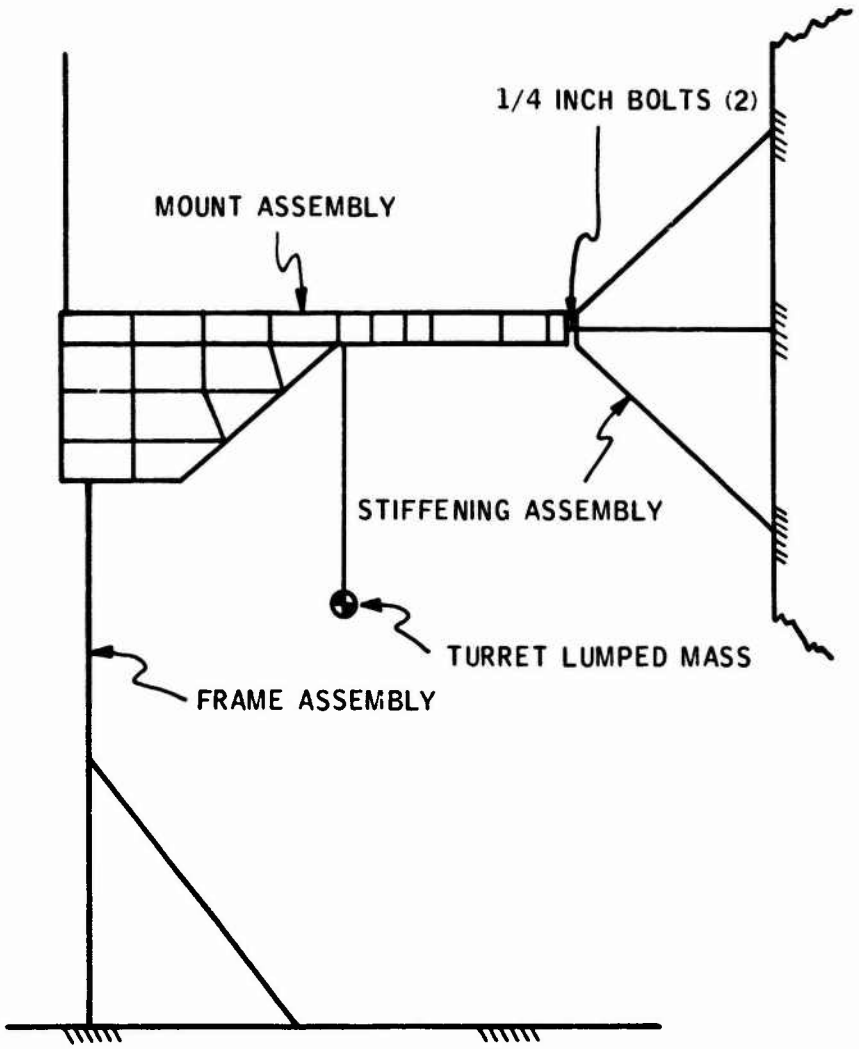

Figure 14. M-28 Stiffened Functional Test Stand

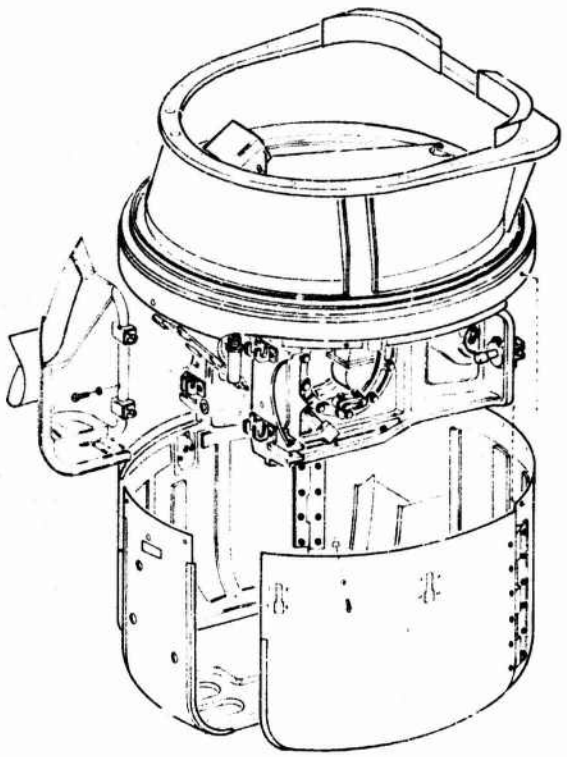

Figure 15. M-28 Turret Primary Structure

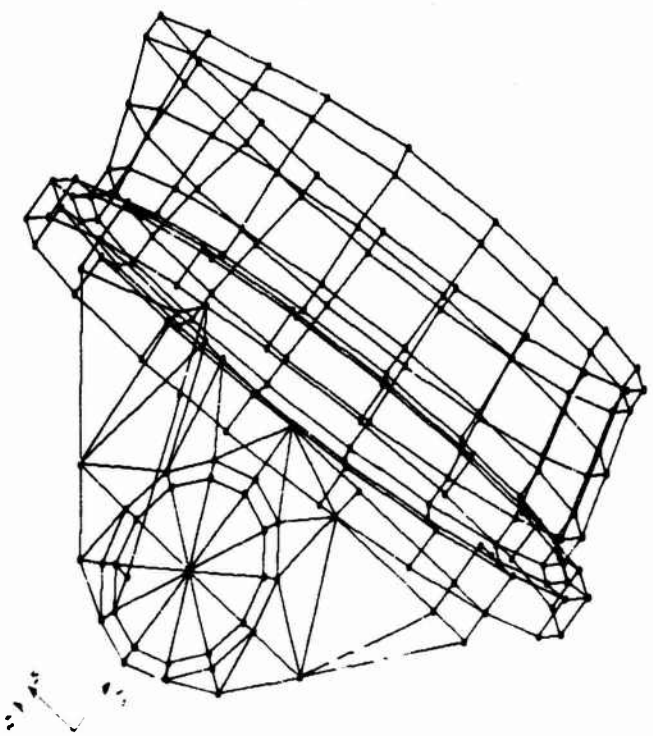

Figure 16. M-28 Turret (X_1)

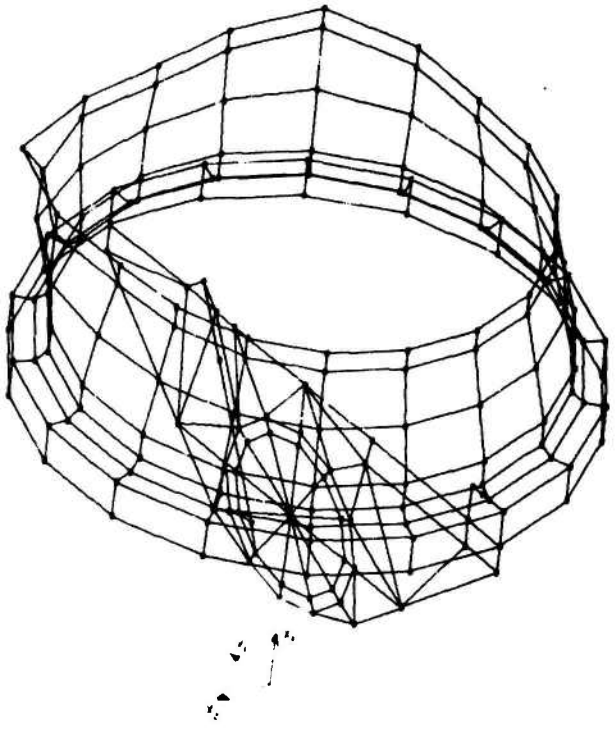

Figure 17. M-28 Turret (X_2)

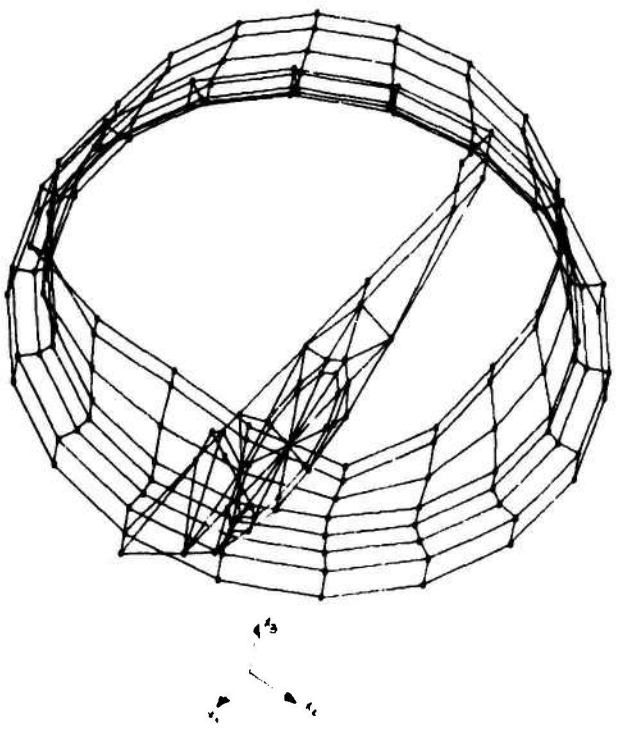

Figure 18. M-28 Turret (X_3)

RESONANT FREQUENCY (Hertz)	DESCRIPTION OF RESPONSE
46.8	Clean rotational motion of gun assembly on bearings in elevation axis due to hydraulic actuator flexibility.
47.8	Clean rotational motion of turret ring and gun assembly on bearings in azimuth axis due to flexibility of gear drive.
81.2	Fore-aft rocking motion of entire turret assembly in the X_1 axis due to flexibility of supporting shell structure.
116.1	Rocking motion of the turret gun assembly in second mode, again coupling with rotational motion in the azimuth axis.

Thus, based on the math model simulation, one would not expect any structural resonances in the turret below 40 Hz when mounted to a fairly rigid interface. The actual AH-1G gun turret mount interface qualifies as a relatively rigid mount based on observations made by Honeywell and ARMCOM personnel at Edwards AFB. Resonance tests were made at Edwards (See Appendix); however, they do not verify the lack of resonances below 40 Hz. They indicate resonances in both elevation and azimuth axes at approximately 17 Hz. These resonances were relatively clean (no cross coupling) and very heavily damped. This leads the analyst to believe that these resonances are in the drive train and correspond to the 47-Hz and 48-Hz resonances in the math model. The basic reason for the mismatch between analysis and testing is due to a poor stiffness choice by the analyst for the drive train.

The drive train stiffness was approximated in the math model rather grossly. This is a result of the complexity of the system. Two critical stiffness terms exist in the math model which totally control the resonances in the drive train. In the elevation axis, the hydraulic actuator is modeled as a beam between two nodes. The axial stiffness of this beam controls the rotation of the gun saddle assembly in the bearing. This stiffness was approximated by a closed cylinder with a piston at the half-way point. Needless to say, this will provide an upper bound to the stiffness since valve leakage and line flexibility has not been included. The azimuth Axis resonance is controlled by the gear train flexibilities coupled with the stiffness of the hydraulic motor. Again, an upper bound was used to approximate the stiffness by assuming the ring drive gear (part 5, Figure 60, Reference 3) to be attached rigidly to the support structure at its base. Thus, it would appear that these stiffness choices were relatively poor and should be modified to reflect the data obtained at Edwards AFB (See Figure 19 for illustration of these assemblies).

Now that the facts are known, the test results can be correlated with the analysis. For example, consider a simple spring mass system, as follows:

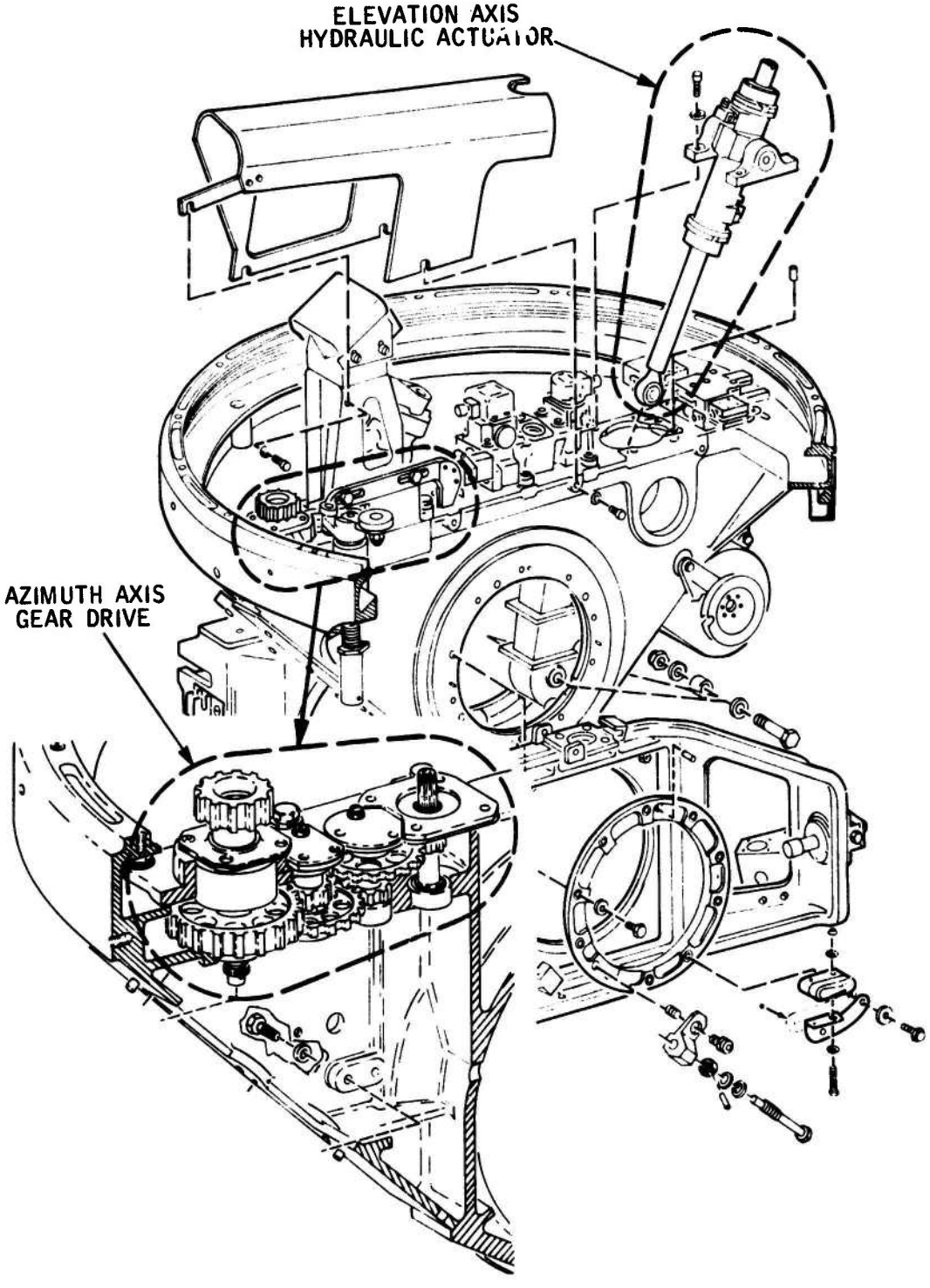

Figure 19. M-28 Turret Drive Assembly

K_s

M_s

K_T

M_T

s - Designates support structure to the turret itself

T - Designates internal turret structure

Since $f_n = \frac{1}{2} \frac{k_n}{M_n}$

and $\frac{1}{f_n^2} = \frac{1}{f_s^2} + \frac{1}{f_T^2}$

A combined resonance for the system can be easily calculated where f_s comes from the math model f_T = 17 Hz and f = test measurements. Following are calculations for the test stand, stiffened test stand, and the helicopter mount.

. Function Test Stand (No Support)

-- Elevation Axis

$$\frac{1}{f_n^2} = \frac{1}{(9.95)^2} + \frac{1}{(17)^2}$$

$$f_n = 8.6 \text{ Hz}$$

-- Azimuth Axis

$$\frac{1}{f_n^2} = \frac{1}{(16.2)^2} + \frac{1}{(17)^2}$$

$$f_n = 11.7 \text{ Hz}$$

. Stiffened Functional Test Stand

-- Elevation Axis

$$\frac{1}{f_n^2} = \frac{1}{(33.7)^2} + \frac{1}{(17)^2}$$

$$f_n = 15.2 \text{ Hz}$$

-- Azimuth Axis

$$\frac{1}{f_n^2} = \frac{1}{(36.8)^2} + \frac{1}{(17)^2}$$

$$f_n = 15.4 \text{ Hz}$$

. Helicopter (AH-1G) Mount

-- Elevation Axis

$$\frac{1}{f_n^2} = \frac{1}{(\infty)^2} + \frac{1}{17^2}$$

$$f_n = 17 \text{ Hz}$$

-- Azimuth Axis

$$\frac{1}{f_n^2} = \frac{1}{(\infty)^2} + \frac{1}{17^2}$$

$$f_n = 17 \text{ Hz}$$

STRUCTURAL ANALYSIS CONCLUSIONS AND RECOMMENDATIONS

. The functional test stand for the M-28 helicopter gun turret is not a stable dynamic test fixture, for it has resonances lower than those in the turret.

. The turret has a resonance at 17 Hz in both the elevation and azimuth axes which is due to the hydraulic fluid compressibility in the elevation axis actuator assembly and the gear train flexibility in the azimuth axis.

. The M-28 gun turret mount interface with a AH-1G helicopter is essentially rigid since it mounts into the primary structure.

. Basic structural resonances of the turret (excluding the drive train) are 40 Hz and above. Thus, current resonance problems can be eliminated by stiffening the drive train without too much risk of higher frequency coupling problems.

. The stiffened functional test stand should give reliable dynamic response data below 15 Hz. If higher frequency inputs are desired, additional stiffening will be required. Note that response will always be a worse case on the test stand than on the actual AH-1G.

SECTION IV

SENSOR CONTROLLER DESIGN

SYSTEM DESCRIPTION

The Fluidic Armament Turret System (FATS) was designed to be a hybrid system using both hydrofluidic and electronic technology. The system schematic is shown in Figure 20.

A heart of the system is the hydrofluidic package which was designed to be mounted in the center of the elevation bearing. This package includes two vortex rate sensors, two hydrofluidic amplifiers, and two transducers. A photo of this package is shown in Figure 21.

The package was designed to put both sensors "on the gun" -- that is, on the turret inner gimbal which holds the guns -- because of the significant reduction in complexity of mechanical and hydraulic hardware. Vortex rate sensors are used mainly because of their inherent ruggedness and reliability. A single fluidic amplifier was added to increase the rate signal and to provide better impedance matching between the sensor and the pressure transducer.

The rest of the system is designed using electronics to allow for ease of modification and because of the significant complexity required. The entire system is shown in Figure 22. It includes the hydraulic power control, the sensor package, and the electronics package.

MECHANIZATION

The system analysis discussed in Section II determined the required gains for the system. As shown in Figure 7 of the system analysis, the gain of 21.2 degrees per second per degree per second was required. In addition, the system includes a 1-second high pass and a 1-second lag. This gain requirement was allocated to the system as shown in Figures 23 and 24. In addition to these gains, the cosine of the elevation angle was also used in the azimuth control. This signal was available from the elevation synchro and was used to vary the gain of a multiplier in the azimuth FATS circuit. The details of this circuit are given in Section V.

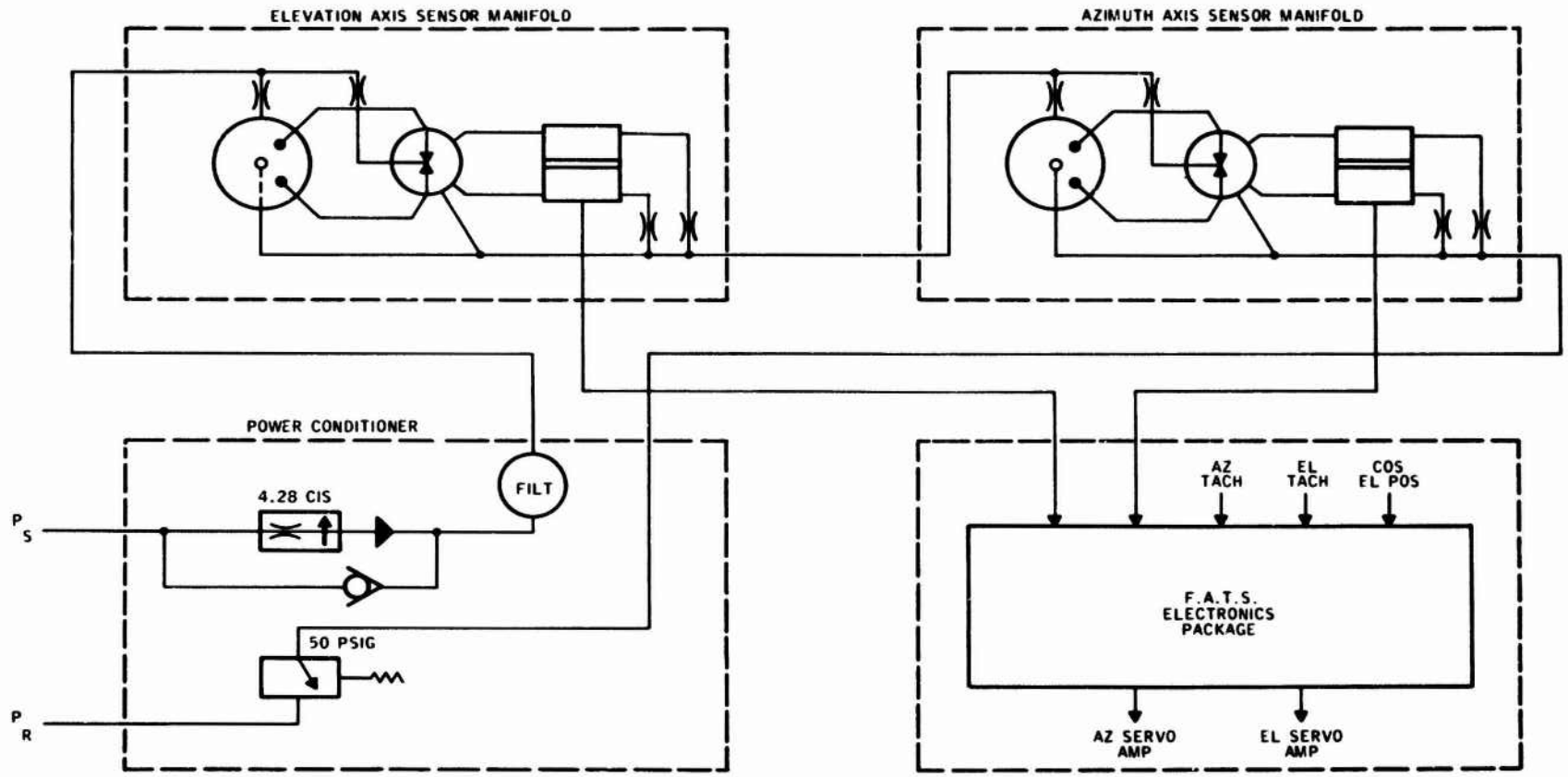

Figure 20. Schematic Diagram of the Fluidic Armament (dwg) XG1144A01 Turret System

Figure 21. FATS Two-Axis Sensor Package

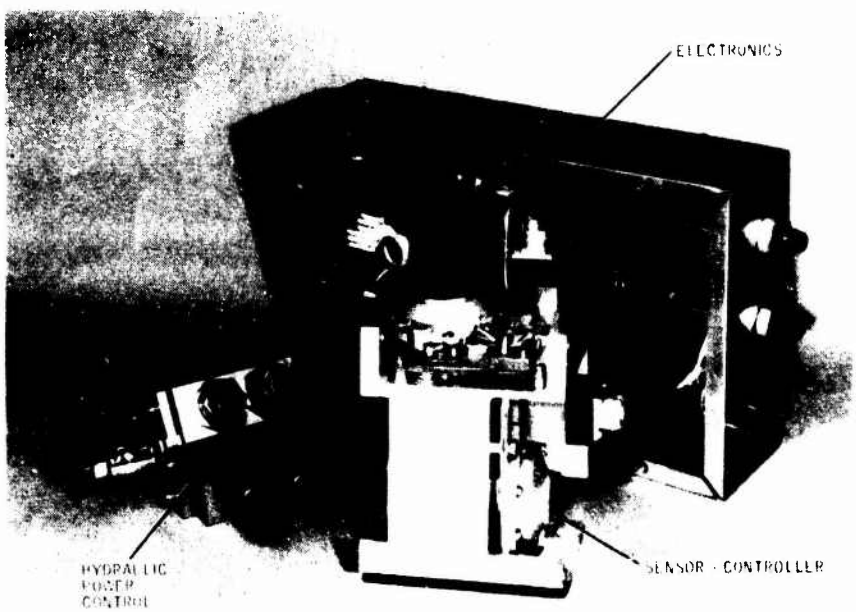

Figure 22. FATS System

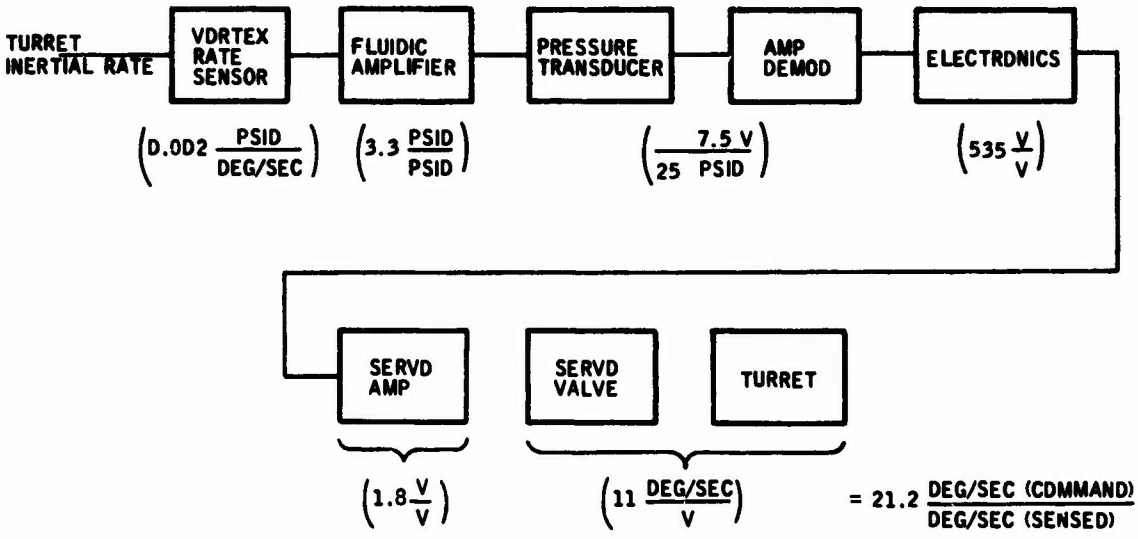

VRS GAIN

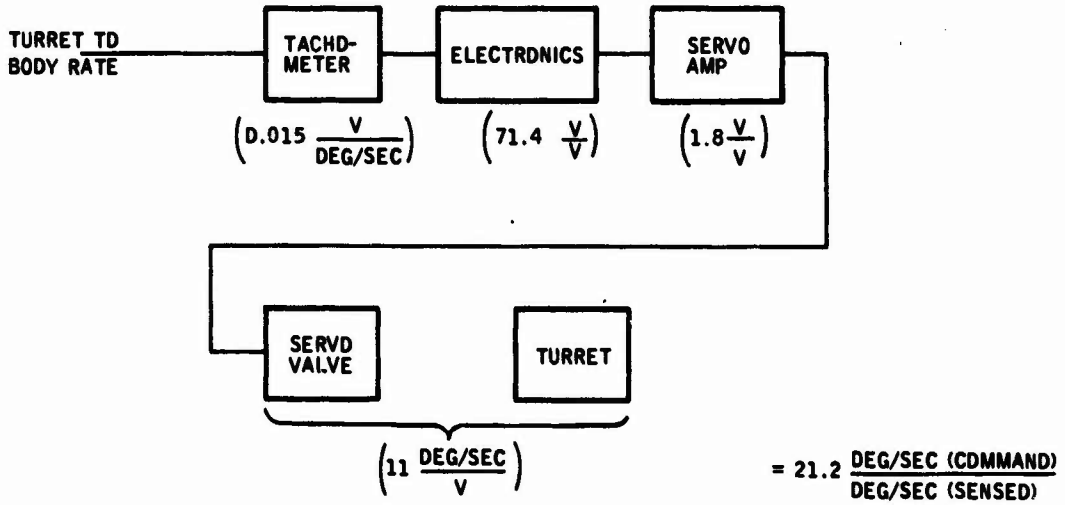

TACHOMETER GAIN

Figure 23. Azimuth Axis Gain Allocations (a) VRS Gain (b) Tachometer Gain

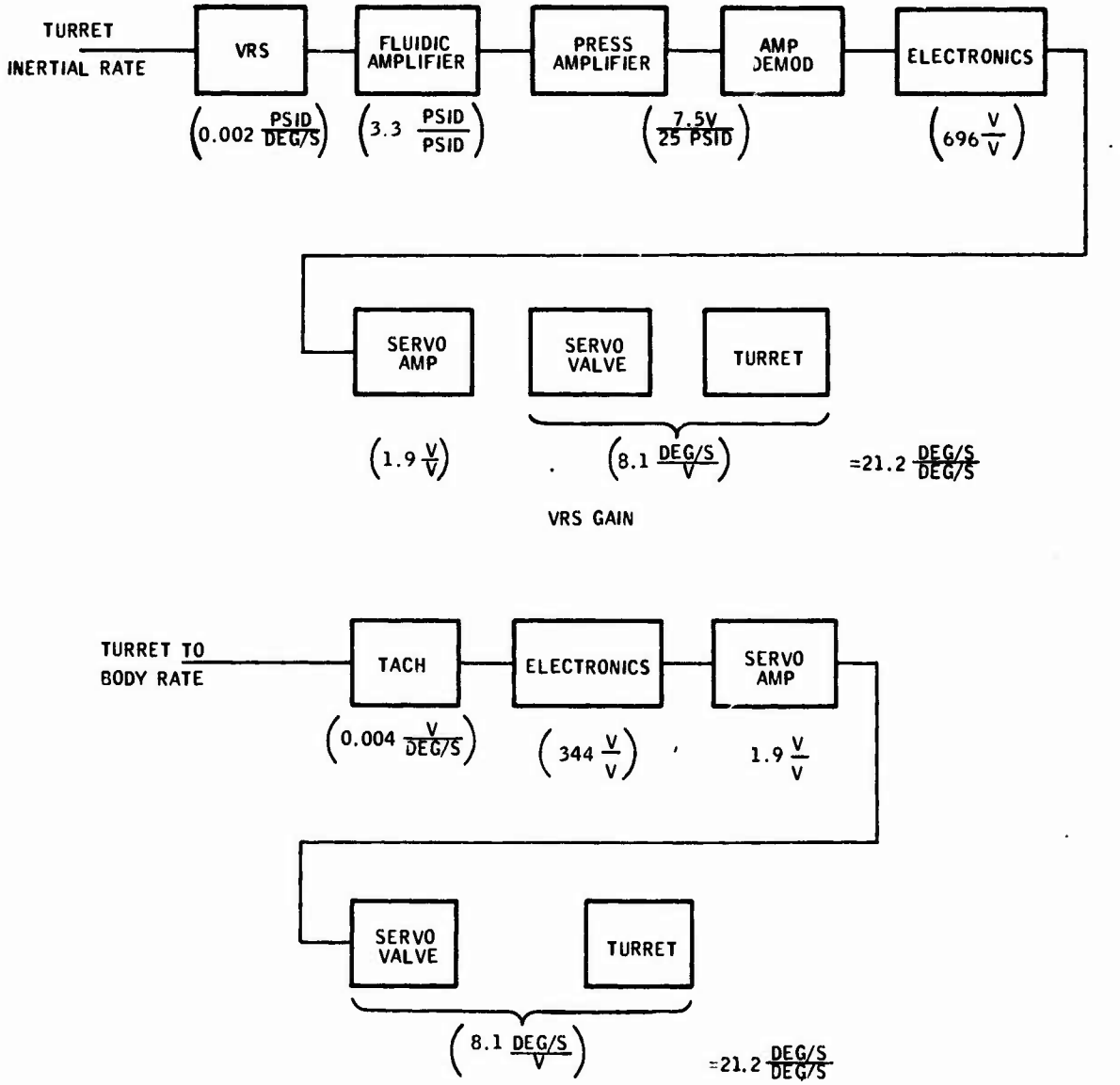

Figure 24. Elevation Axis Gain Allocations (a) VRS Gain (b) Tachometer Gain

SECTION V

COMPONENT DESIGN

The component design was divided into two main efforts: hydrofluidic, and Electronic.

HYDROFLUIDICS COMPONENTS

The hydrofluidics portion of the FATS design is divided into components, which are discussed individually in the following paragraphs.

Rate Sensor Design

The rate sensors for this system are designed around the vortex concept as used in several previous Army contracts, such as DAAF03-72-0021. In this case the sensors (two identical) were designed under the following ground rules:

Flow - 1.0 gal/min.
Scale factor - 0.005 psid/deg/s (loaded into the amplifier)
Response - 0.010 s time delay
Temperature sensitivity - ±30% on scale factor (over oil operating range 60° to 180° F).

These ground rules lead to a basic sensor with dimensions as shown in Figure 25.

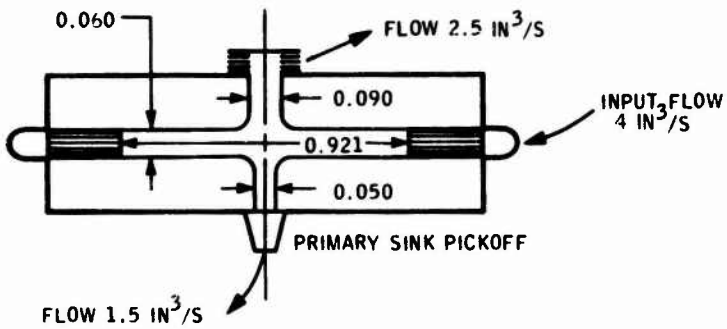

FIGURE 25. Basic Sensor Design Dimensions

The sensor uses about 1.0 gal/min. of hydraulic flow, has a loaded scale factor of 0.005 psid/deg/sec, has a theoretical response delay time of 0.010 and the temperature sensitivity is better than required.

Experience has shown that the theoretical time delay of a sensor is difficult to obtain in hardware if the signal is to be processed in any way, and especially if a large transducer is used to sense the signal (large capacitance).

A rate sensor with the type pickoff used in this case has an output impedance of approximately 400 psi/in^3/s. With a transducer capacitance (of 0.000012 in^3/psi) as shown in the following calculation, a first order lag with a time constant of 0.010 sec and results.

$$T = 400 \frac{\text{psi}}{\text{in}^3/\text{s}} \quad (2) \quad \left(0.00001 \frac{\text{in}^3}{\text{psi}}\right) = 0.010 \text{ s}$$

For this reason it was decided to use a fluidic amplifier to amplify the signal (power) and effectively reduce the sensor output impedance (transducer now sees the 60 ohms output impedance of the amplifier).

$$\frac{E_{out}}{\text{Rate in}} = \left(\frac{1}{1 + 0.002S}\right)\left(e^{-0.015S}\right)$$

The resulting response of the rate sensor, amplifier, and transducer combination can be approximated by the above transfer function as determined imperically.

This response time, therefore, would not quite satisfy the 0.010-s time delay requirement. To increase the sensor response, a new coupling element was developed that changes the sensor response such that it is best approximated by a lag lead. Figure 26 shows the configuration that was first tested.

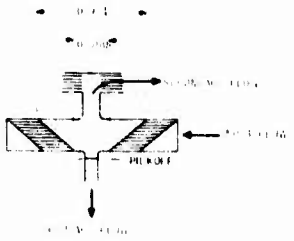

FIGURE 26. Lag-Lead Coupling Element

This configuration resulted in response characteristics that were better than required, but at the sacrifice of scale factor. The approximate transfer function, as determined by experiment, is:

$$\frac{E_{out}}{\text{Rate in}} = \left(\frac{1}{1+0.005S}\right)\left(\frac{1}{1+0.002}\right)$$

sensor transducer

As a result the final configuration was determined to be a compromise of the first two, as shown in Figure 27.

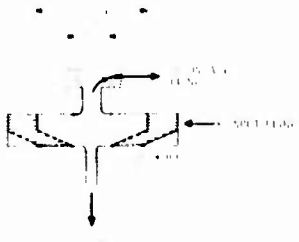

FIGURE 27. Final Coupling Design

Figure 28 shows the rate sensor disassembled in an exploded view.

An approximate transfer function for this device as determined empirically is:

$$\frac{E_{out}}{Rate_{in}} = e^{-.010S} \quad \frac{1}{1 + 0.002S}$$

Figure 29 shows a sensor manifold with a transducer and a hydrofluidic amplifier assembled. The rate sensor has been removed and partly disassembled to show the coupling elements and the two flow sinks. See Figure 29.

Hydrofluidic Amplifier Design

No new amplifier designs were studied as a part of this program. Several amplifiers which had already been developed were considered for this application. The main purpose of an amplifier in this application is to improve the match of the impedance of a vortex rate sensor to a transducer. Amplifiers of different sizes were considered, as well as amplifiers with restricted inputs to raise the input impedance. The final choice was made based on tests of these various configurations, and the amplifier to be used is one with a 0.025-by/0.025-inch power port and corresponding output legs, but with 0.010-by-0.025 inch control ports. This provided higher input impednace and therefore raised the effective pressure gain of the rate sensor (draws less flow) while having lower output impedance to reduce the RC time constant of the transducer input. With this amplifier, the noise-to-gain ratio at the output of the transducer amplifier-demodulator was also less than with any other configuration. See Figure 25.

Sensor Manifold Design

The manifolds used in each axis were fabricated using the electroformed conductive wax process. This process starts with a stainless baseplate and, using a mold, conductive wax paths are laid on the surface of the baseplate. Finally it is nickel plated and the wax removed leaving connecting paths between components. See Figure 29.

Transducer Design

The plan for this program called for an off-the-shelf transducer. The Celesco variable reluctance transducer (model P21D-25; see Figure 29) was chosen as the best available to meet the very stringent requirements. The following ground rules were established:

- Differential tranducer (oil both sides)
- Self bleeding
- Capacitance less than 0.00003 in^3/psi
- Capable of 1500 psi operating levels
- Minimal temperature shifts
- Maximum scale factor

There was no real competition with Celesco, except for two companies who make almost identical units. Because we had previous experience with Celesco, their transducer was chosen. To minimize capacitance (minimize diaphram deflection), a ±25 psi unit was used in each axis.

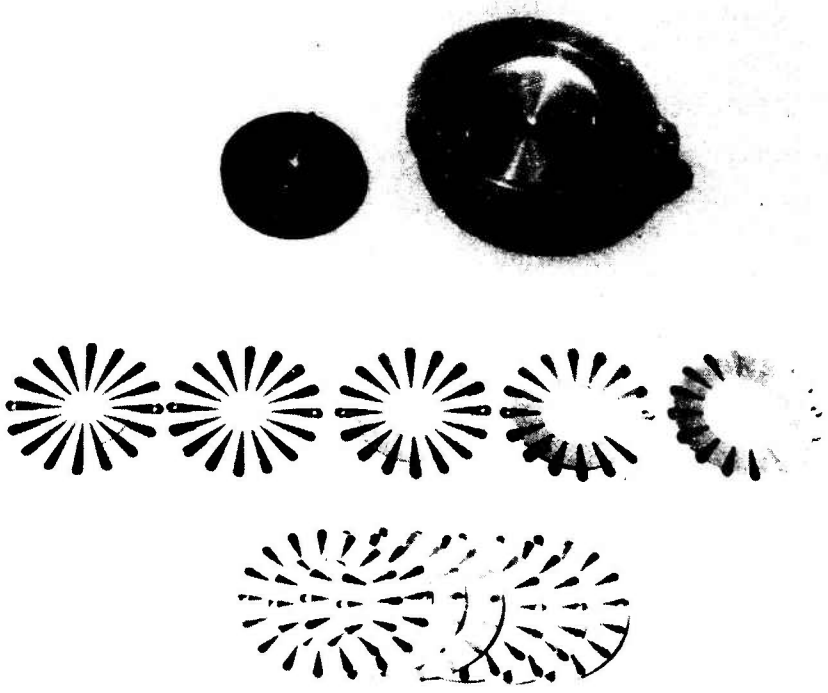

Figure 28. Rate Sensor

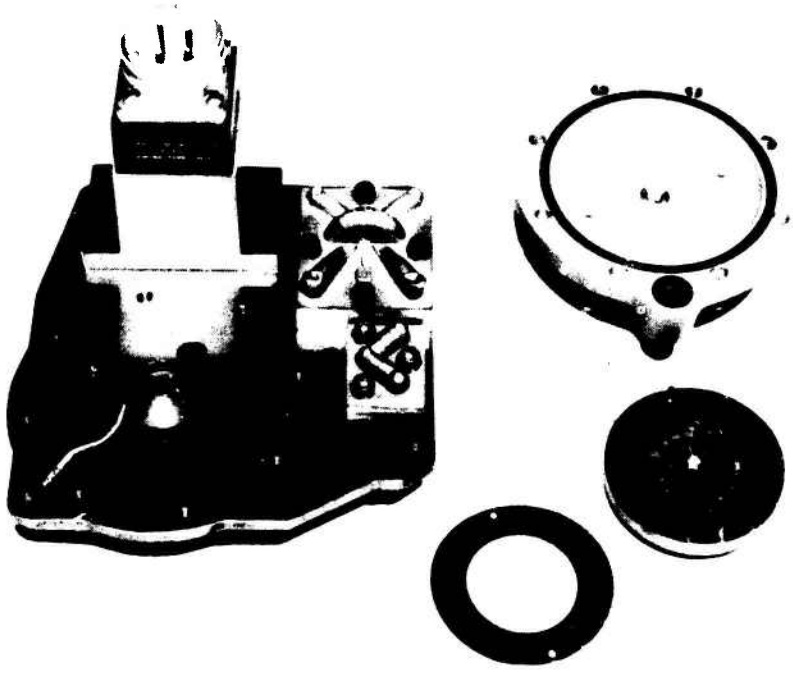

Figure 29. Rate Sensor, Amplifier, Transducer, and Manifold Assembly

A solid state differential transducer would have a big advantage in size, response, and price; but they are not presently available.

Flow Distribution Manifold

This manifold was machined from aluminum and given an anodized finish. This block was mounted in the turret inner gimbal and served as the mounting place and flow source for the sensor manifolds of each axis (see Figure 21).

Hydraulic Power Control

This device includes an aluminum machined housing with a flow control and back pressure regulator installed (Figure 22). The unit was designed to replace a similar porting block on the turret, but with the addition of the two valves. The flow control valve is a standard industrial grade device purchased from Waterman Hydraulics (Model No. 3912-1.00), and the back pressure regulator consists of the inner parts of a standard device available from Tescom Corp.

FATS ELECTRONICS

The FATS electronics package contains two channels of electronic control functions for azimuth and elevation control of a helicopter gun turret. It is designed to operate from +28 Vdc and -28 Vdc power obtained from the M28A1 turret control system. The inputs to the control channels consist of the following signals:

Azimuth Axis

- Azimuth rate which is generated in a turret mounted hydrofluidic vortex rate sensor and converted to an electrical signal in a differential pressure transducer.
- Azimuth tachometer which is a dc electrical signal from a turret driven tachometer.
- Cosine of elevation angle which is a 400-Hz signal from the elevation resolver in a M28A1 turret control system.

Elevation Axis

- Elevation rate which is generated in a similar manner as azimuth rate.
- Elevation tachometer which is a dc electrical signal from a turret driven tachometer.

The pressure transducers in the vortex rate sensor assembly are energized from individual carrier demodulator units located in the FATS electronic package. The carrier demodulators operate from +28 Vdc and generate a 5-kHz excitation voltage for the variable reluctance pickoff in the pressure transducer. Signals produced by the pressure transducer are then amplified and demodulated in the carrier demodulator. Because of the excellent signal-to-noise ratio in the variable reluctance transducers, high gain in the electronic channels is possible to achieve the required output voltage levels for controlling the turret system without excessive noise.

The functional diagram of the FATS electronics is shown in Figure 30 as the electronics functions were originally built. In the elevation axis the rate sensor signal from the carrier demodulator is summed with the elevation tachometer signal into an op-amp. Signal shaping is provided in a 1-second high pass and a 1-second lag circuit. A gain control is provided at the input to the final op-amp. Switching at the output allows for changing from the normal to the stabilization modes of operation.

In the azimuth axis the rate sensor signal from the carrier demodulator is amplified and fed into a divider circuit on the Z input where the divider function is $\frac{10Z}{X}$. The X input is the demodulated cosine function of the elevation angle obtained from the elevation resolver. The multiplier output is high passed and summed with the high passed azimuth tachometer signal. Additional signal shaping is provided by a 1-second lag. Gain adjust and switching functions are provided as in the elevation axis.

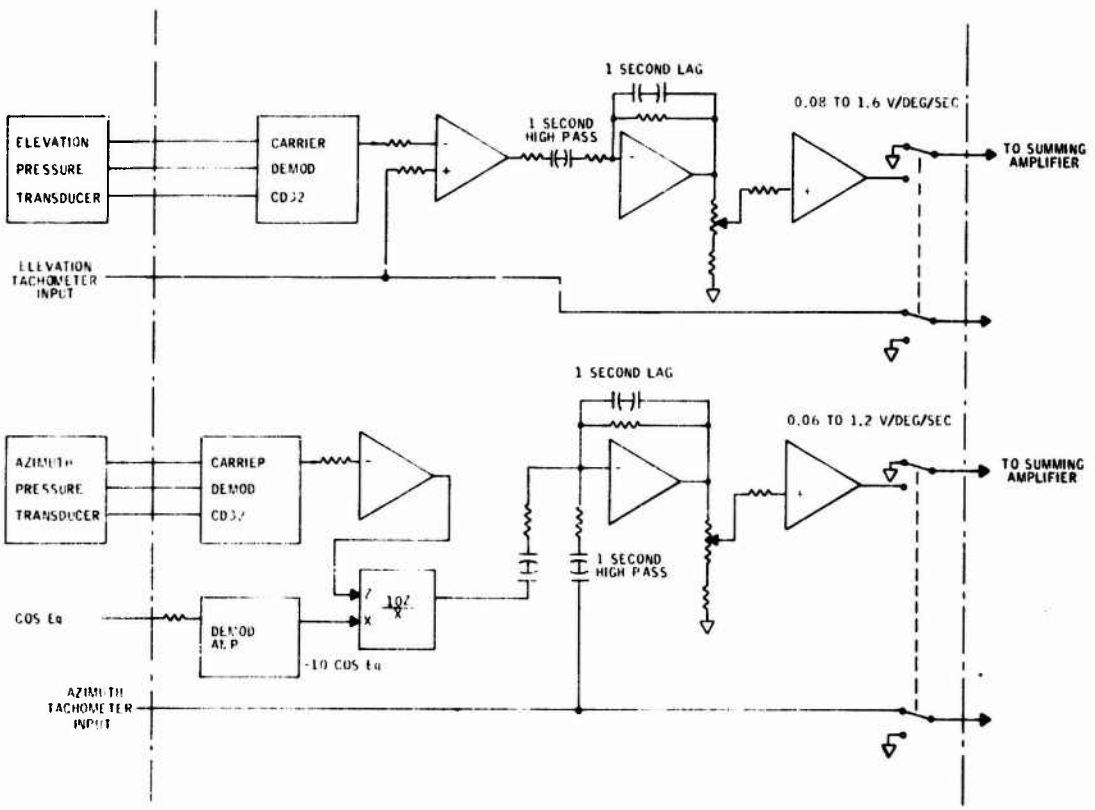

Figure 30. Original FATS Electronics Functional Diagram

SECTION VI

COMPONENT AND SYSTEM TESTS

COMPONENT DEVELOPMENT TESTS

Developmental tests on the hardware were limited mostly to tests on various rate sensor, amplifier, and transducer combinations. As discussed in the design section, a vortex rate sensor with a 0.010-second transport delay was designed and built. This basic sensor had a deadended gain of 0.010 psid/deg/s and a loaded gain of 0.005 psid/deg/s. The response characteristics are shown in Figure 31. This response curve shows the effects of the RC lag caused by the transducer. Where a 0.010-s sensor should have 90 degrees of phase lag at 25 Hz, this sensor shows 90 degrees of phase lag at 17 Hz.

Figure 32 shows the response of the lag lead sensor described in the design section. This curve shows a 90-degree phase lag at 50 Hz with some rolloff in amplitude. The gain was 0.002 psid/deg/s deadended.

These results indicate a sensor that was faster than required, but the gain was down by a factor of five.

The final sensor design used a combination coupling element (part lag-lead and part transport delay). The gain was now 0.005 psid/deg/s deadended, and the response was as shown in Figure 33. This curve shows about 90-degree phase lag at 25 Hz.

During the experiments run above on various coupling elements, it was also noted that the signal-to-noise ratio decreased when the gain decreased. So a tradeoff is indicated between response-and-gain, or signal-to-noise ratio. The final experiments run on the FATS sensing system were on the use of various amplifiers between the rate sensor and the transducer. Four general concepts were listed. First, a small 0.015-by 0.015-inch power nozzle amplifier with 0.015-by 0.015-inch control ports (10047850-101); then a standard 0.025-by 0.025-inch amplifier, with 0.025-by 0.025-inch control ports (10047850-103); a 0.025-by 0.025-inch amplifier with orifices in front of each control port; and finally, a 0.025-by 0.025-inch amplifier (10047850-102) with small 0.010-by 0.025-inch control ports. The selected amplifier provided a pressure gain of 3.3 at 120°F oil temperature.

The first configuration gave good performance in all ways, but its output impedance was too high, resulting in poor frequency response. The second and third had good response, and lower signal-to-noise ratio. The last configuration had good response and the best signal-to-noise ratio.

HARDWARE BUILD AND TEST

The electronics package was built and tested for functional operation prior to tying the rate sensor inputs to the carrier demodulators. A gain increase was made in the electronics channels to compensate for the lower than anticipated output from the vortex rate sensors.

After installation in the helicopter, the ground checkout of the system revealed several problems which were corrected. The first was the correction of tachometer phasing, and the second was the need for additional gain. The third was the summing of the azimuth rate and azimuth tachometer signals after the high pass functions. In the original mechanization, the

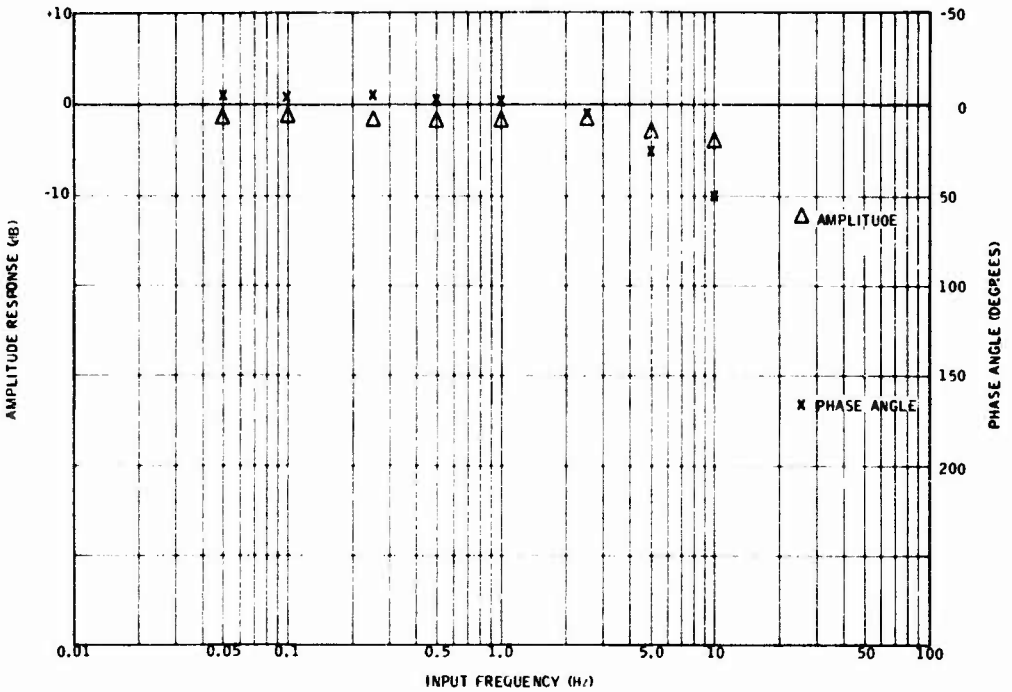

Figure 31. Frequency Response FATS Pickoff #2, Regulator Elements

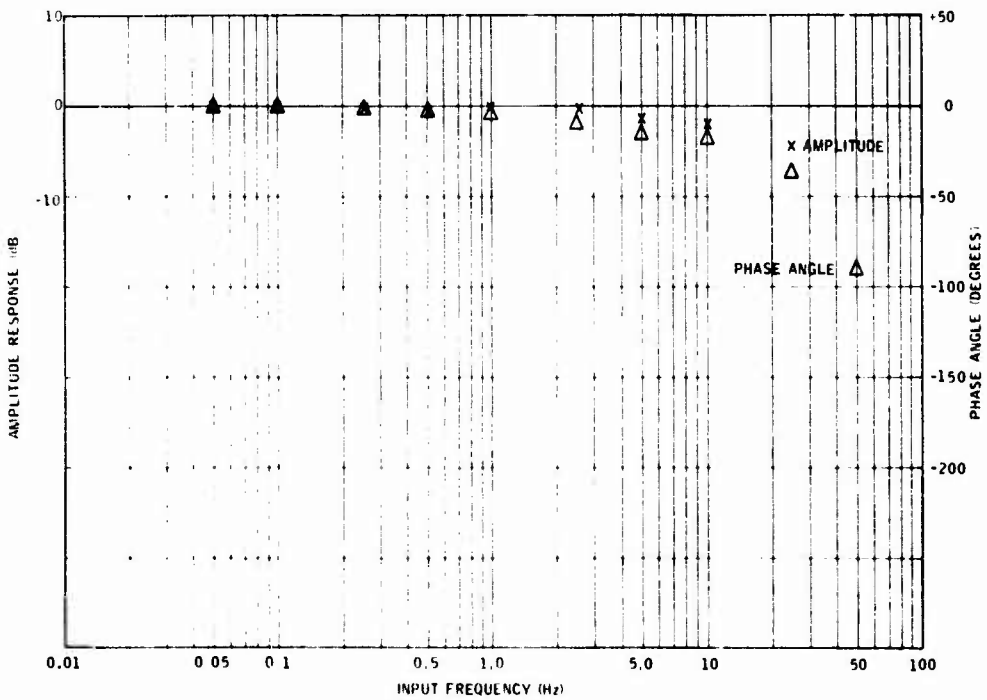

Figure 32. D.E. FATS Pickoff #2, T=120°F, Lag-Lead Coupling Elements

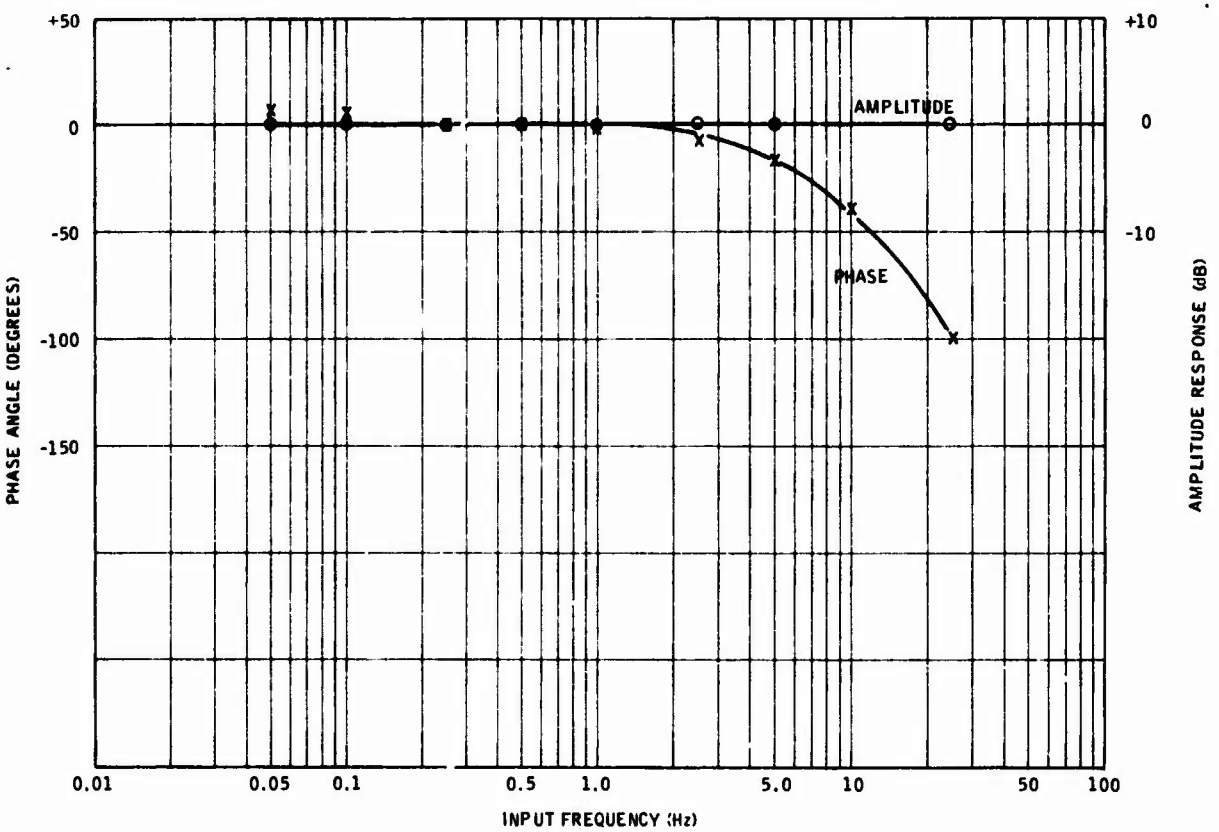

Figure 33. Final Design Frequency Response, Elevation Axis (T=120°F)

high-pass constants were set to be within approximately 3% of each other. Because the rate and tachometer signals are cancelling, a small difference in time constant produced instability. An additional op-amp was added to the azimuth channel to allow summing the rate and tachometer signals ahead of a common high-pass. See Figure 34.

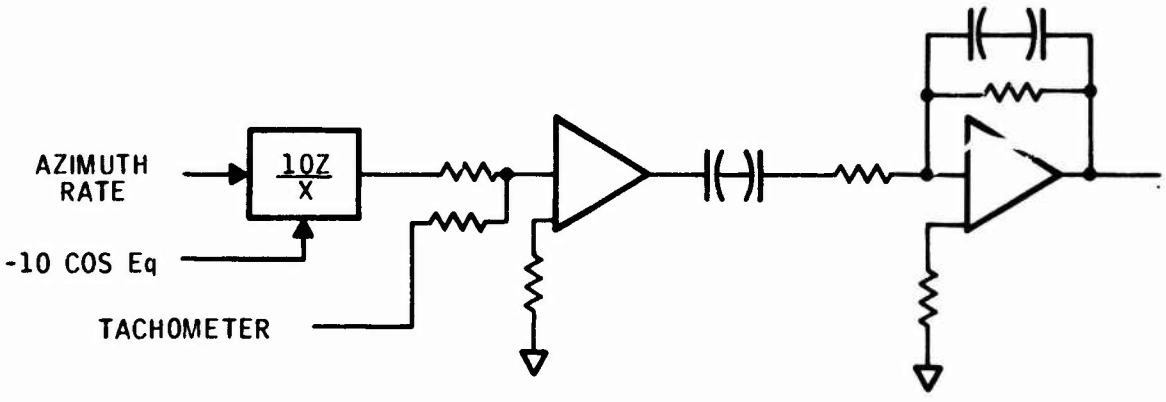

FIGURE 34. Azimuth Channel Summing Change

To balance the tachometer and rate sensor signals more closely, gain adjustments were added to the tachometer input. The gain was adjusted by driving the turret manually and nulling the difference signal at the output of the summing amplifier with the tachometer gain adjust.

To provide for flight records of the rate sensor output without loading the circuit with the recorder, isolation amplifiers were added to the electronics package for recording outputs. The functional block diagram in Figure 35 shows the final configuration.

FLIGHTWORTHINESS TEST

System flightworthiness tests were conducted on the hydrofluidic section of the system. Test requirements were set up to establish performance limits under various environmental conditions. These limits are described in the following paragraphs.

Requirements for Performance Tests

Scale Factor - The scale factor of each axis shall be determined using an x-y plotter. The plotter shall be calibrated in volts versus rate, in degrees per second. The amplifier demodulator shall be calibrated for a scale factor of greater than 0.00125 V/deg/s. The actual recording shall be retained for inclusion in the report.

Output Noise - The output noise of each axis shall be determined by estimating the peak-to-peak noise observed in the x-y plot taken in par 1.1. Noise shall be less than 1.5/s peak-to-peak.

Range and Linearity - The linear output range of each axis shall be greater than ±30 deg/s. Within this range the actual curve of par 1.1 shall be within 5% of full scale from the best straight line.

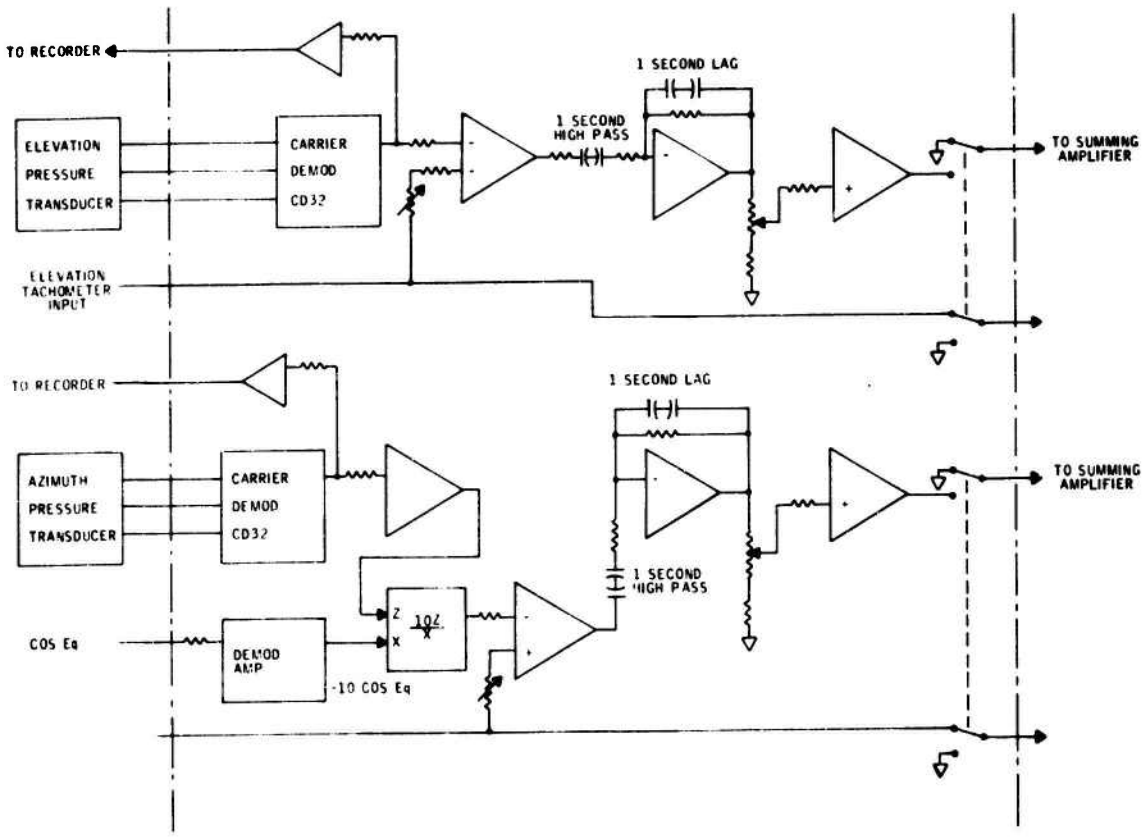

Figure 35. Final FATS Electronics Functional Diagram

Null Offset - With the amplifier demodulator null set, the range of null shift over the full temperature range shall be within ±0.4 V.

Phasing - Clockwise rotation of each axis shall provide a positive voltage output from the system demodulators. Clockwise rotation shall be determined when looking at the top of each rate sensor.

Cross Coupling - When rotating the system about either axis the output of the other axis shall be less than 2% of the first axis.

Response - The amplitude response relative to the dc scale factor shall be less than +2 dB and greater than -2 dB for frequencies up to 16 Hz. From 16 Hz to 25 Hz the amplitude ratio shall be between +1 dB and -4 dB.

The phase lag shall be less than 45° at 9 Hz and less than 90° at 18 Hz.

A curve of the frequency response between 0.1 Hz and 25 Hz shall be plotted and retained for the report.

Requirements for Environmental Tests

Temperature - The system performance tests of Par 1.0 shall be run before, during, and after exposure of the system to three oil temperatures of 60°F, 120°F, and 180°F.

All performance tests are to meet the requirements of par 1.0 except the scale factor of 60°F must be greater than 0.0006V/deg/s and the noise at 180°F must be less than 3/deg/s peak-to-peak.

Vibration - The system shall be subjected to the performance tests of par 1.0 before and after the following vibration test and normal flow will be maintained during vibration.

A vibration scan of 5-500-5 Hz shall be made over a period of 15 minutes in each of three mutually perpendicular axes. The level from 5 to 20 Hz shall be 0.1 in double amplitude, and from 20 to 500 Hz, 2.0 g.

All resonant points shall be noted and corrective action will be required along with a retest for any resonances below 25 Hz.

The system shall have no output greater than ±1/deg/s during the vibration test with the exception of noise at frequencies above 25 Hz.

Test Results

The system was set up for all flightworthiness tests using the FATS system hydraulic power control and the system amplifier demodulators. The hydrofluidic and hydraulic components were exposed to the environments in each case.

Performance tests were run on the system before, during, and after each temperature test, and also before and after the vibration test. During vibration the output of each axis was monitored with no angular rate inputs, and no outputs were observed.

The performance of the hydrofluidics package met all of the stated requirements with only one exception. This involved noise in the elevation axis at 180°F; 10 deg/sec peak-to-peak at 180°F oil temperature, with a requirement for less than 3 deg/sec. This high noise level only occurs above 170°F and therefore should not affect the performance of the turret in the aircraft during the performance evaluation.

Typical data at 120°F are shown in Figures 36 through 39. Table 2 summarizes the more significant data at various temperature and for post vibration testing.

TABLE 2. SUMMARY OF FLIGHTWORTHINESS TEST DATA

Test Condition	Scale Factor V/deg/s		Null (volts)		Noise (deg/s peak-to-peak)		Response Phase Angle at 18 Hz (degrees)	
	El	Az	El	Az	El	Az	El	Az
60°F	0.0007	0.0006	-0.15	+0.22	0.85	1.0	-66	-64
120°F	0.0014	0.0013	+0.02	-0.2	0.70	0.75	-72	-60
180°F	0.0015	0.0015	+0.35	-0.3	10.0	2.0	-73	-70
120°F Post Vibration	0.0020	0.0016	-0.625	+0.02	1.2	0.3	-78	-75

SYSTEM TESTS

Frequency response and gain of the complete FATS system (including electronics) were determined just prior to installation on the aircraft and turret. This curve, Figure 40, shows the system response to be very near to the theoretical calculations, with the addition of improved phase characteristics in the mid-frequency range. The gains were set at the required values for each axis with the system at 120°F. These gains were 1.06 V/deg/s azimuth and 1.37 V/deg/s elevation.

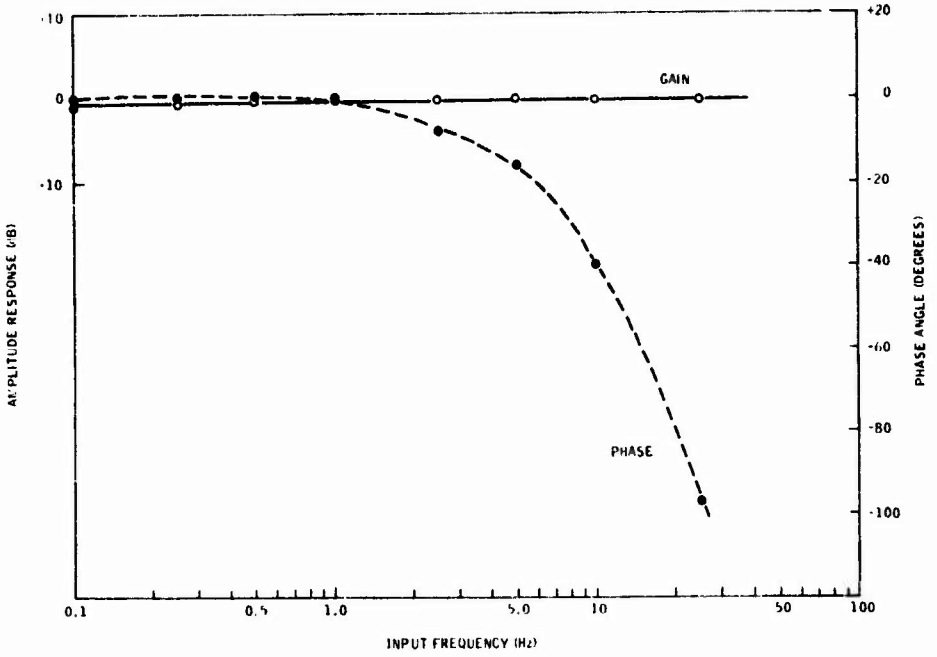

Figure 36. Response, Elevation Axis, T=120°F

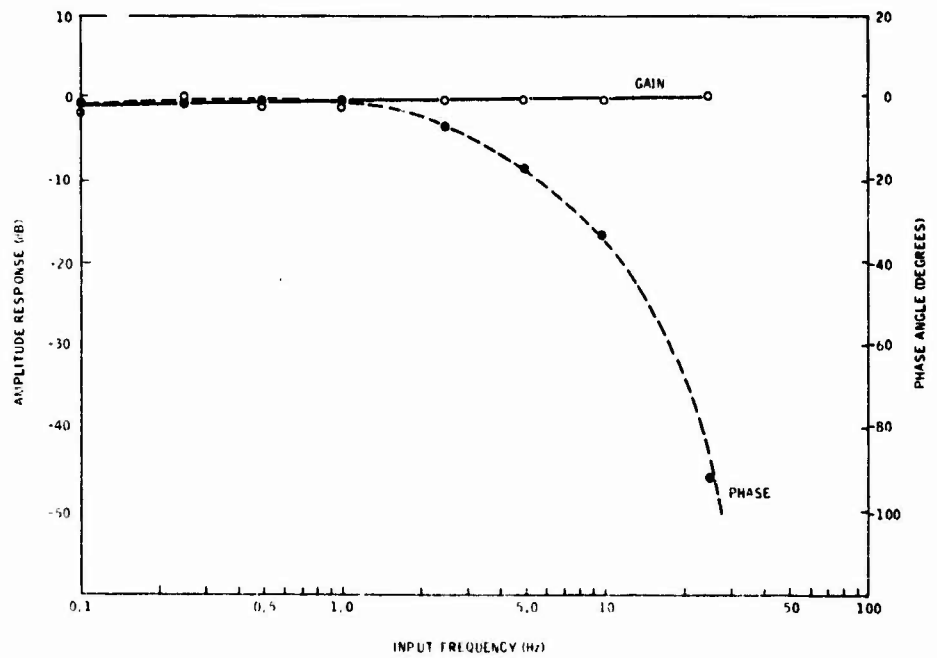

Figure 37. Response, Azimuth Axis, T=120°F

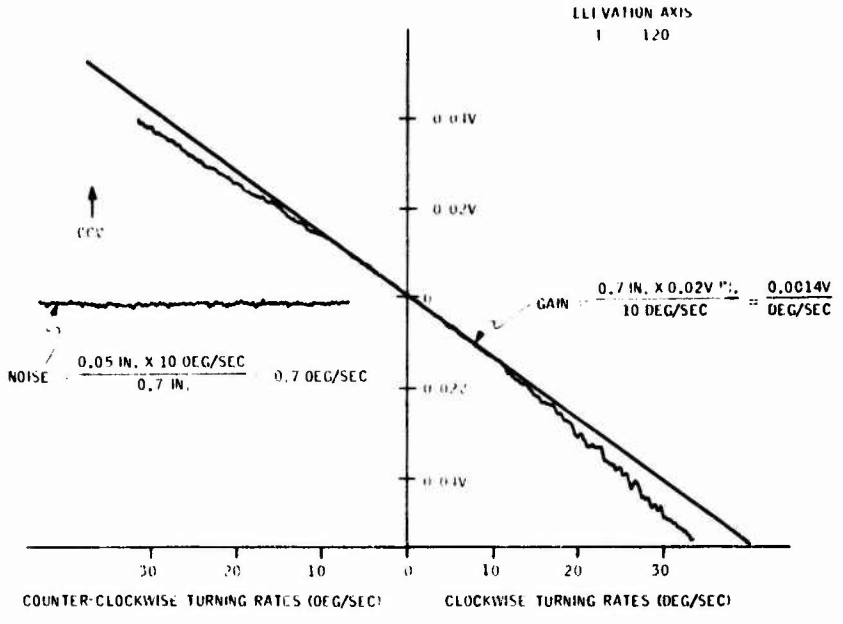

Figure 38. Gain, Elevation Axis, T=120°F

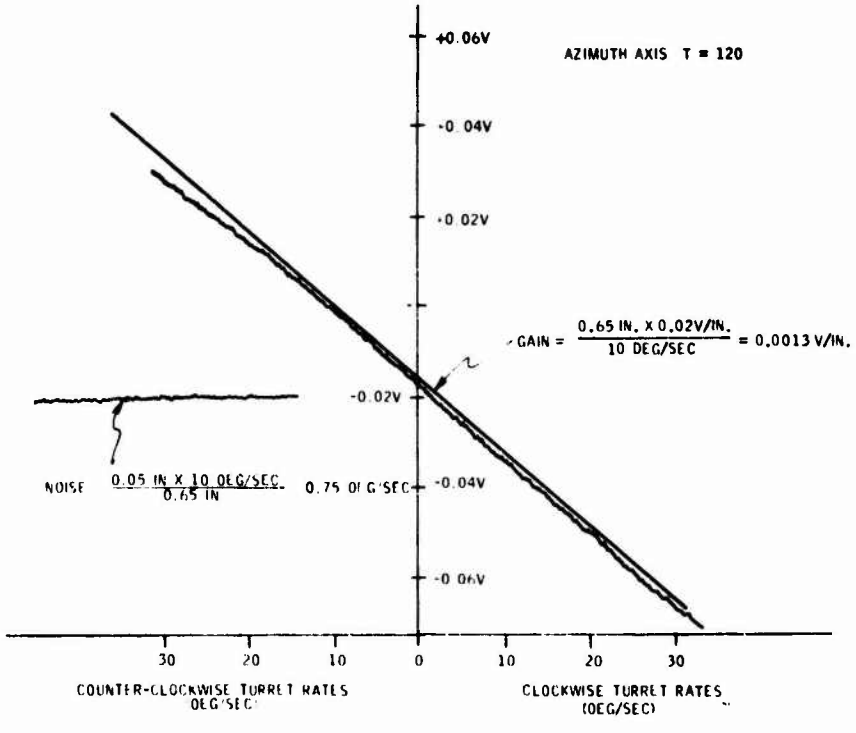

Figure 39. Gain, Azimuth Axis, T=120°F

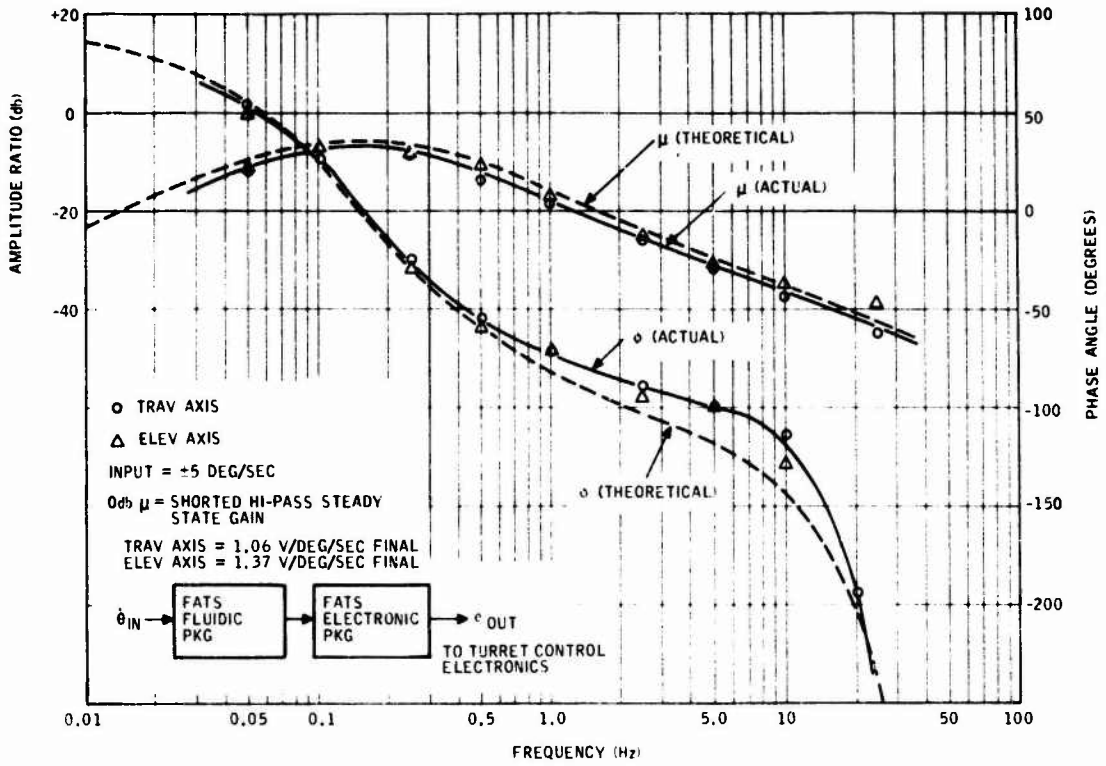

Figure 40. FATS System Response and Gain Prior To Firing Tests

SECTION VII

AIRCRAFT MOUNTED SYSTEM TESTING

The FATS was installed on the AH-1G, SN 69-16441, at the Honeywell Minneapolis flight operations. Testing consisted of (1) Frequency response of the complete M-28 Armament System, (2) Airborne stabilization with and without gun firing, and (3) Ground firing tests. All firing testing was conducted at the Honeywell Proving Grounds, located north-east of Elk River, Minnesota. This section describes this effort and presents analysis of the test results.

INSTALLATION

Figure 41 illustrates the M-28 turret location on the AH-1G helicopter. The FATS Fluidic Sensor Package located in a space just forward of the gunners cockpit. Figure 42 shows the FATS Fluidic Package. It is seen that it is shaped to fit within the turret elevation gimbal (see Figure 43). The fluidic package was powered by the turret hydraulic system pressure and required a flow control valve and back pressure regulator for proper hydraulic power conditioning. The standard turret hydraulic manifold (see Figure 43) was replaced with a special manifold containing the power conditioning apparatus so that hydraulic hose connections could be made from the supply manifold to the fluidic package and still retain the standard turret hydraulic power plumbing connections. The AH-1G Helicopter came in equipped with an M28E1 Armament System. In this system, the elevation gimbal was configured with ribs on the inner portion of the gimbal. The FATS fluidic package, however, had been configured to fit the gimbal on an M28A1 turret which had no ribs. To facilitate installation of the FATS fluidic package it was necessary to exchange the M28E1 turret for an M28A1 turret. Figure 44 shows the fluidic package installed within the turret elevation gimbal.

Since the weapons on hand went with the M28A1 Armament System, it was necessary to exchange the M28E1 Weapon Controllers (see Figure 41) for M28A1 Weapon Controllers. The weapon system was checked out by dry cycling the weapons to verify that all safety circuits, etc., were operational.

The necessary test instrumentation (gyros to measure aircraft rates and a recorder) was installed on a wooden panel and was mounted in the ammunition bay (in the fuselage aft of the turret) in place of the ammunition containers (Figures 41 and 45). Since limited firing was to be done, partially filled ammunition belts were adequate for firing tests.

TURRET FREQUENCY RESPONSE TO ELECTRICAL INPUTS - GROUND CHECKS

Allowing installation, frequency response measurements were made on the stabilized turret using airborn recording instruments to verify performance. Major results are shown in Figures 46 through 48.

Figures 46 and 47 show the responses to simulated sight inputs for elevation and azimuth respectively. The test points are compared to theoretical response curves. The data verifies that adequate turret response to sight inputs is maintained with the added stabilization feedback and that no undesirable closed-loop resonances are generated. The major deviation between the test data and the theory occurs between 1.6 and 15.6 Hertz. Most of this deviation is attributed to gain mismatch between the tach and the vortex rate sensor (VRS). The test data comes closer to the

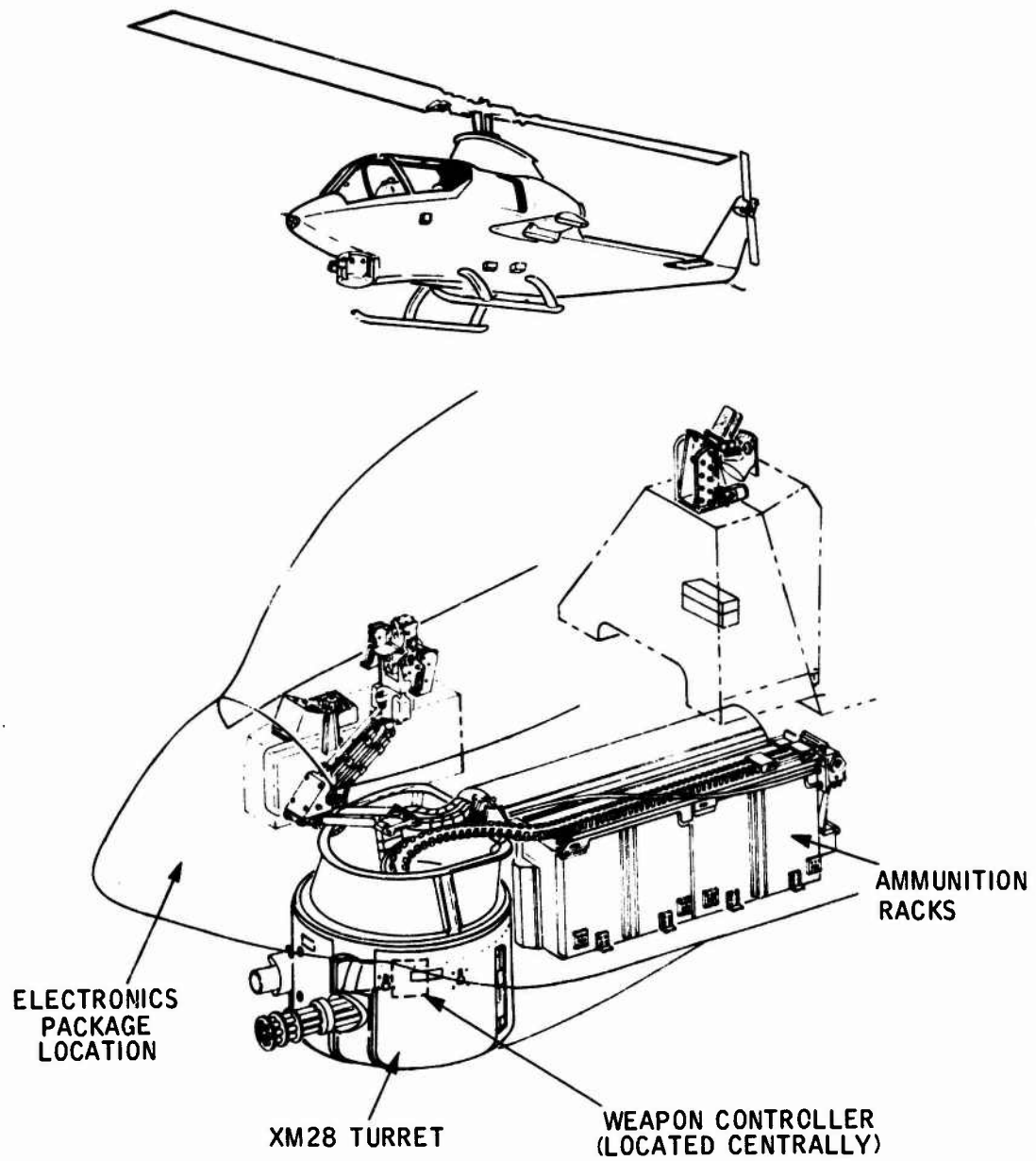

Figure 41. M-28 Turret Location

Figure 42. FATS Fluidic Package

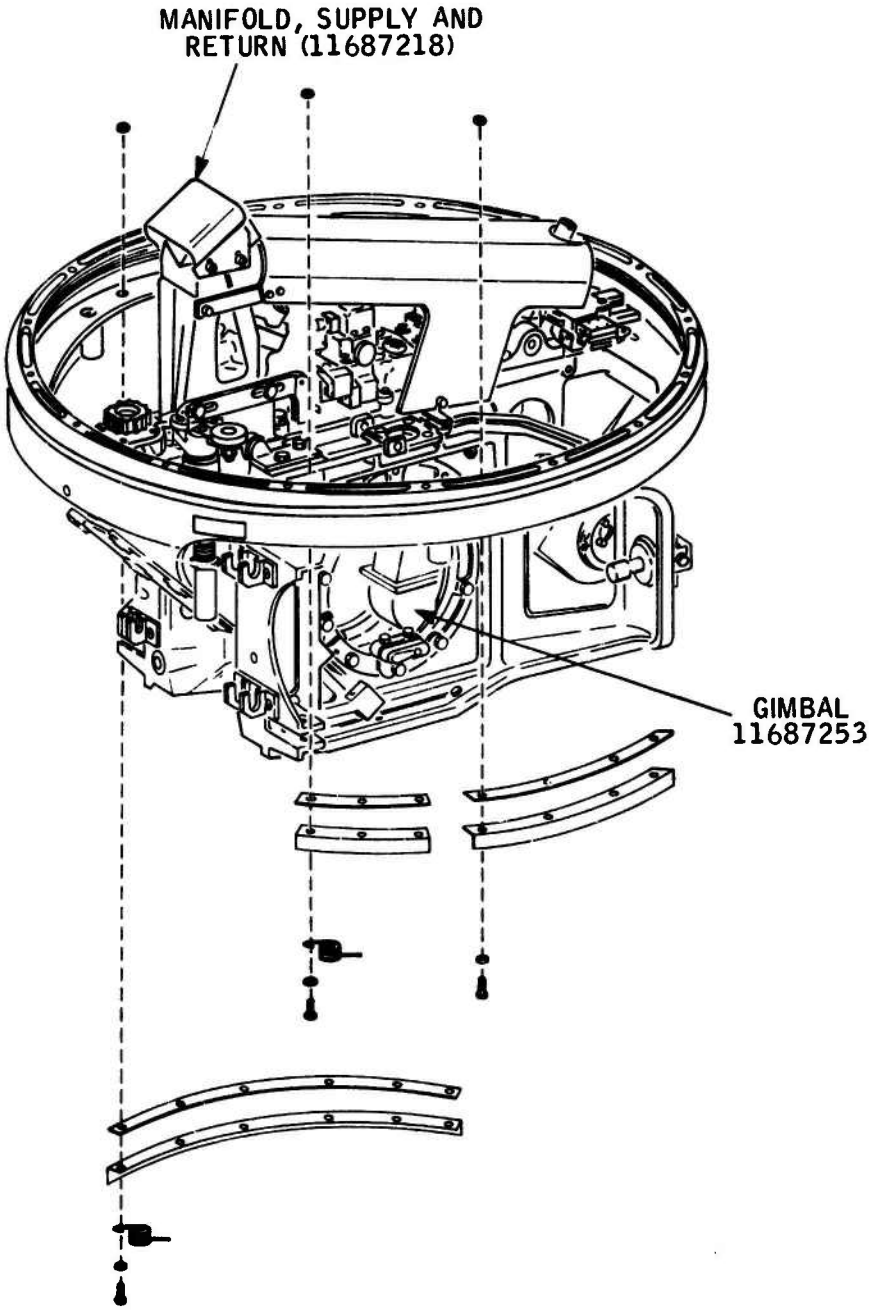

Figure 43. Helicopter Weapon Turret M-28, Partially Exploded View

Figure 44. Sensor Controller Installation

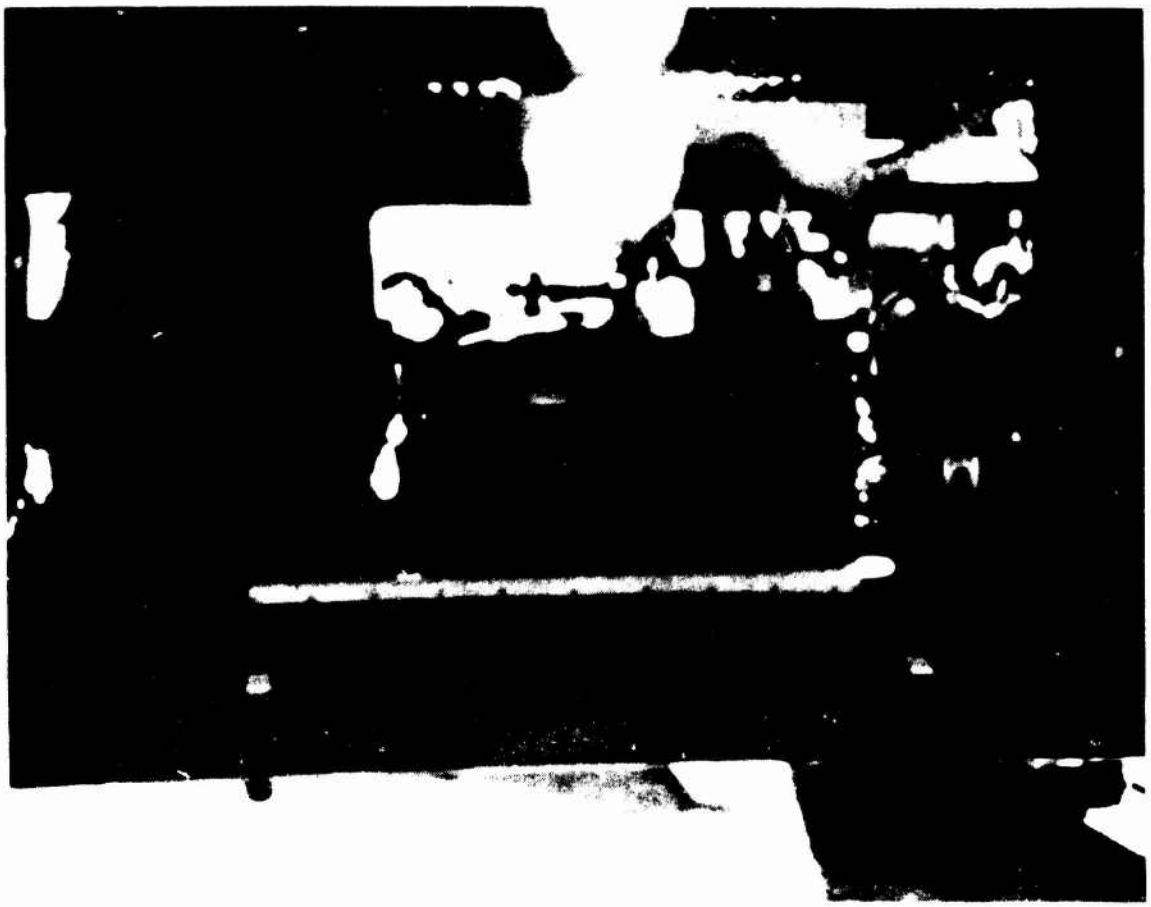

Figure 45. Test Instrumentation Installation

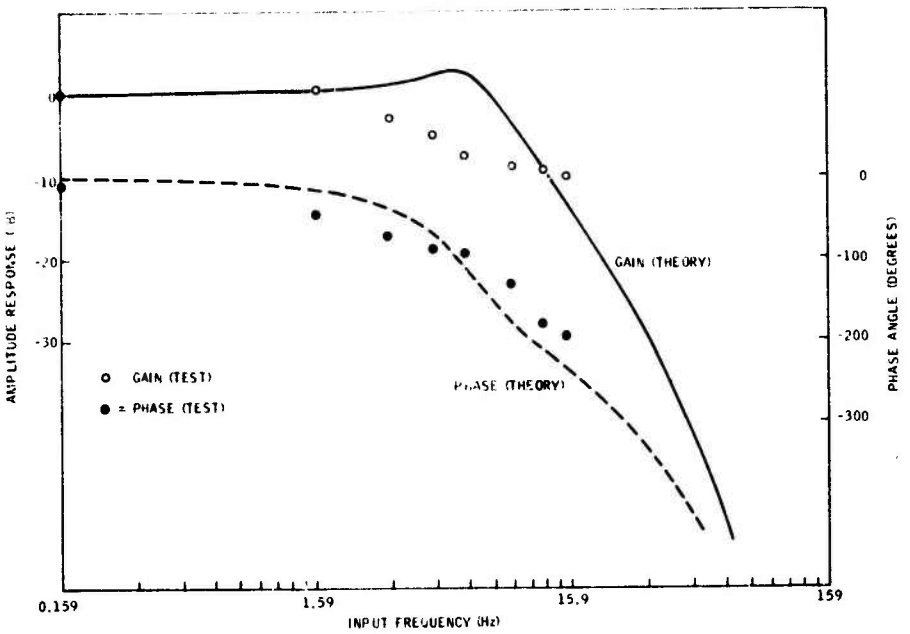

Figure 46. Stabilized Elevation Response to Sight Inputs

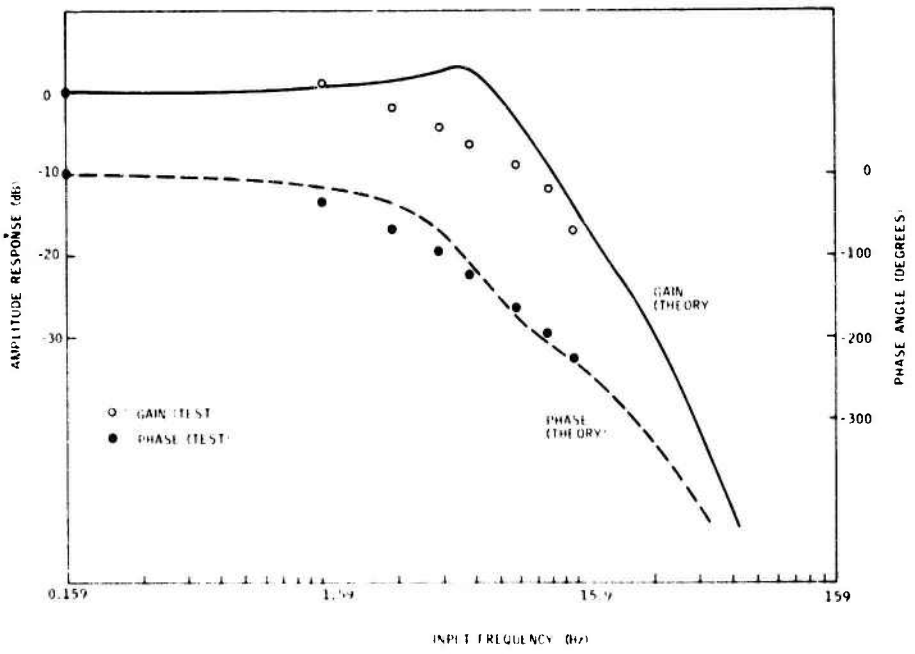

Figure 47. Stabilized Azimuth Response to Sight Inputs

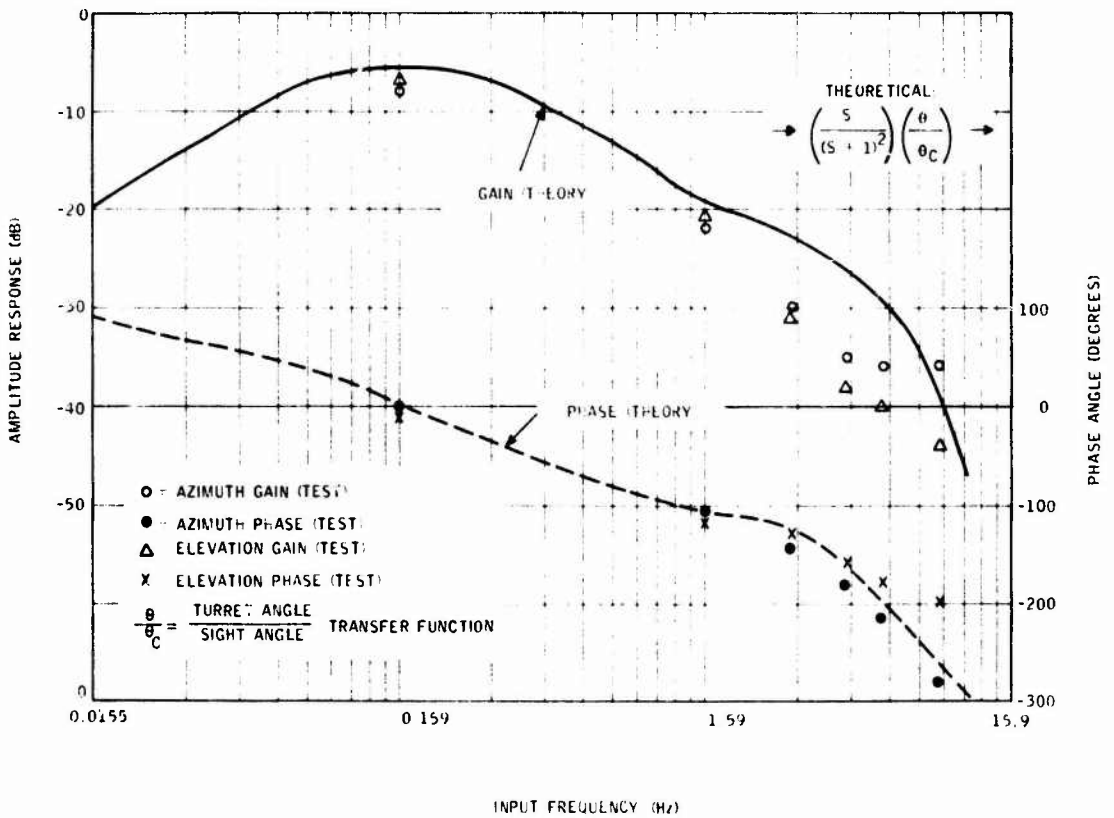

Figure 48. Response to Inputs at Rate Sum Point

theoretical performance with no stabilization added, indicating that the actual dynamic tracking between tach and VRS is somewhat better than that exhibited by the dynamic models used in the theoretical derivation.

The responses of both axes to electrical inputs applied at the VRS/tach sum points (see Figure 35) are illustrated in Figure 48. The data indicates that.

1. The stabilization gains are somewhat below ideal in both axes, about 20% low in elevation and 30% low in azimuth.

2. The lower gains above 1.59 Hz reflect the results of Figures 46 and 47.

The low stabilization gains resulted primarily from VRS gains below nominal. The latter did not compromise tach/VRS mismatch, since the tach gains were trimmed to match the associated VRS gains prior to testing. The effective turret stabilization of inertial inputs will be degraded, however, by the lower gains, the amount dependent on the nature of the disturbance. For frequencies around 1 Hz, a 30% low stabilization would result in about a 65% reduction in turret motion, in contrast to a 90% reduction produced by the nominal system.

RANGE TESTING

The turret system was evaluated and compared with and without the fluidic stabilization system on and with and without gun firing (7.62 and 40 mm). Most data was obtained from instrumentaion located in the ammunition bay (see Figure 41), ground firing testing was also evaluated from the targets.

The range testing was conducted in two time sequences: December 7, 8, 1973, and December 20, 21, 1973. The first sequence was plagued by aircraft grounding (rotor blade inspection) turret malfunction (40 mm limit switch, broken wires, jammed ammunition belts), and obtaining gas from near the range (local airports ran out). Between the two periods, the turret was reworked, the system recalibrated, and instrumentation was reviewed. The second series of tests were accomplished without major difficulty, the one problem being a broken electrical wire in the azimuth circuit, rendering the stabilization system (in that axis) inoperative.

Limiting Factors

One factor hindering the evaluation of all airborne testing was the lack of a compensation signal from the turret stabilization system to the sight reticle; i.e., with the gunner in the loop, errors were caused due to the gunner being unaware of stabilization system input; with the sight pinned (gunner out of the loop), nothing corrected for low frequency inputs (below about 0.48 Hz).

Another factor limiting the testing was due to the tight space the pilot had to maneuver in. (The range was built in a deep ditch.) This probably accounted for the difficulty the pilot had in getting 1.27 Hz type inputs into the helicopter (optimum for the system) and prevented pitch type maneuvers when firing. It may be noted that the so called "optimum" frequency of 1.27 Hz merely reflects the frequency at which the system produces maximum attenuation (see Figure 9). This results from a combination of designing for no attenuation around 0.159 Hz and designing for adequate system stability. The dominant disturbance frequencies actually experienced in the testing were around 0.48 Hz as shown in Figure 56.

A third factor involved the temperature at times reaching -8°F, which required repeated warm-up of the turret power system. This was aggravated by the fact that the fluidic system was not temperature compensated, thus requiring additional warm-up time.

Data Obtained

Data were obtained for the following test procedures and are discussed below:

Flight Testing

- Hover testing (trying to get 1.27 Hz input), with and without FATS, and sight pinned (azimuth only).
- Hover testing (step input), with and without FATS, and sight pinned (azimuth only).
- Hover testing (1.27 Hz input), with and without FATS, and gunner in loop (azimuth only).
- Controller Hover (pilot trying to hold helicopter steady), with and without FATS. A broken wire was found in azimuth following this test and time problems prevented repeat of the test.

Test Results

Turret Stabilization in Flight - The stabilized turret was operated in flight and tested under both helicopter attitude and weapon firing disturbances. The former were applied primarily by pilot inputs in pitch and yaw. The resulting turret motions were measured and compared to the corresponding vehicle motions to determine the degree of stabilization attained. In some cases the 40 mm and 7.62 mm weapons were fired to determine impact dispersion. These results are reported in a separate section.

The results of a hover stabilization test (run 12/20/73) of the azimuth axis are illustrated in Figure 49. The three helicopter body rates are recorded, plus shaped position error signals in azimuth and elevation. The shaped error signal is the difference between sight angle and turret angle after being shaped by the loop lag-lead filter:

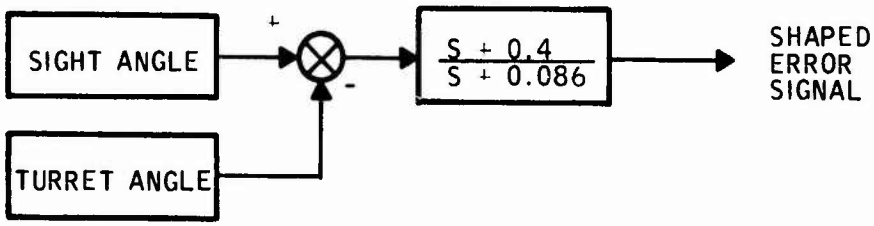

With a "pinned" sight (zero gunner command), the shaped error signal is a direct measure of the stabilization input. Note that the data for the shaped error signals is expressed in terms of the high frequency (above 0.4 r/s) relationship to actual position error, it being of primary significance to the frequency range of the stabilization system. In terms of steady state (nonvarying) signals, therefore, the indicated degrees of error on Figure 49 would be about a factor of 4.7 lower.

The results of Figure 49 may be summarized as follows:

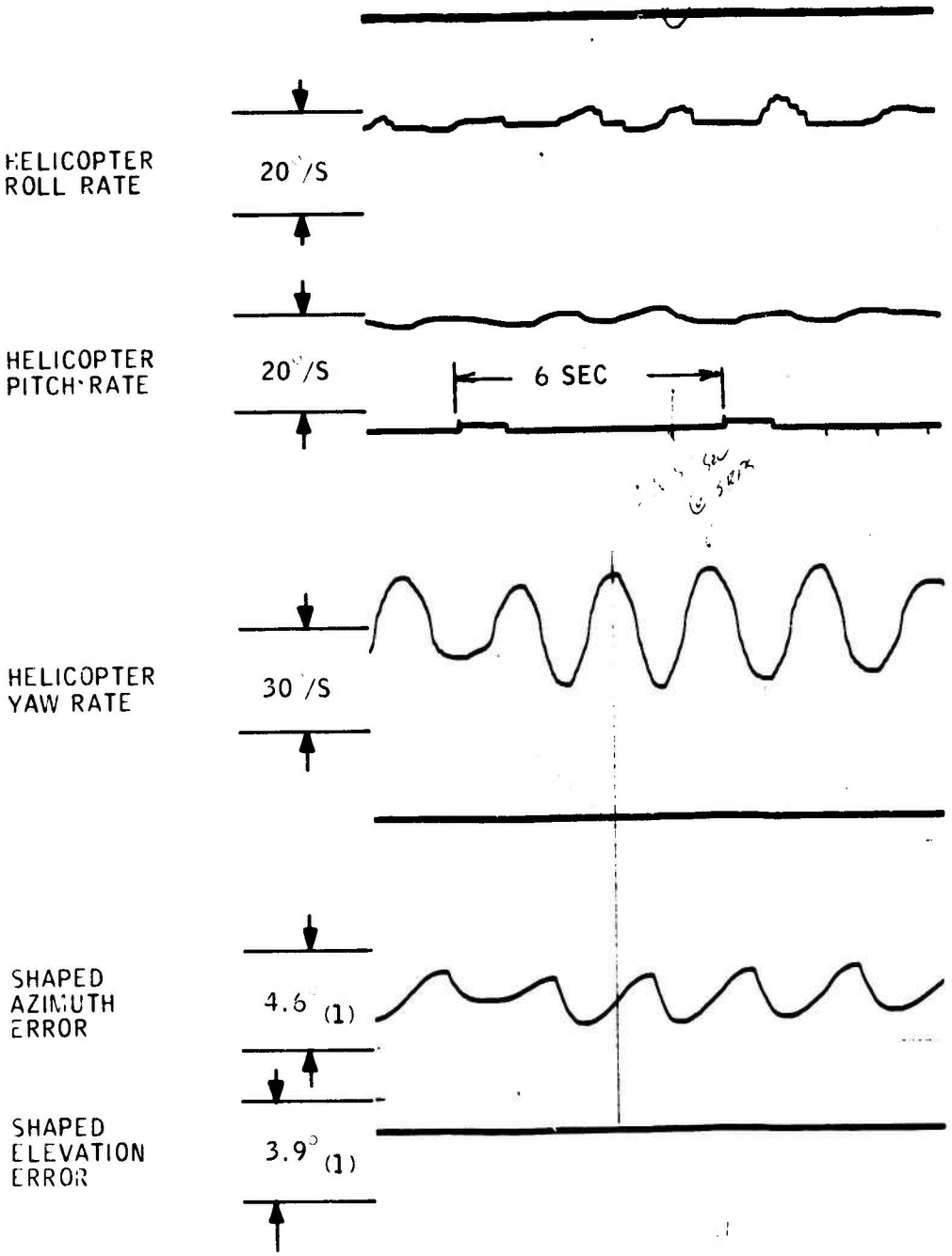

1: SCALE FACTOR FOR FREQUENCIES ABOVE 0.064 Hz

Figure 49. Azimuth Stabilization During Hover, Pinned Sight

1. The excitation in yaw amounts to an approximate sinusoid at a frequency of 0.46 Hz and a helicopter body amplitude of ±5.7°.

2. The turret is moving opposite to the helicopter at an amplitude (relative to the helicopter) of ± 1.2 degrees.

3. Hence the absolute turret motion in yaw is ±4.5°, for an attenuation by the stabilization system of -2 dB. Allowing for the 30% low stabilization gain, the theoretical attenuation at this frequency should be -3 dB.

Similar data (run 12/20/73) for the elevation axis is illustrated in Figure 50. These results are as follows:

1. The excitation in pitch amounts to an approximate sinusoid at frequency of 0.38 Hz and an amplitude of ±3.1°.

2. The turret is moving opposite to the helicopter at a relative amplitude of ±1.2°.

3. Hence the absolute turret motion in elevation is ±1.9° for an attenuation by the stabilization system of -4.3 dB. The theoretical attenuation at this frequency should be -2.5 dB.

Figure 51 illustrates simultaneous disturbances from both the pilot and weapons firing (test 12/21/73). Here both the elevation and azimuth stabilization systems are active, with the pilot applying a rudder kick, accompanied by a 40 mm burst using a pinned sight.

Based on a 3-second portion of the Figure 51 data (as noted on Figure), the associated helicopter heading change and turret motion relative to the helicopter were computed and plotted on Figure 52. The absolute turret motion is the sum of the two motions. Note that the peak turret motion due to the stabilization is 4.5°, a value about half of that theoretically expected for the given disturbance. The data illustrates the fact that the stabilization is only transient in nature (by design), and that considerable absolute turret motion may be expected under the situations normally encountered.

A problem with the current installation is illustrated by Figure 51 by the elevation deflection during 40 mm operation (12/21/73). This is believed to be caused by magnetic pickup from the gun motor, either by the fluidic-to-electrical transducer or by the tach. The problem is primarily in elevation. A comparable test (12/21/73) without the stabilization systems activated is illustrated in Figure 53. Here no turret deflections are experienced. Figure 54 shows a similar rudder kick during 7.62 mm firing (12/21/73), stabilizer on. The interference with the gun motor is again evident.

Added hover stabilization data is shown in Figure 55 (run 12/8/73). Here the azimuth tachometer output is recorded and compared to that produced by a nominal system under an identical helicopter yaw disturbance time history. The turret motion being produced relative to the helicopter is about ±4°. The yaw helicopter motion is about ±10°. System performance compares reasonably well with theory.

Figure 56 presents data plotted on the theoretical nominal system response curve. As can be seen the data compares fairly well. It is also noted that most pilot induced input motions fell at lower frequencies than was originally assumed.

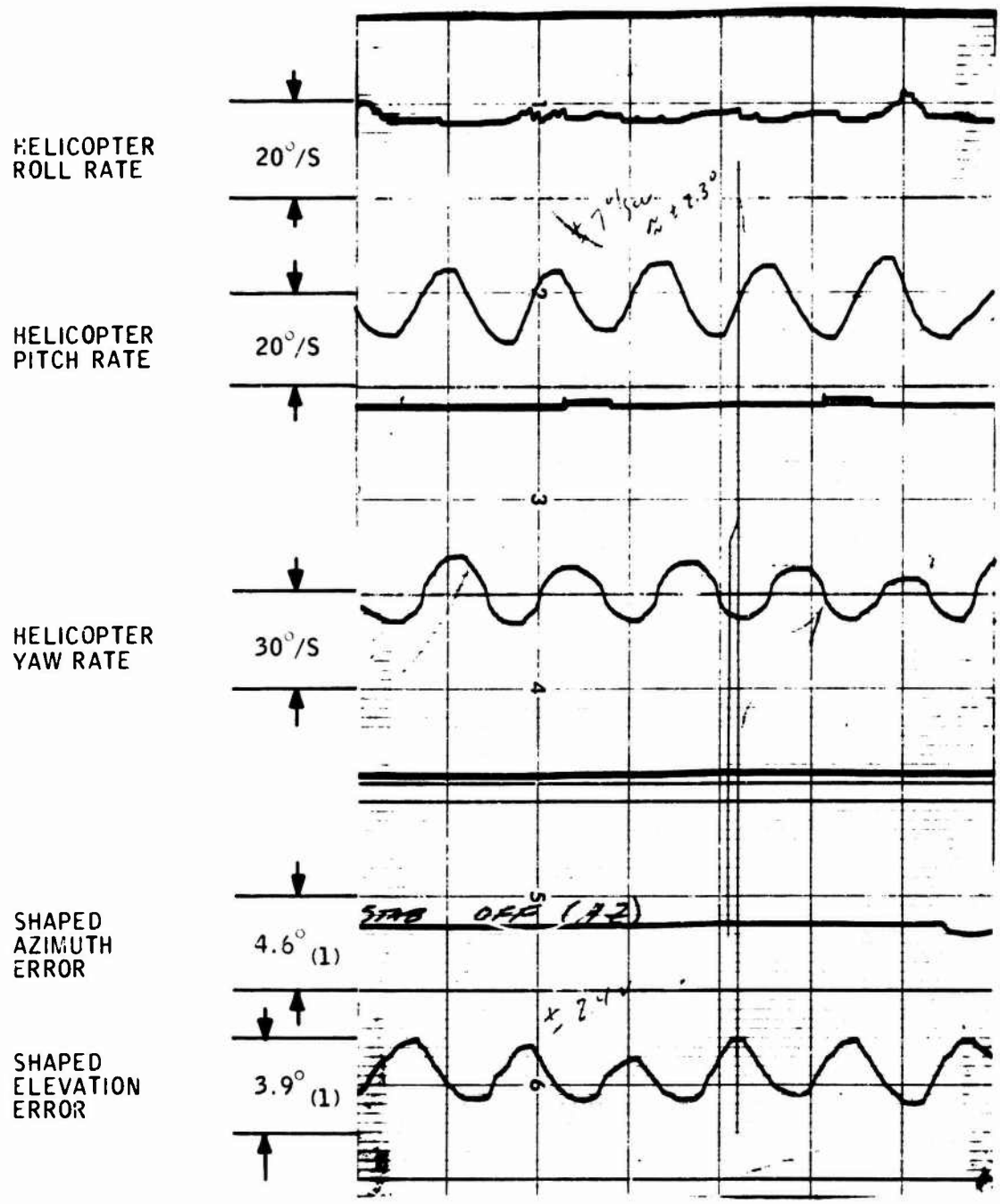

(1) SCALE FACTOR FOR FREQUENCIES ABOVE 0.064 Hz

Figure 50. Elevation Stabilization During Hover, Sight Pinned

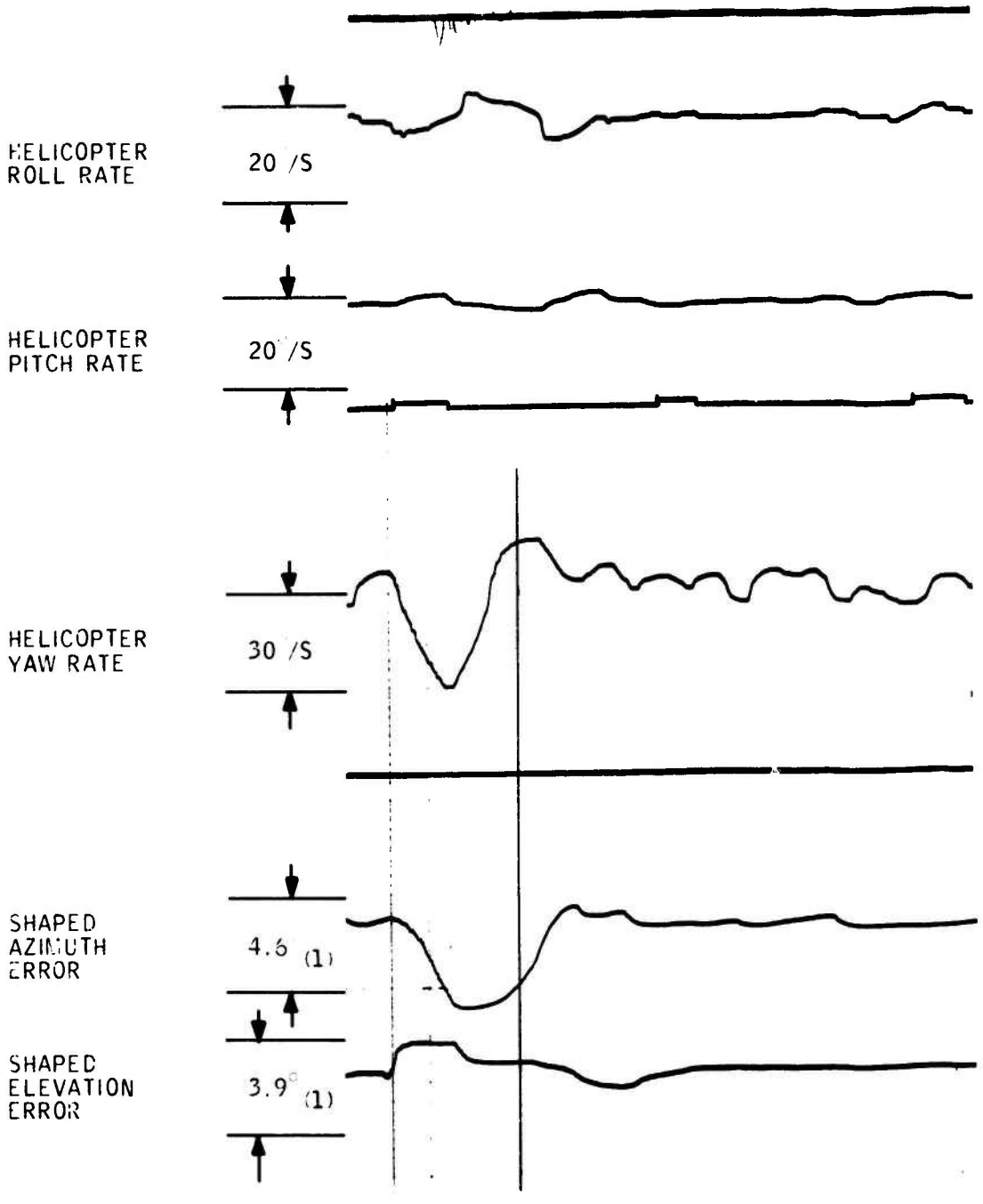

Figure 51. Stabilization During Hover, Rudder Kick Plus 40MM Firing, Sight Pinned

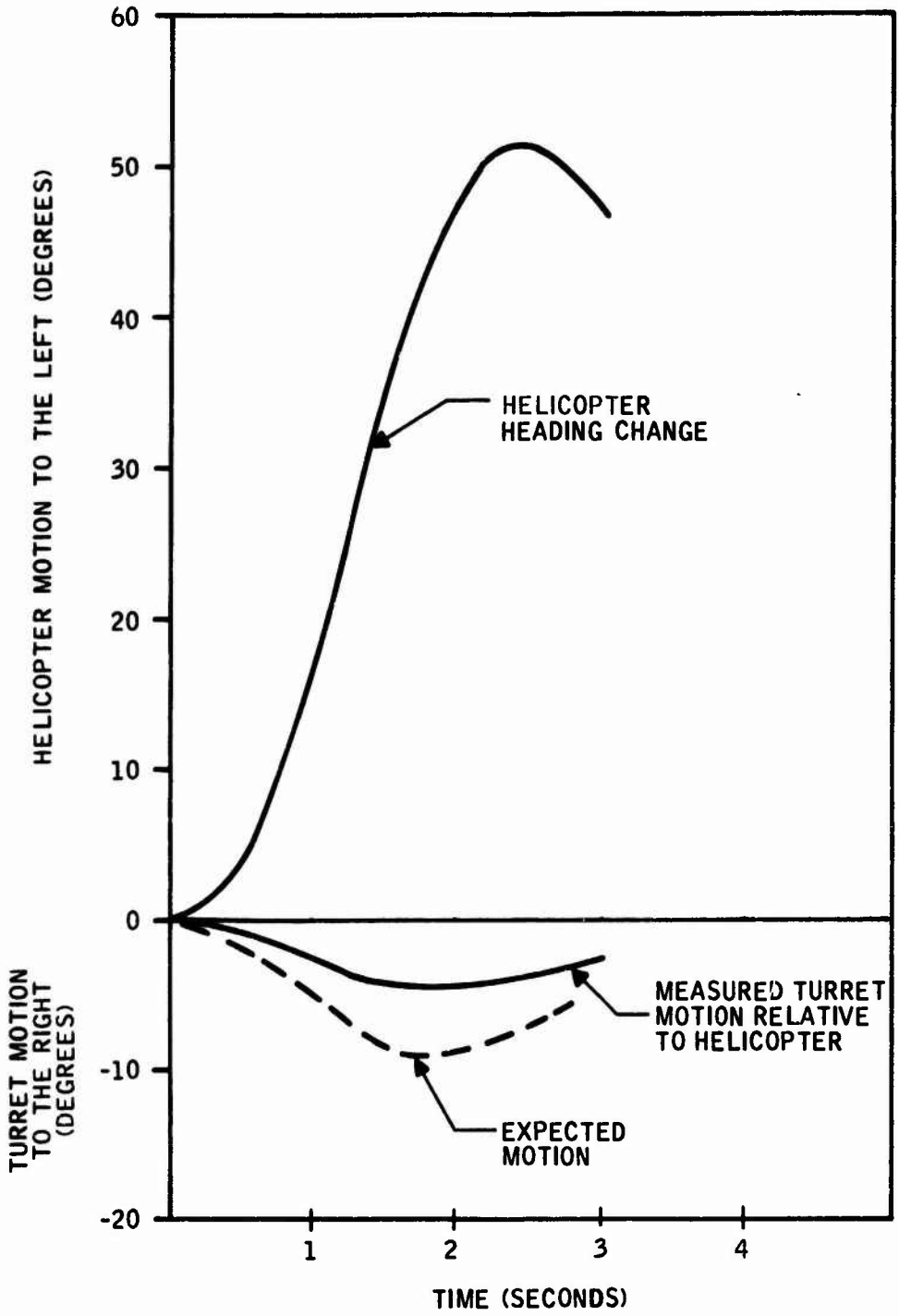

Figure 52. Helicopter and Turret Motion During Rudder Kick

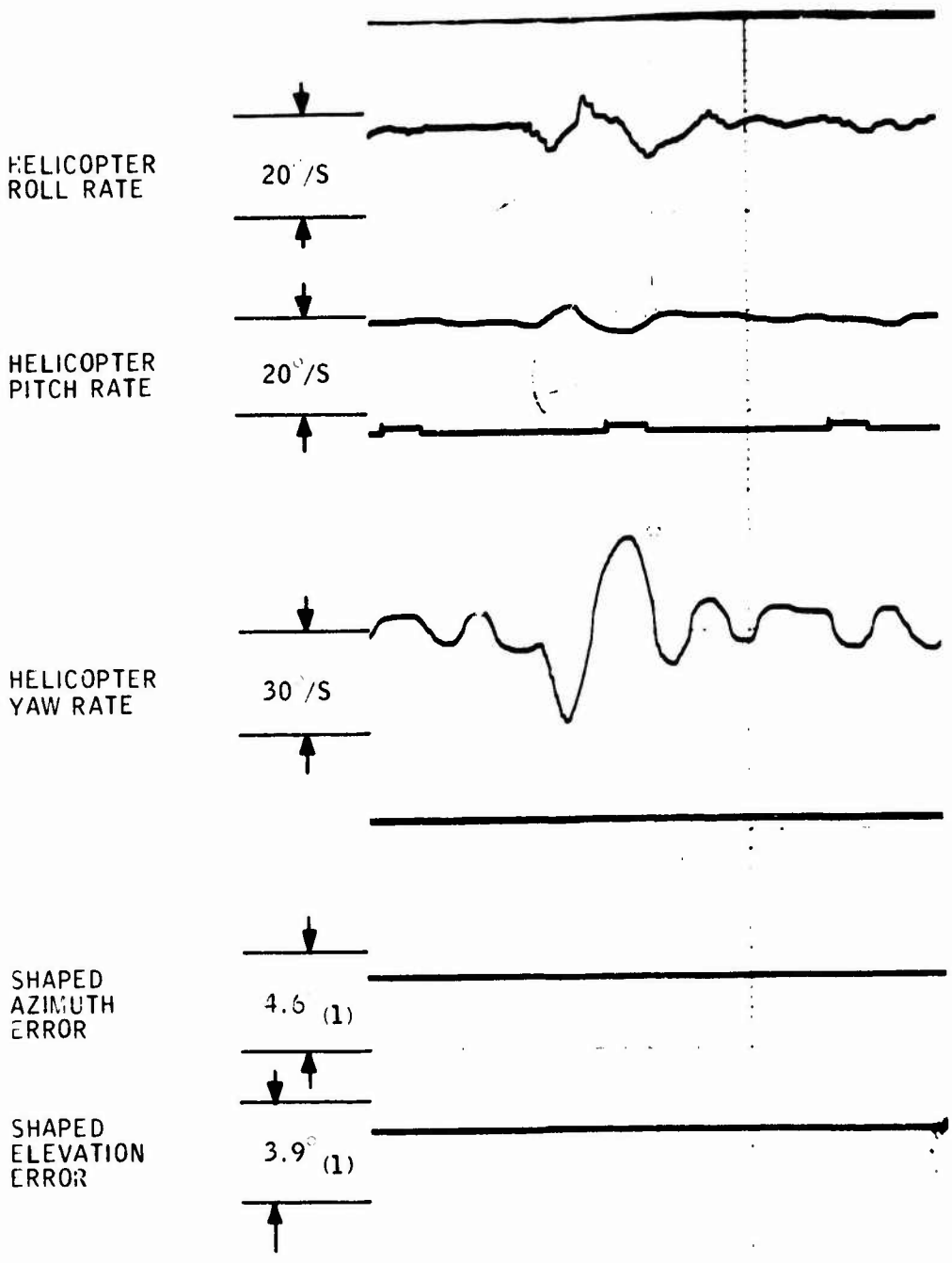

Figure 53. Normal Mode During Hover, Rudder Kick Plus 40MM Firing, Sight Pinned

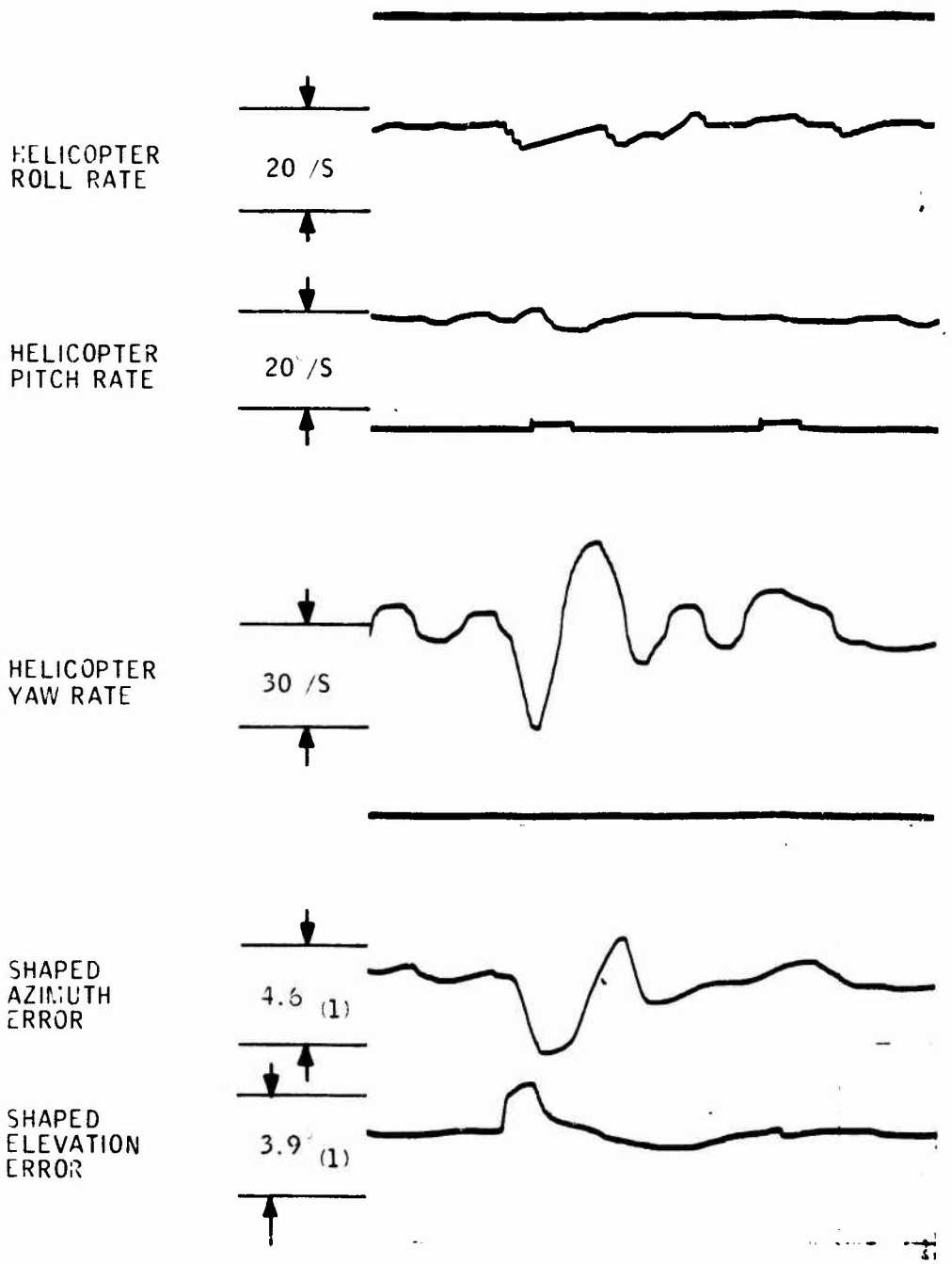

1. SCALE FACTOR FOR FREQUENCIES ABOVE 0.064 Hz

Figure 54. Stabilization During Hover, Rudder Kick Plus 7.62MM Firing, Sight Pinned

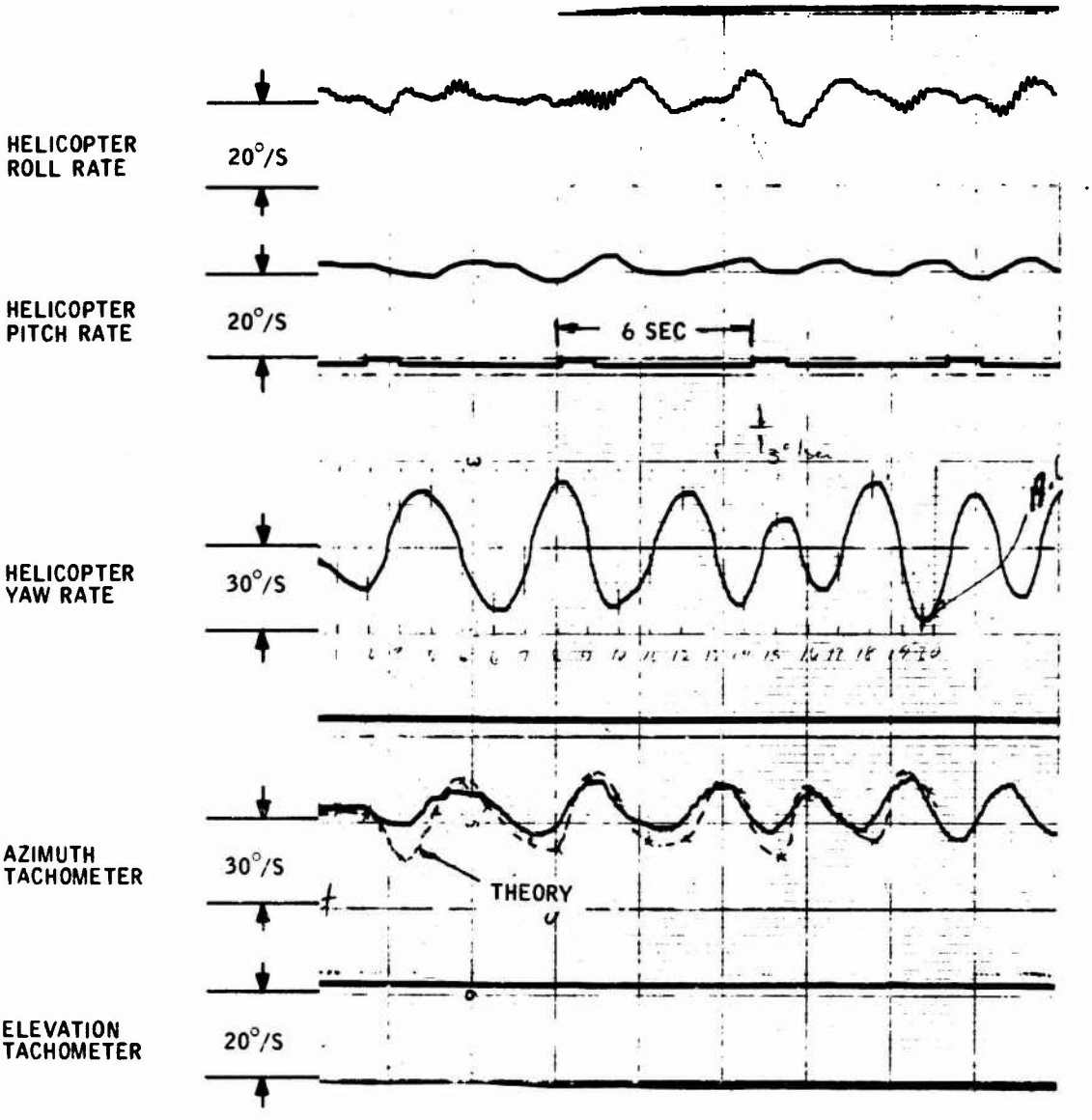

Figure 55. Azimuth Stabilization During Hover, Sight Pinned, Comparison to Theory

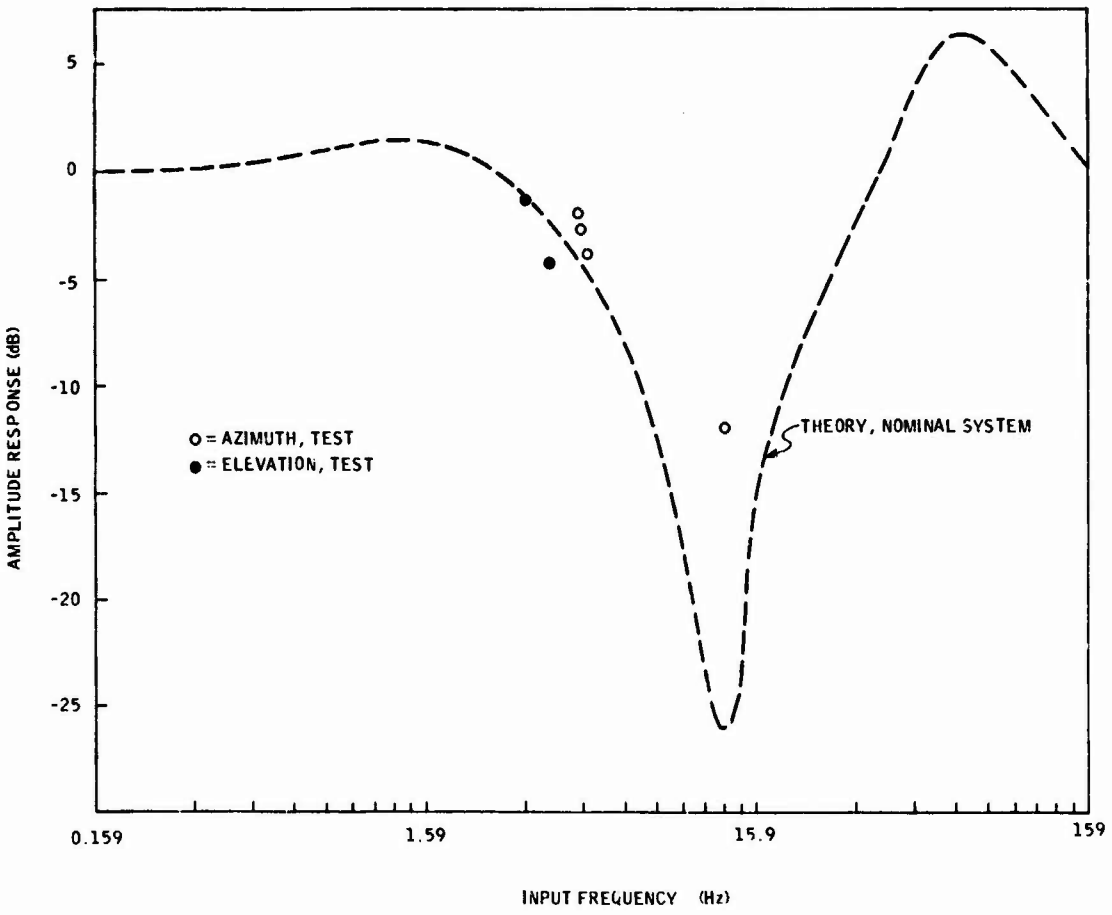

Figure 56. Ratio of Absolute Turret Amplitude to Absolute Helicopter Amplitude

Grcund Firing Tests - Weapon firing with the helicopter on the ground, sight pinned, was tested to determine the effects of the stabilization system. It was expected that the stabilization system would have little effect, unless significant angular deflection of the aircraft structure occurred due to recoil forces. It was found that the stabilization system had a degrading influence (in terms of gun-to-helicopter deviation) due to magnetic pickup (from the gun motor). Figure 57 illustrates results from a test on 12/21/73. About a 2 degree deviation results in elevation, and about a half degree in azimuth, when the gun motor is operated.

Figure 58 illustrates comparable ground firing (run 12/7/73) with no stabilization system on. Here the azimuth and elevation tachometer outputs are recorded instead of the position errors used previously. The tachometer outputs are considerable, particularly in elevation, where a 4 degree-per-second equivalent output appears. For the 3-s duration of the firing, this would equal a 12 degree turret deviation, well beyond anything which actually occurred (based on impact dispersion). This indicates an interference situation. The tachometer is used for both the stabilized and normal modes, but it is high passed at a very high break frequency (8 Hz) in the latter, so the interference would be less significant. Lack of such is substantiated by the results of Figure 53.

Target Evaluation

The first system firing tests (ground tests) were conducted with the aircraft approximately 1000 inches from a 8 by 8-ft plywood target (see Figures 59 and 61). The second sequence of firing (hover testing, see Figures 60 and 66) utilized a 8 by 16-foot target. Because of the limiting factors (lack of sight compensation and limits of a aircraft maneuverability), previously discussed, most system effectiveness evaluations were obtained from the on-board instrumentation. Except for ground firing testing, only qualitative evaluation of targets could be made.

Ground Firing - Figures 61 and 62 show the dispersion patterns for the 40 mm firing, with FATS OFF and with FATS ON, respectively. Figures 63 and 64 present the patterns for the 7.62 minigun. Table 3 tabulates the maximum horizontal and vertical dispersion as measured from the targets. The data was taken with the helicopter grounded in idle and the gunner's sight pinned.

TABLE 3. GROUND FIRING DISPERSION DATA

Condition	7.62 Minigun Dispersion (Inches)		40 mm Grenade Dispersion (Inches)	
	Horizontal	Vertical	Horizontal	Vertical
FATS OFF	28	24	15	10
FATS ON	12	18	4½	14

An examination of the target patterns reveal the effects of the magnetic pickup in elevation previously discussed. As can be seen, the resultant dispersion is much greater in the elevation axis, also, the affects are much greater for the 40 mm grenade launcher than for the minigun, although some interference is noted. Future systems would have to include shielding of the tachometers.

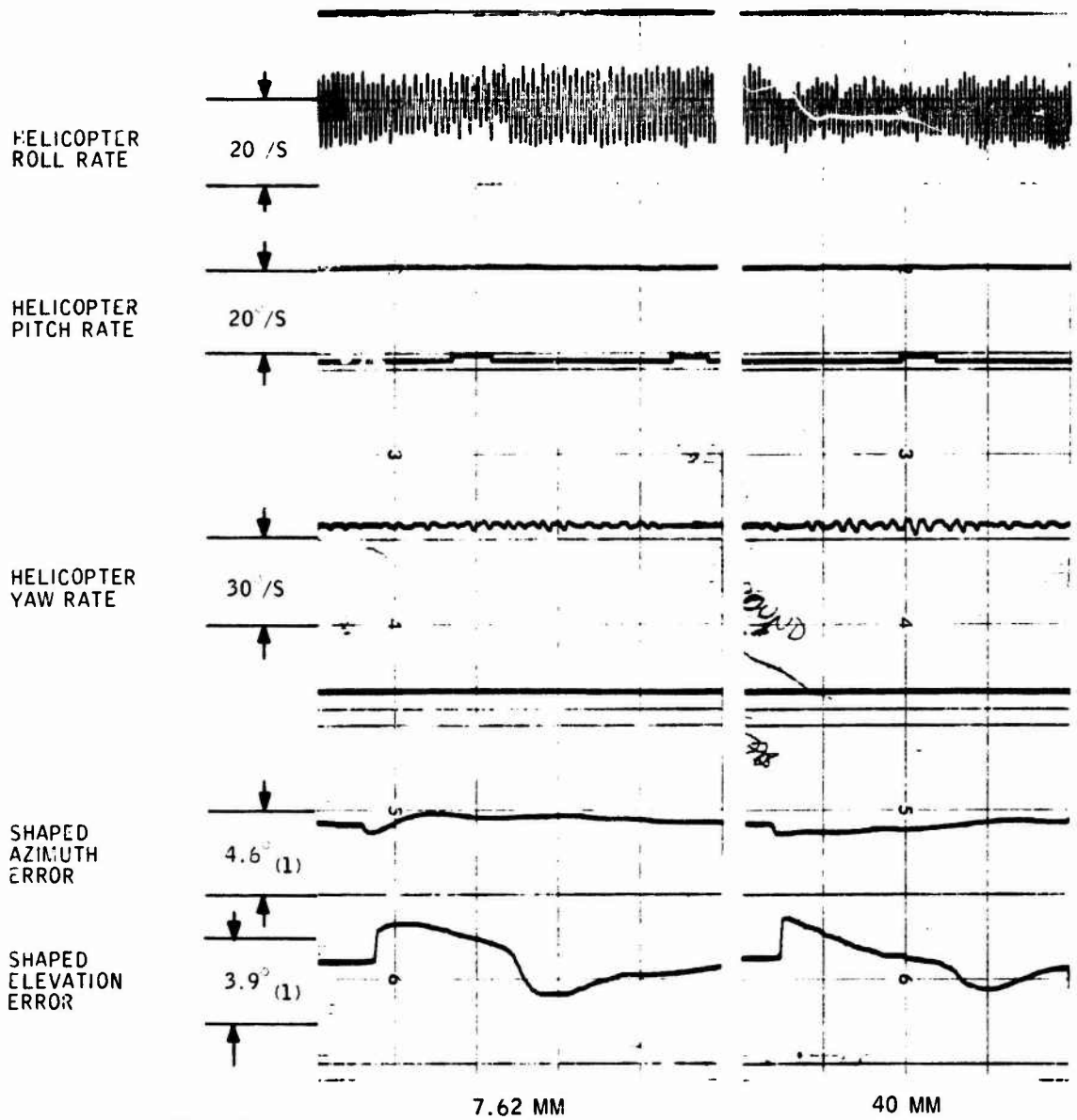

(1) SCALE FACTOR FOR FREQUENCIES ABOVE 0.064 Hz

Figure 57. Stabilized Firing Results, Helicopter on Ground, Sight Pinned

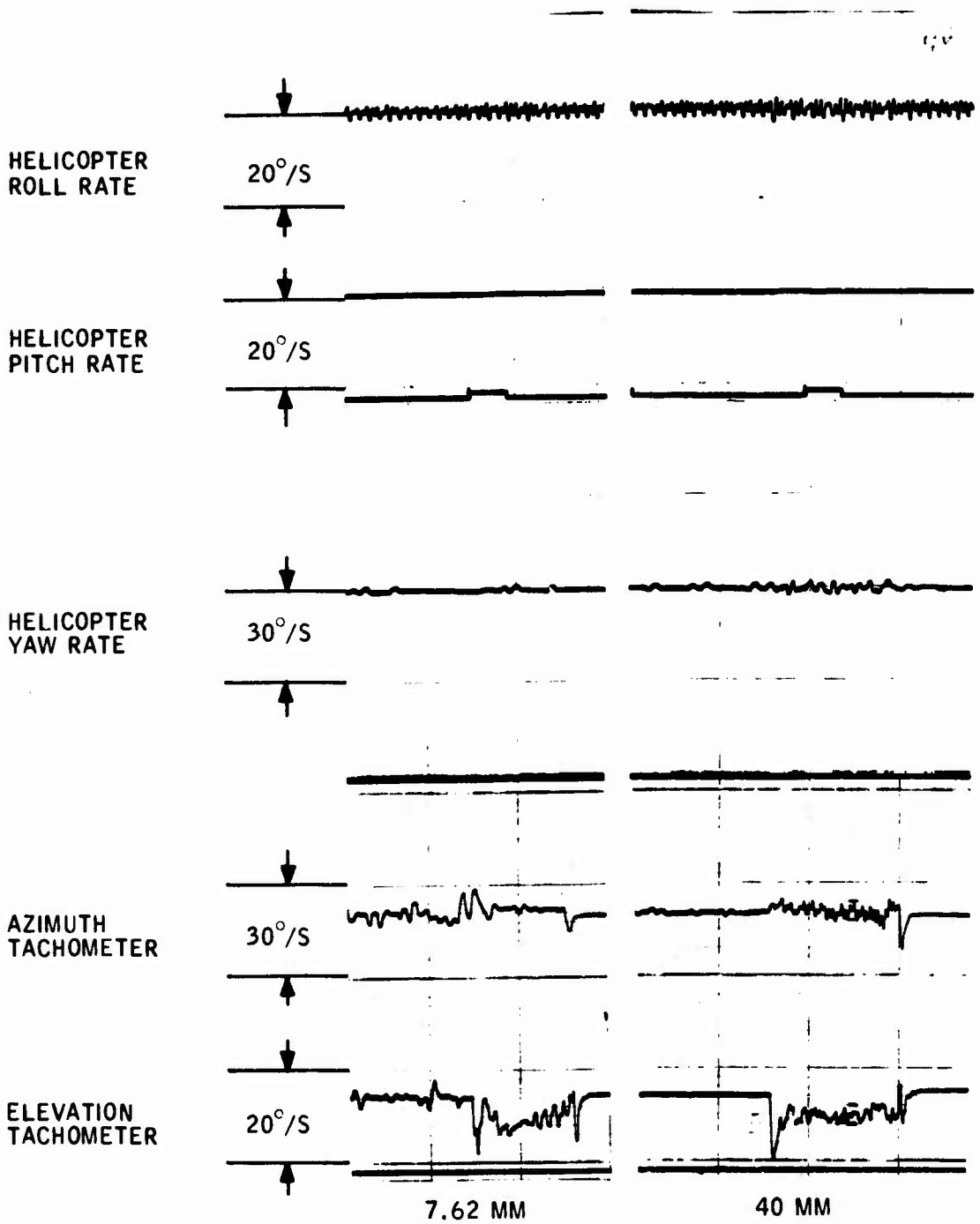

Figure 58. Normal Turret Firing Results, Helicopter on Ground, Sight Pinned

Figure 59. System Firing Tests from 1000 Inches at 8 by 8-Foot Plywood Target (Ground Firing Tests)

Figure 60. Hover Firing Test Setup

Figure 61. 40MM Pattern, SAS Off

Figure 62. 40MM Pattern, SAS On

Figure 63. 7.62MM Pattern, SAS Off

Figure 64. 7.62MM Pattern, SAS On

The data concludes that gun firing causes a structural motion within the control band of the FATS system. The system effectivity corrects for 70% of this motion for the 40 mm and 57% for the minigun, in the azimuth (horizontal) axis. The interference in the elevation axis prevented accurate evaluation, although a 30% reduction in minigun dispersion is indicated.

Hover Firing - Hover firing testing was limited to inputs in the azimuth axis only due to the confined area for helicopter maneuvering. Two basic tests were conducted to evaluate the system.

- Step input with and without FATS, sight pinned; Pedal-kick timed with firing.
- Gunner interaction tests with and without FATS, gunner in loop, pilot trying to oscillate helicopter at 1.27 Hz.

Figure 65 shows the results of the step input testing. As expected, due to the 1-second high-pass in the system, the only difference between FATS ON and FATS OFF condition is the initial accumulation of rounds with FATS ON, and then as the high-pass "charges up", the system reacts as though it were in FATS OFF condition. Figure 66 shows this initial accumulation for the minigun firing. Figure 65 also shows the vertical magnetic interference: the round pattern moves up as the helicopter moves from right to left.

Figure 67 shows the results of the gunner interaction testing. As expected, without a stabilization system compensation of the sight retical, the dispersion is actually greater (both in azimuth and elevation) with the system on than with the system off -- approximately double.

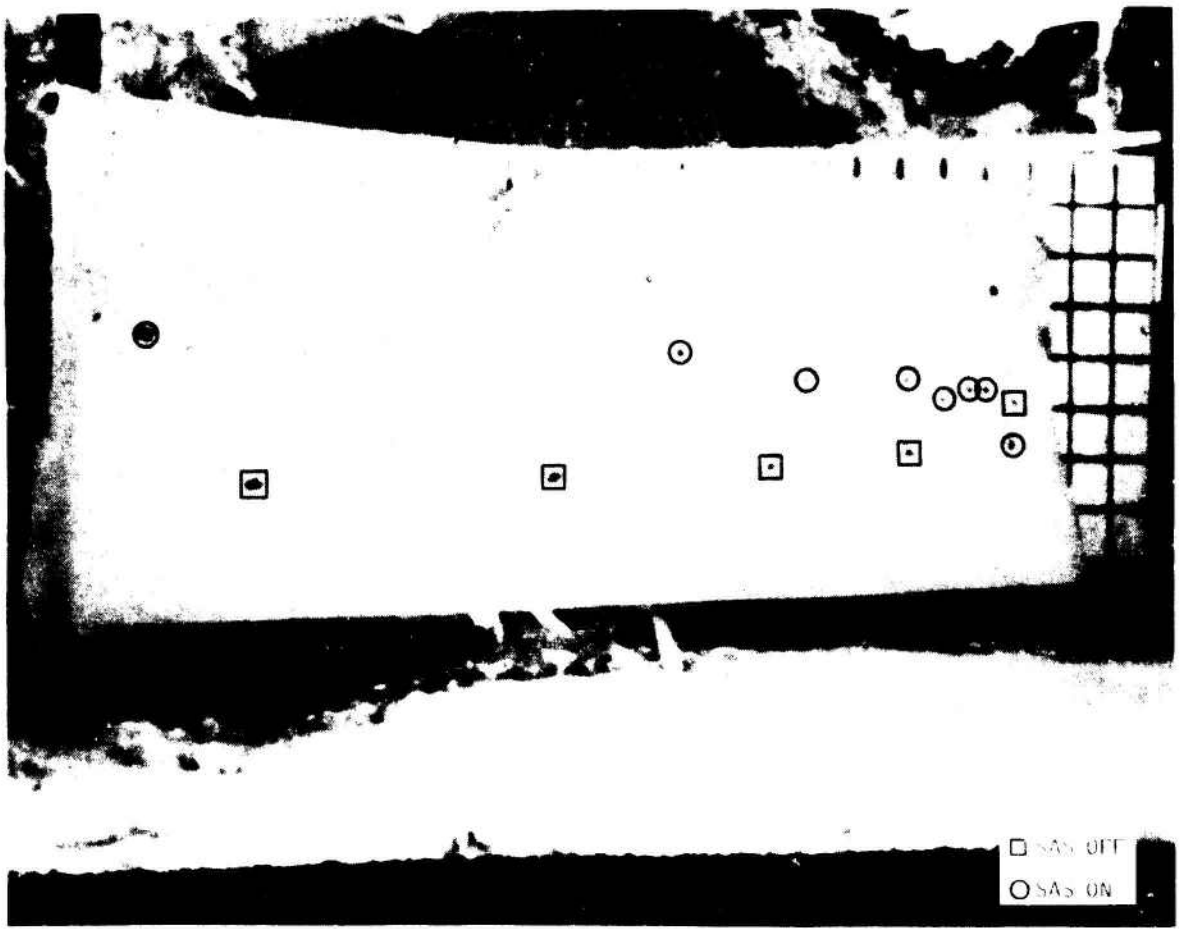

Figure 65. 40MM Step Input, SAS On and Off

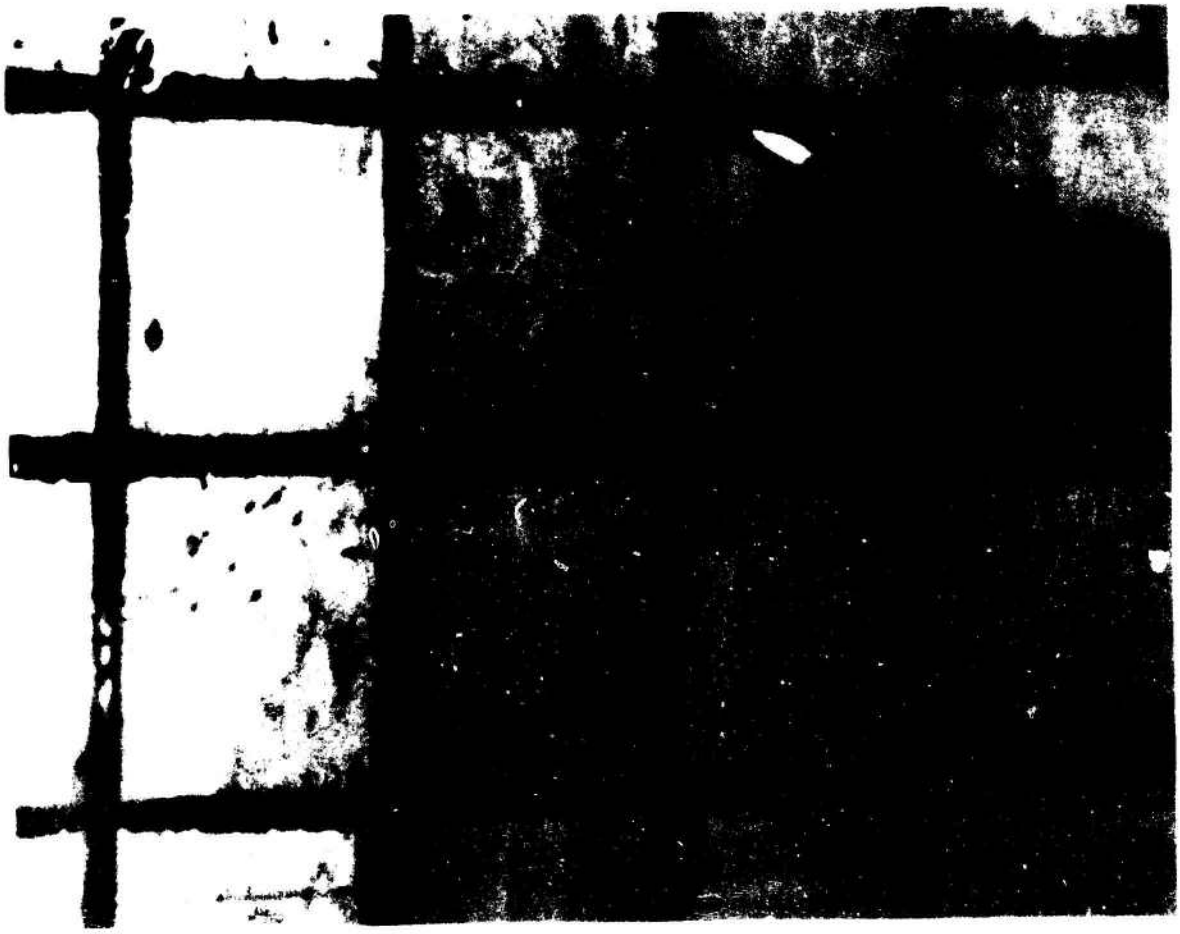

Figure 66. 7.62MM Step Input, SAS On

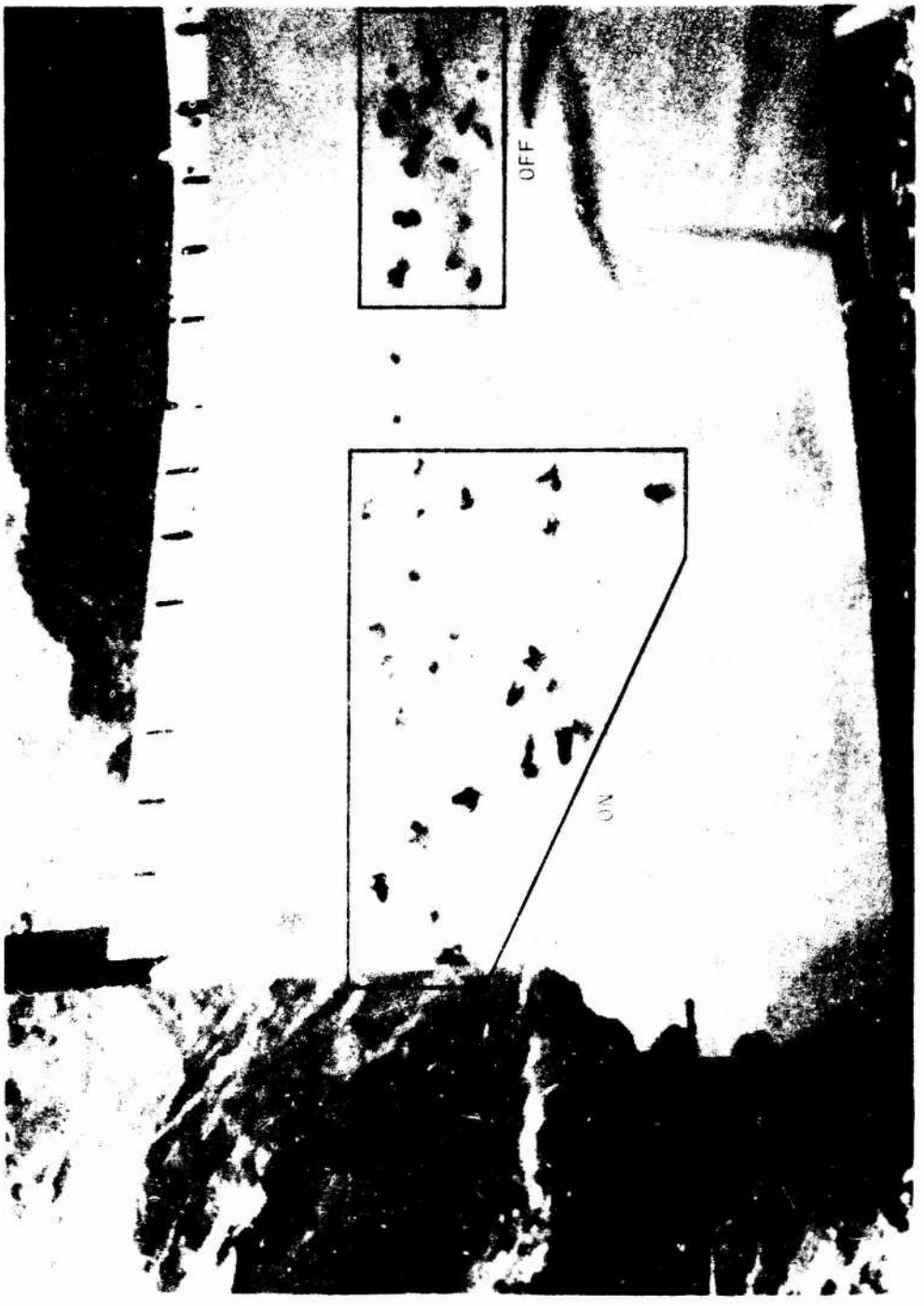

Figure 67. Gunner Interaction Test

SECTION VIII

CONCLUSIONS AND RECOMMENDATION

CONCLUSIONS

Due to a number of factors, the test results are not as visually conclusive as desired. However, from data analysis, limited target analysis, and taking into account known errors such as magnetic interference from the gun motors, it is believed that the program reached its major objective of proving that hydrofluidic systems could be utilized to provide stabilization of aircraft mounted guns, improving round dispersion up to 70%. The following major conclusions are drawn from the overall program effort.

Turret Structural Resonance

- Both rigid test stand and actual aircraft response testing confirmed that the lowest resonance frequency in the turret is about 17 Hz in both the elevation and azimuth axes. Analysis showed that this was caused by hydraulic fluid compressibility in the elevation actuator assembly and by gear train flexibility in the azimuth axis.

- The M-28 gun turret mount interface with the AH-1G helicopter is essentially rigid.

- The gear train could be stiffened without too much risk of higher frequency coupling problems.

- A higher pressure system utilizing a smaller volume elevation actuator would drive the 17 Hz resonance upward.

Fluidic Armament Control System (FATS)

- The general concept of hydrofluidic turret stabilization for future turrets was verified. The ability to interface hydrofluidics subsystems with electronic systems was demonstrated.

- The hydrofluidic system was unaffected by the turret firing environment. No affects due to firing shocks were noted. It is concluded that hydrofluidic systems are suitable for applications requiring environmental ruggedness.

- Some difficulty during testing was encountered due to low gain caused by low oil temperature. Future fluidic systems for this application should be temperature compensated.

- An optimized system that includes gunsight reticle compensation (for stabilization system inputs) would effectively reduce round dispersion.

Feedback Control Loop Interaction Effects

The analysis of the turret control loops assumed that angular acceleration of the turret resulted in negligible angular motion of the helicopter structure to which the turret was attached. Such motion could be due to both rigid helicopter rotation (in flight) and to structural deformation (probably mostly the latter). It could constitute an added feedback path

through the VRS, and at worst result in dynamic instability of the turret control loop. Because of adequate correlation between predicted and measured frequency response, it was concluded that the above coupling was negligible.

The test results confirm that the coupling is negligible.

RECOMMENDATIONS

The basic value of fluidic systems as applied to control of future turrets has been demonstrated. It is felt that systems for some applications could be mechanized now, others would require additional development. The following recommendations are made:

- A cost effectiveness study involving the value of improvement in dispersion considering mission and target mix factors, turbulence environment, gunner human factors and related developments in alternate sight/control means should be conducted.

- A development program involving combining a FATS type system with gun sight reticle compensation for stabilization input signals should be considered.

- The FATS system should be considered to provide stabilization for the case of the pilot firing from the stowed position; the system would be energized as the pilot fired the guns and the system high-pass would be removed, to allow low frequency operation.

- Hydrofluidic systems should be considered for other applications involving environmental ruggedness.

APPENDIX I

APPENDIX I

DEVELOPMENT & EVALUATION LAB

ENGINEERING TEST REPORT

DATE February, 1973	REPORT NO. AEX 72-0143
	PAGE 1 OF 4

1.0 ABSTRACT

Object - Conduct frequency response tests on a XM-28 Helicopter gun turret with the turret mounted in the aircraft.

Summary - Response data is presented graphically both for azimuth and elevation. Tests were conducted at ± 10°/sec and ± 30°/sec with the guns parallel and 90° left and right to the aircraft's longitudinal axis, and forward but depressed about 30°. Significant structural resonance was not detected as noted previously during test stand operation. The gun barrel assembly appeared to reach resonance at about 17 Hz in elevation as shown in the amplitude plots.

2.0 UNIT TESTED

One XM-28 Helicopter Armament Sub-system used on the AH-1G Huey Cobra Helicopter. Tests were conducted at Edwards AF Base on Helicopter SN69-16410.

ATTACHMENTS:

1. Six (6) Graphs
   Three (3) Photographs

REQUESTED BY: J. R. Sjolund	DATA BOOK 07030 PAGE 51
DEPARTMENT: F.F.S.	DEVELOPMENT NO. W0522-A1-5000
WRITTEN BY: E. R. Whyte	DATE TESTING COMPLETE: 12/12/72

3.0 PROCEDURE AND RESULTS

3.1 Procedure

Response tests were conducted open loop on the helicopter mounted gun turret. Input rates were ± 10°/sec and 30°/sec. Phase lag and amplitude ratio were recorded for frequencies between 1 and 30 Hz. The input signal was fed directly to the Moog values from a Bafco Frequency Analyzer through a dummy amplifier card extender inserted in the electronic control assembly. Turret motion was sensed by a GG445A1 rate gyro mounted on the left hand weapon saddle and by the internal tachometers. Access to the tachometer outputs was through a dummy amplifier card inserted in J6 in the electronic control assembly.

The input signal was a sine wave, with frequency varied by octaves from 1 to about 30 Hz for both elevation and azimuth.

Data was recorded with the guns orientated as follows:

A. Motion in Azimuth Mode

1. Guns level - forward
2. Guns level - 90° left
3. Guns level - 90° right
4. Guns depressed 28° - forward

B. Motion in Elevation Mode

1. Guns forward
2. Guns 90° left — (Motion through the Horizontal Plane)
3. Guns 90° right
4. Guns forward, depressed about 30°

Cross-talk data was recorded for three gun positions:

1. Guns forward, level - motion in azimuth
2. Guns forward, level - motion in elevation
3. Guns forward, depressed about 30°, motion in elevation

3.2 Results

Phase lag in degrees and amplitude response in db's were plotted graphically for each of the positions tabulated in the procedure; the

3.2 Results (Continued)

graphs are attached to the report.

Graph No. 1 compares the results between the turret's tachometer and the rate gyro. The output from the elevation tachometer was unreliable when fed into the frequency analyzer although the wave form and signal level appeared normal on a scope. The problem was left unresolved due to time limitations on aircraft availability. The difference between the two readouts for the azimuth data may be due to back lash in the gear train associated with the hydraulic motor.

There was no significant turret resonance observed as experienced on the test stand except for the 7.62 gun assembly. The barrel assembly appeared to go into resonance at about 17 Hz. The natural frequence of the entire aircraft was observed to be about 5.5 Hz.

For offset gun positions during frequency operation in the opposite mode, it was necessary to hold the gunners action switches closed and aim the sight to the desired angle. The switches were taped closed and the sight was clamped at the selected angle for this operation.

With the guns depressed during an azimuth input, there were random, low level step changes in gun position. This was attributed to the elevation amplifier loop since the tachometer amplifiers had been removed.

4.0 INSTRUMENTATION

A Honeywell GG445A1 rate gyro was used in the tests and was calibrated for response and output levels in Minneapolis prior to leaving for Edwards AFB and after return. The post test data was used to correct the gyro response data. Output level of the gyro was monitored on a scope to set the desired turret rate input.

The gyro output signals were demodulated internally in the frequency analyzer and displayed directly in phase angle and amplitude. (db's) Photographs attached to the report show gyro orientation and the general instrumentation set up.

SIGNATURES AND APPROVALS

By _____
E. R. Whyte, Engineering Aide
Development and Evaluation Lab

Approved _____
J. C. Armstrong, Manager
Development and Evaluation Lab

_____
B. G. Johnson, Group Supervisor
Development and Evaluation Lab

ATTACHMENT NO. 1

Six (6) Graphs
Three (3) Photographs

K&E SEMI-LOGARITHMIC 46 4973
KEUFFEL & ESSER CO

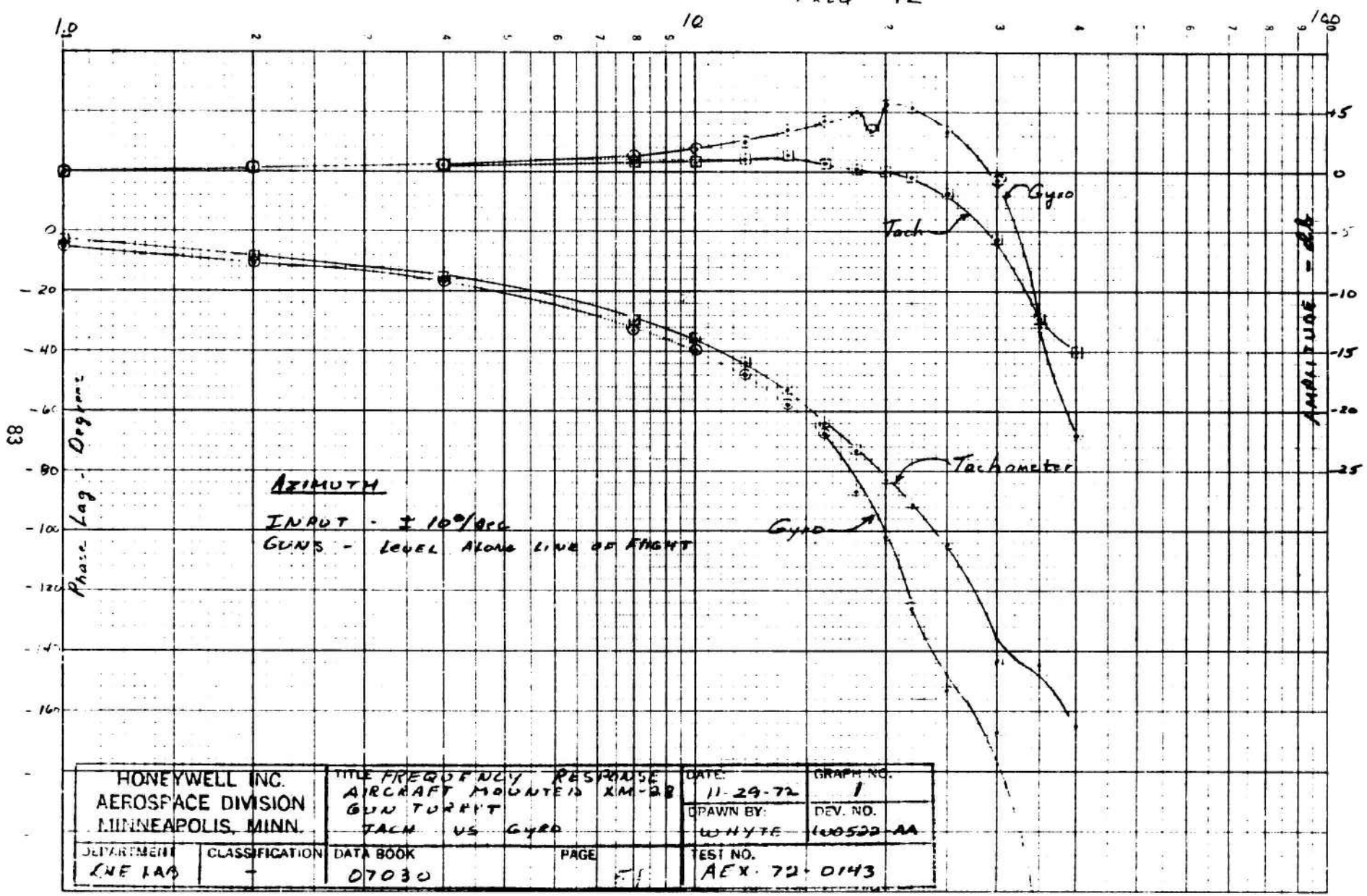

HONEYWELL INC. AEROSPACE DIVISION MINNEAPOLIS, MINN.		TITLE FREQUENCY RESPONSE AIRCRAFT MOUNTED XM-28 GUN TURRET TACH VS GYRO		DATE: 11-29-72	GRAPH NO. 1
				DRAWN BY: WHYTE	DEV. NO. 100522-AA
DEPARTMENT CNE 1A3	CLASSIFICATION -	DATA BOOK 07030	PAGE	TEST NO. AEX-72-0143	

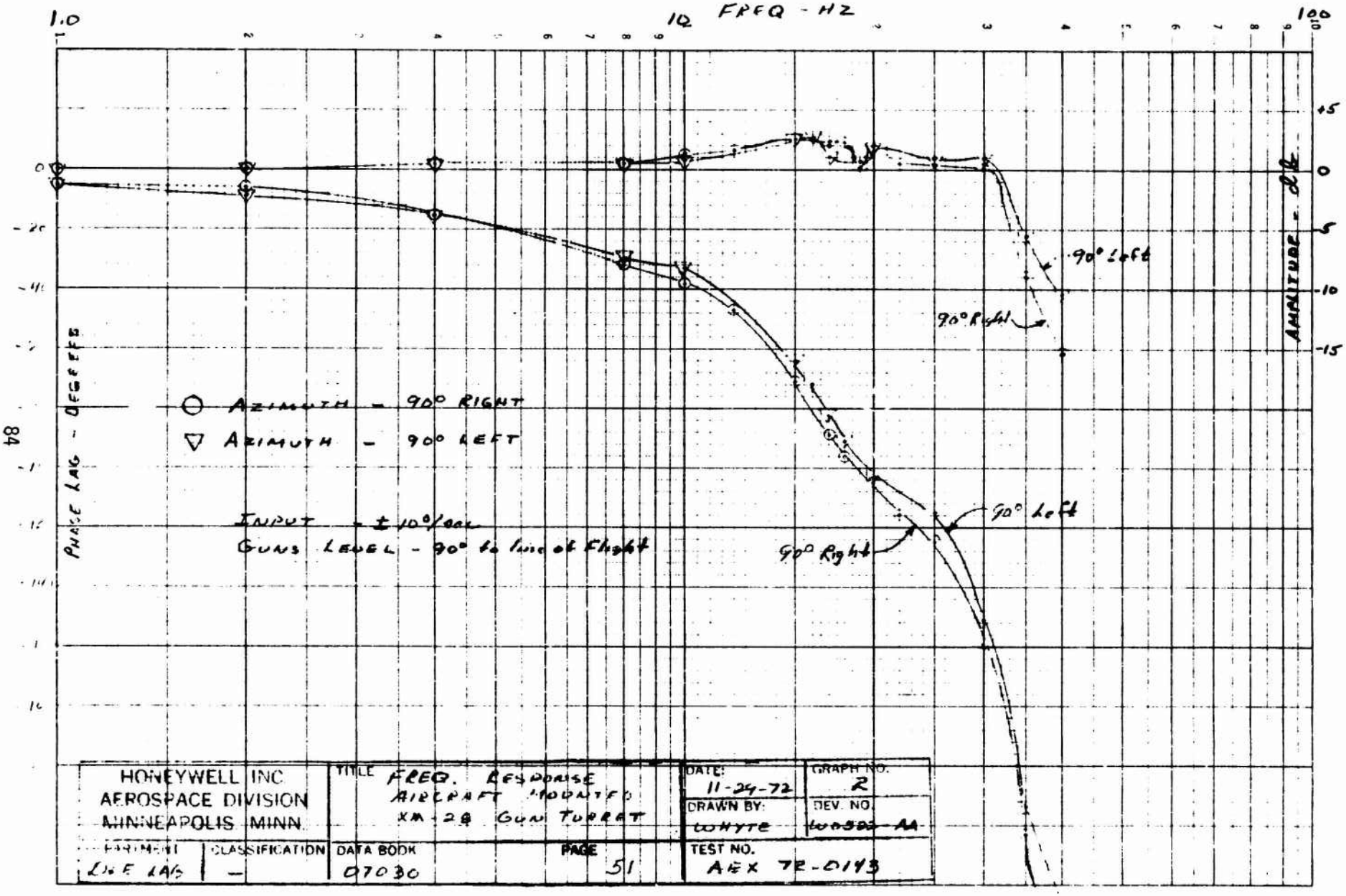

HONEYWELL INC. AEROSPACE DIVISION MINNEAPOLIS MINN.	TITLE FREQ. RESPONSE AIRCRAFT MOUNTED XM-28 GUN TURRET	DATE: 11-24-72	GRAPH NO. 2
		DRAWN BY: LOWYTE	DEV. NO. [illegible] AA
DEPARTMENT L & E LAB	CLASSIFICATION –	DATA BOOK 07030	PAGE 51
		TEST NO. AEX 72-0143	

K&E SEMI-LOGARITHMIC 46 4973
KEUFFEL & ESSER CO.

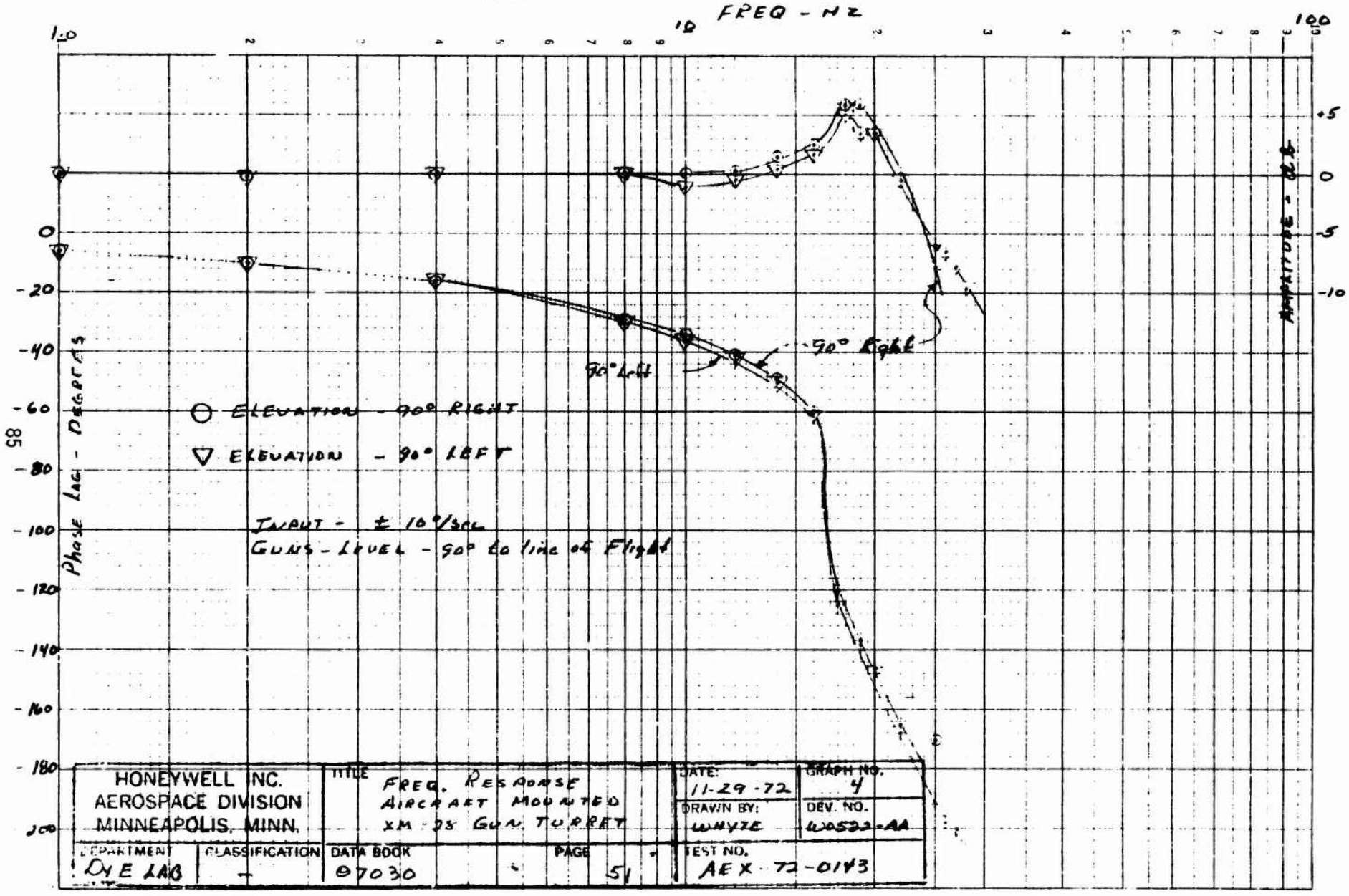

HONEYWELL INC. AEROSPACE DIVISION MINNEAPOLIS, MINN.	TITLE: FREQ. RESPONSE AIRCRAFT MOUNTED XM-28 GUN TURRET		DATE: 11-29-72	GRAPH NO. 4	
			DRAWN BY: WHYTE	DEV. NO. W0523-AA	
DEPARTMENT: DYE LAB	CLASSIFICATION: -	DATA BOOK: 07030	PAGE: 51	TEST NO.: AEX-72-0143	

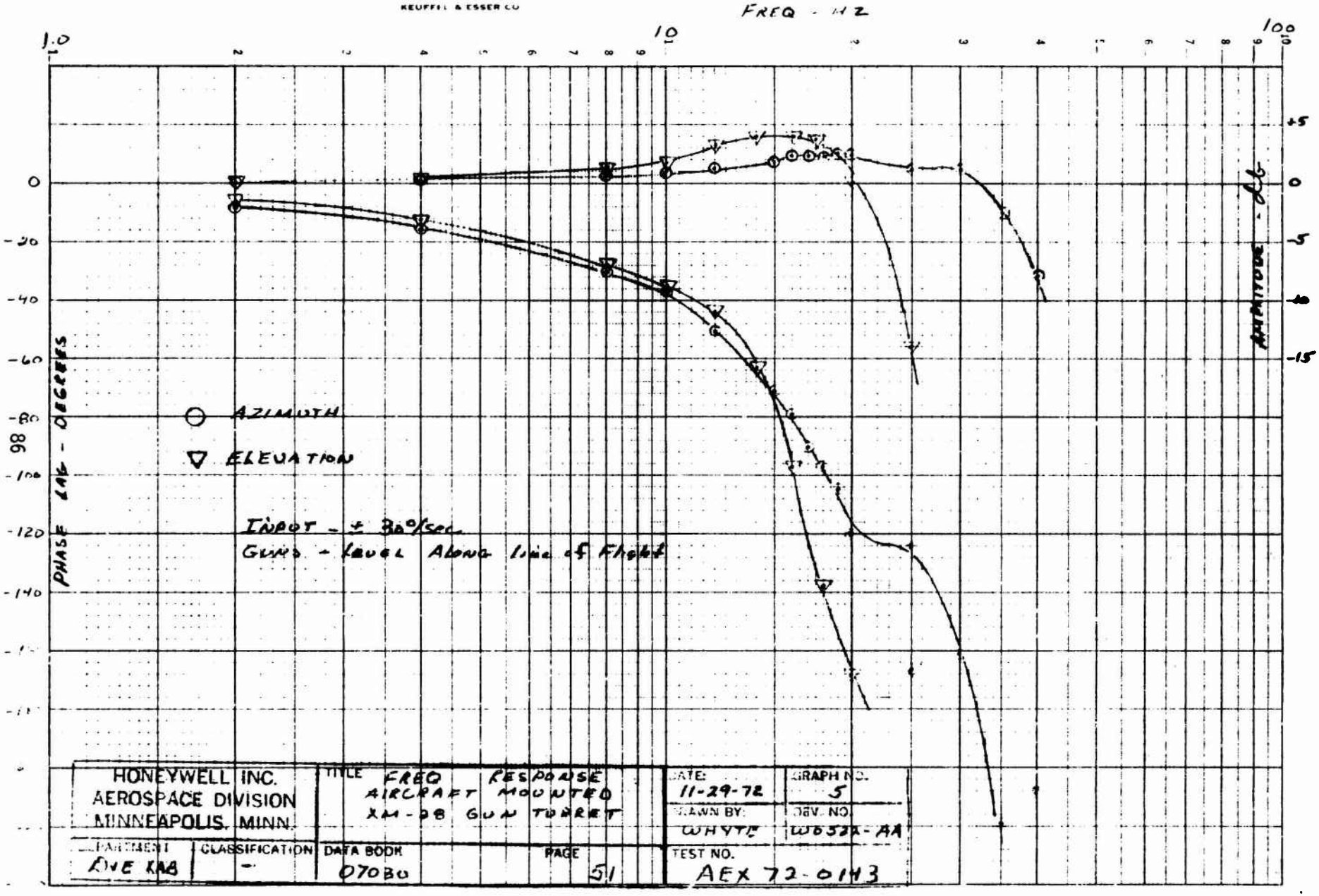
K·E SEMI-LOGARITHMIC 46 4973
KEUFFEL & ESSER CO
FREQ - HZ
1.0
10
100
PHASE LAG - DEGREES
AMPLITUDE - db
0
-20
-40
-60
-80
-100
-120
-140
+5
0
-5
-10
-15
AZIMUTH
ELEVATION
INPUT - ± 30°/sec
GUNS - LEVEL ALONG LINE OF FLIGHT
HONEYWELL INC.
AEROSPACE DIVISION
MINNEAPOLIS, MINN.
TITLE FREQ RESPONSE AIRCRAFT MOUNTED XM-28 GUN TURRET
DATE: 11-29-72
GRAPH NO. 5
DRAWN BY: WHYTE
DWG. NO. W6528-AA
DEPARTMENT DNE KAB
CLASSIFICATION -
DATA BOOK 07080
PAGE 51
TEST NO. AEX 72-0143

K&E SEMI-LOGARITHMIC 46 4973
2 CYCLES X 70 DIVISIONS
KEUFFEL & ESSER CO.

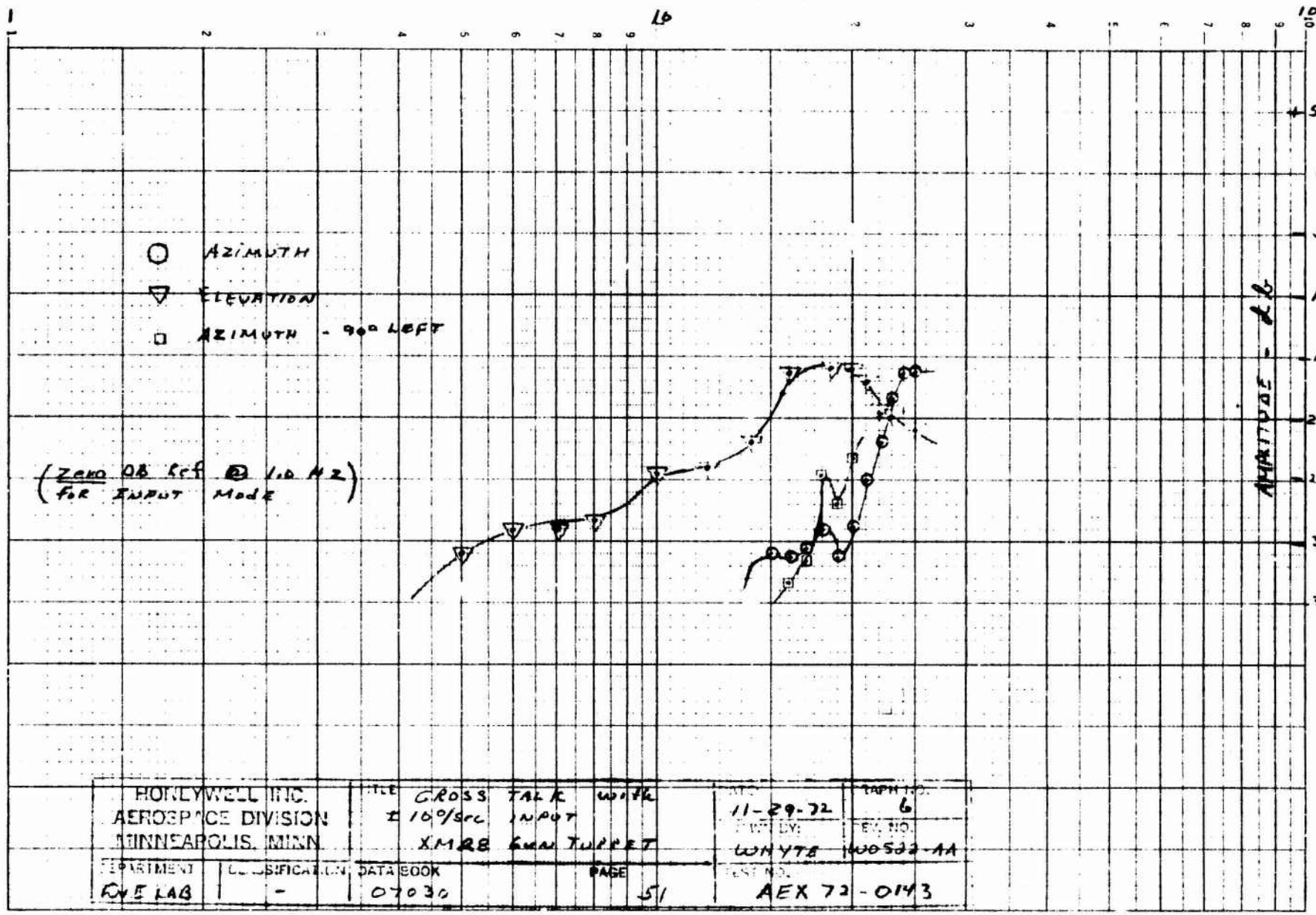

HONEYWELL INC. AEROSPACE DIVISION MINNEAPOLIS, MINN.	TITLE: CROSS TALK with ± 10°/sec INPUT XMRB Gimbal Turret		DATE: 11-29-72	TAPE NO.: 6
			DWG. LEV: WHYTE	DWG. NO.: 1100522-AA
DEPARTMENT: Sys E LAB	CLASSIFICATION: -	DATA BOOK: 07030 PAGE 51	TEST NO.: AEX 72-0143